The orchestration of DNA-protein crosslink recognition and repair in mammalian cells

A DISSERTATION

SUBMITTED TO THE FACULTY

OF THE UNIVERSITY OF MINNESOTA

BY

Maram Magdi Essawy

IN PARTIAL FULFILLMENT

OF THE REQUIREMENTS FOR THE DEGREE OF

DOCTOR OF PHILOSOPHY

Advisor: Colin Campbell, PhD

January 2023

Acknowledgements

I would like to express my deepest appreciation to Dr. Colin Campbell for the mentoring and support that he has provided me during my time in his lab, as well as the time Colin has spent teaching me how to approach my experiments independently and confidently. Colin has taught me to use my strengths and overcome my weaknesses to become a better scientist, has taught ‘do or do not, there is no try’, and showed me through his words and by example what it means to give my all to every task that I am faced with. The lessons I learned from Colin are never-ending, and I am grateful to have had a PhD advisor who is committed to the success and well-being of his trainees.

DEDICATION

I would like to dedicate this thesis to my parents, Magdi Essawy and Karima Koraiem, who left their home country and lived for decades away from their own parents, friends, and family, to provide me with the tools and opportunities that would help me achieve my dreams. My mother gave up her own dreams to achieve a PhD in order to raise my brothers and me, and to that sacrifice, I owe my degree. I am grateful to have been raised by parents who have such a strong work ethic and thirst for knowledge, which they also worked tirelessly to instill in me. My parents provided me with constant support, without which I may not have been able to overcome the many challenges of graduate school. I am eternally grateful to my parents for their never-ending love and support.

Table of Contents

ABBREVIATIONS

DNA-Protein Crosslink (DPC)

8-oxoguanine (8-oxoguanine)

Oxoguanine glycosylase (OGG1)

Quantitative polymerase chain reaction (PCR)

Strand-specific primer extension-quantitative polymerase chain reaction (SSPE-qPCR)

Nucleotide Excision Repair (NER)

Homologous Recombination (HR)

Non-Homologous End Joining (NHEJ)

Microhomology-Mediated End Joining (MMEJ)

Base Excision Repair (BER)

Immunoprecipitation (IP)

Sodium Dodecyl Sulfate (SDS)

Apurinic (AP)

Apyrimidinic (AP)

Topoisomerase (TOP)

Tyrosyl-DNA-Phosphodiesterase (TDP)

Cycle threshold (Ct)

Small Ubiquitin-Like Modifier (SUMO)

LIST OF TABLES

List of Figures

List of Supplemental Figures

ABSTRACT

DNA-Protein Crosslinks (DPCs) are large, bulky, and cytotoxic DNA lesions that are subject to repair by Nucleotide Excision Repair (NER) and Homologous Recombination (HR), and post-translationally modified prior to their repair. The orchestration of DPC repair by multiple, redundant repair pathways is not fully understood. A limitation of DPC repair research is that drugs used to form genomic DPCs form other kinds of DNA damage as well. To address this limitation, I have developed a site-specific, chemically homogenous model DPC substrate that can be manipulated to allow for independent study of different kinds of DPCs. DPC substrates were transfected into cell-based or cell-free systems and analyzed utilizing a variety of assays, including qPCR-based and non-qPCR-based assays. I showed that these systems can be used to study DPC repair, removal, and post translational modifications. Genetic manipulation of transfection conditions allows for the study of repair intermediates formed via NER-mediated or HR-mediated DPC repair, independently. Using the tools described above, I found that DPC removal via NER and HR is ubiquitin dependent, however pathway specific removal is modulated by differential polyubiquitination of the crosslinked protein. I also showed that DPC removal by NER, but not HR is proteasome dependent. Finally, I found that DPCs are also modified with SUMO1 and SUMO2/3 proteins, and that DPC ubiquitination and SUMOylation are interdependent, however the mechanisms underlying this interdependence remain to be investigated.

Chapter 1

Introduction

I. DNA-PROTEIN CROSSLINK FORMATION

Cellular genomes are subjected to a variety of insults that can result in several different forms of mutational and/or deleterious types of genomic lesions [1, 2]. One form of genomic lesion is called the DNA-protein crosslink (DPC). DPCs are formed when proteins become irreversibly trapped on DNA and can be formed by a variety of endogenous and exogenous factors [3-7]. Endogenously derived DPCs can be formed by enzymatic or non-enzymatic mechanisms **(Figure 1.1)**. Non-enzymatic DPCs form when nuclear proteins become trapped to DNA following exposure to endogenous or exogenous reactive compounds. Enzymatic DPC formation occurs as a result of trapping of DNA-modifying enzymes onto DNA during cellular processes including DNA replication, transcription, and repair [8]. The mechanisms by which some of these DPCs form are described below.

Enzymatically derived DPCs can be formed following the trapping of proteins like topoisomerase 1, topoisomerase 2, polymerase beta, and PARP-1 to DNA [8-10]. DNA topoisomerases relieve excessive torsional strain in the DNA double helix (which forms as a result of helix unwinding during DNA replication) by forming single-stranded breaks (topoisomerase 1) or double-stranded breaks (topoisomerase 2) in the backbone, which are then re-ligated following relaxation of the double-helix [11]. During this process, topoisomerases form a transient catalytic intermediate (top-cc), (**Figure 1.2A)** which, in the case of misalignment of the DNA due to mismatches, abasic sites, and even nicks in the vicinity of the topoisomerase cleavage site, can become irreversibly trapped

to DNA, and then are referred to as top-DPCs [10]. Second, a common enzymatically induced DPC is formed during aberrant repair of oxidative DNA damage [12]. Oxidative damage to DNA is repaired by the base excision repair (BER) pathway, which mobilizes polymerase β for DNA synthesis as well as cleavage of the 5′-deoxyribose phosphate (dRP) formed following DNA strand incision by apurinic/apyrimidinic (AP) endonuclease [13, 14]. During attempted excision of chemically reduced AP residues polymerase β can become covalently trapped to the DNA, resulting in a DPC [8]. Another example of enzymatically induced DPC is the Poly (ADP-ribose polymerase 1 (PARP-1) DPC. (PARP-1), also known as NAD+ ADP-ribosyltransferase 1 or poly[ADP-ribose] synthase 1, is a DNA-binding protein that is involved in multiple nuclear processes, including the detection of DNA damage, DNA repair, and the regulation of transcription [15, 16]. One of the main functions of PARP-1 is ADP-ribosylation, which occurs when PARP-1 uses NAD + to synthesize poly ADP ribose (PAR) and transfers these PAR moieties to proteins [17]. PARP-1 also has a strong affinity for abasic sites and single-strand breaks, including those formed as intermediates of the BER pathway [9]. Following the binding of PARP-1 to these lesions, PARP-1 conducts PARylation of BER repair enzymes to promote their recruitment to the site of DNA damage [18]. However, the persistence of abasic sites in DNA can create conditions in which PARP-1 becomes covalently crosslinked to DNA. This is thought to occur when PARP-1 cannot regenerate NAD +. In the absence of this oxidizing agent, the Schiff base formed between a primary amine in PARP-1 and the C1’ atom of the

deoxyribose in the AP site is reduced, forming a stable covalent bond between PARP-1 and the DNA backbone [19].

Non-enzymatic DPCs are formed following the exposure of cells to endogenously existing crosslinking agents, such as aldehydes or reactive oxygen species, or exogenous crosslinking agents, such as UV light, ionizing radiation, and DNA-damaging agents including many cancer chemotherapeutics [2, 20]. Aldehydes are strongly electrophilic, highly reactive, and relatively long-lived compounds that are produced in the cell as byproducts of cellular reactions, such as the metabolism of alcohols, amino acids, and neurotransmitters. Lipid peroxidation of cellular phospholipids results in the formation of a variety of aldehyde species, including formaldehyde, which is also formed as a byproduct of histone demethylation [21]. Although cells contain robust aldehyde detoxification mechanisms, aldehydes that escape these mechanisms can react with DNA and proteins to form DPCs. Formaldehyde induces DPC formation when it is attacked by the primary amine of a lysine residue (forming a methylol adduct). A dehydration reaction then occurs to form a transient Schiff base, which further reacts with the amino groups of aromatic DNA bases to form a stable DPC [22]. Similarly, reactive oxygen species (ROS) are formed endogenously as byproducts of cellular activities, such as ATP production, peroxisome activity, and the unfolded protein response. However, high ROS levels can cause multiple forms of biomolecular damage, including DPC formation [23, 24]. While the aberrant repair of oxidative DNA damage can result in the formation of DPCs, as described above, multiple other direct mechanisms of DPC induction by ROS exist. For example, lysine residues of DNA-interacting proteins such as histones can form

a transient Schiff base with oxidized abasic sites, which occurs with slow kinetics and can be converted into a stable covalent bond [25, 26].

A variety of environmental agents are capable of inducing DPC formation in cells. For example, UV irradiation can form purine and pyrimidine free radicals, which then form covalent bonds with nearby proteins [27, 28]. Similarly, ionizing radiation induces unstable DNA radical cations as well as protein radicals, which, when in close proximity to one another, can react or recombine to form a covalent bond. Additionally, industrial chemicals such as 1,2,3,4-Diepoxybutane (DEB) can react with the N7 atom of guanine to generate an adduct that can form crosslinks with the nucleophilic amino acid residues of nearby proteins [29-39].

One of the most used and most effective classes of anti-cancer therapeutic agents is DNA-damaging drugs [40-43]. Examples of DNA-damaging drugs include the topoisomerase inhibitors camptothecin and etoposide, which induce cytotoxicity by stabilizing topoisomerase 1 or topoisomerase 2 cleavage complexes, respectively inhibiting the religation step and subsequent dissociation of topoisomerase from DNA, resulting in a top-DPC [44]. Nitrogen mustards, the first DNA-damaging chemotherapeutic to be used, are alkylating compounds that can form DPCs by multiple mechanisms, including by reacting with the N7 position of guanine, which can then covalently bond to cysteine residues of nearby proteins [7, 38, 45-55]. Platinum-based chemotherapeutics such as cisplatin exert cytotoxicity following activation in the cell by reacting with nucleophilic DNA and protein residues, such as the N7 atom on purine residues and sulfhydryl group-containing amino acids such as cysteine, which can then

react together to form a DNA protein crosslink [56]. The therapeutic agents described above all create other forms of DNA damage in addition to DPCs, including DNA monoadducts and DNA-DNA interstrand and intrastrand crosslinks [57]. While 5-aza-2'-deoxycytidine (5-azaDC) is a cancer therapeutic that only forms one form of DNA lesion (DPC), it nevertheless exerts its cytotoxic effects by multiple mechanisms, including depletion of cellular DNA-methyltransferase I (DNMT1) stores and inhibition of DNA methylation (as 5-azaDC is incorporated during replication to replace cytosine residues in DNA) [58, 59]

Cancer cells can become resistant to DNA-damaging drugs through a variety of mechanisms, limiting the success of this widely used class of antineoplastic drugs in cancer therapy [60]. Since failed DNA repair promotes mutagenesis, and enhanced DNA repair capability represents a potential avenue through which cancer cells become drug-resistant, there has been great interest in identifying the major mechanisms of DPC repair [61, 62].

II. DNA-PROTEIN CROSSLINK REPAIR MECHANISMS

To protect the genome from these frequently formed and highly cytotoxic lesions, organisms have evolved mechanisms to remove DPCs. Some types of DPCS, notably topoisomerase-1/2-DPCs and spo11 DPCs, are subject to specialized repair mechanisms [63, 64]. Tyrosyl-DNA phosphodiesterase 1 (TDP1) and tyrosyl-DNA phosphodiesterase 2 (TDP2) are highly conserved repair enzymes dedicated to the excision of top-1 and top-2 DPCs, respectively [65]. Following the recognition of a topoisomerase 1 DPC, the

proteosome or SPRTN proteolytically degrade the protein component of the DPC (known as debulking), allowing for access of TDP 1to the tyrosyl-DNA linkage. TDP 1 then hydrolyses the phosphotyrosyl bond (**Figure 1.2B)**, freeing the broken DNA end(s) and allowing for break targeted DNA repair factor [such as polynucleotide kinase phosphatase (PNKP) and X-ray repair cross complementing 1 (XRCC1) for single-strand break repair or homologous recombination/non-homologous end joining for double-strand break repair]. TDP2 functions mechanistically like TDP1 to hydrolyze phosphotyrosyl bonds but is targeted to top-2 DPCS rather than top-1 DPCs [11, 65-67].

Spo11 is evolutionarily related to archaebacterial topoisomerases [68-70] and is required for the initiation of meiotic recombination in several species, including humans [71]. Tyrosine residues of two dimerized spo11 proteins nucleophilically attack DNA, generating a covalent linkage between the spo11 residue and a 5′ phosphate in the DNA backbone, resulting in the formation of a DSB to which spo11 is trapped. Like topoisomerase, spo11 is first proteolyzed then removed *via* endonucleolytic cleavage from DSB ends (by mre11 nuclease), resulting in the formation of protein-free DSB ends at which meiotic recombination is initiated [72-75].

Despite the few exceptions in which covalently trapped proteins are removed via their own specific repair mechanisms, the majority of DPCs are repaired by two major DNA repair pathways: nucleotide excision repair (NER) and homologous recombination (HR) [76-84]. The first papers describing NER documented the discovery that bacteria were able to remove pyrimidine dimers, a form of UV-induced damage, from DNA, and that they could identify several genetic mutations that sensitized bacteria to UV

irradiation. It was also shown that the mechanism by which bacteria repaired pyrimidine dimers included an excision step (to remove the damaged bases) and a DNA synthesis step (to fill in the excised spaces) [85-87]. At the same time, another group documented evidence that mammalian cells were also capable of removing UV-induced DNA damage in a repair synthesis-dependent manner, and soon genetic mutations were identified in xeroderma pigmentosum (a disease characterized by sun sensitivity and predisposition to cancer) patients that were linked with an inability to remove UV-induced DNA damage [88, 89]. It is now known that the NER pathway not only removes pyrimidine-dimers formed in response to UV irradiation, but also other forms of bulky DNA lesions, including other chemically induced pyrimidine-dimers and DNA interstrand and intrastrand crosslinks, as well as DNA-protein crosslinks [89]. It has also been established that there are two main subpathways of NER, global genomic NER (gg-NER) and transcription coupled NER (tc-NER) **(Figure 1.3)** [79, 90]. GG-NER removes DNA lesions anywhere in the genome, whereas tc-NER removes DPCs encountered during transcription (which block the elongating RNA polymerase II complex). Both pathways complete the fundamental steps that define NER (damage excision followed by DNA synthesis for gap-filling). The two pathways differ mainly in the steps involved in the recognition of DNA lesions. In gg-NER, the first proteins to be recruited are the xeroderma pigmentosum complementation group C (XPC) protein, centrin 2 (CETN2), and RAD23. In tc-NER, the lesion is recognized by a stalled RNA polymerase II complex, which then recruits the CS complementation group B (CSB) protein [91, 92]. Following DNA-damage recognition by both pathways, Transcription Factor II H

(TFIIH) is recruited to the lesion. TFIIH is a 10-subunit complex that facilitates the opening of DNA around an NER substrate in an XPB ATPase- and XPD helicase-dependent mechanism. Following TFIIH recruitment, an XPF-ERCC1 dimer forms an incision at the 5′ end of the lesion, and XPG forms an incision at the 3′ end, resulting in the release of the damaged oligonucleotide and its flanking sequence. DNA repair synthesis is then completed by DNA polymerase η, ε, or κ, and the DNA is ligated by DNA ligase I and DNA ligase IIIα [93-95].

The second major pathway involved in DPC repair, homologous recombination, was first discovered in the context of genetic recombination in *E. coli* [96, 97]. The mechanism underlying genetic recombination continued to be studied in bacterial and viral genomes [98] and a model describing the mechanism underlying homologous recombination and accounting for gene conversion during recombination (The Holliday junction model) was proposed [99]. Soon after, genetic mutants of *E. coli* that were unable to form recombinants or repair photodamaged DNA were identified (the required gene product was named recA) [100]. Evidence of recombination was also found in in the repair of photodamaged bacterial genomes [101, 102]. Shinohara *et al.,* identified RAD51 in *S. cerevisiae* as a protein involved in recombination and repair and showed that it had structural and functional similarity to the bacterial recA protein, providing the first evidence of recombination in eukaryotes [103]. Further studies have elucidated multiple sub-pathways of recombinational repair in eukaryotes (See **Figure 1.4**). In addition to the role of recombination in meiosis, recombination pathways are mobilized to repair multiple forms of DNA damage, including double-strand breaks, single-strand breaks,

and DNA-protein crosslinks [76, 82, 99, 104-114]. While there are multiple subpathways of HR, the central reactions of all pathways are based on the formation of single-stranded 3′ overhangs around the DNA lesion, which are then coated by replication protein A (RPA). RPA is then replaced with RAD51, which initiates the search for a homologous donor (which is used as the template for error-free repair) and carries out strand invasion of the homologous donor, forming a displacement loop (D-loop). Repair by the subpathway known as synthesis-dependent strand annealing (SDSA) proceeds by displacing the extended break end from the D-loop and annealing the complementary sequence at the complementary end. Repair by the sub-pathway known as Holliday junction dissolution (dHJ) proceeds by forming one or two D-loops between the recombining strands, known as Holliday or Double Holliday Junctions. Repair synthesis is initiated by the invading strand(s), and Holliday junctions are resolved by nucleases and other repair factors [115]. Double strand breaks that have been subjected to 5′ end resection can also be repaired by Single Strand Annealing (SSA), a subpathway that is inhibited by RAD51 and is characterized by DSB formation between homologous repeat sequences. Following the generation of 3′ ssDNA, the flanking homologous sequences then anneal together to form a synapsed intermediate, which is then processed for the endonucleolytic removal of the 3′ssDNA tails. Finally, remaining gaps are filled by polymerase. Repair by SSA results in the loss of genetic information due to deletion rearrangement, and it does not require the presence of a sister chromatid for template-based repair, thus the genetic modulation of this pathway differs from those described above [116].

III. PROTEOLYTIC PROCESSING OF DPCS

In addition to the canonical, nucleolytic repair pathways described above, there is evidence to show that DPC repair mechanisms can also be proteolytic in nature (i.e., preceded by proteolytic processing of the crosslinked protein, as mentioned above in the case of 'debulking' of topoisomerase and spo11 DPCs). This is supported by the observations that NER machinery can only excise DNA containing smaller sized DPCs (less than 14 kDa in size), while the HR machinery preferentially repairs DPCs comprising larger proteins [76, 78]. Proteolysis-coupled repair was first proposed following studies in *S. cerevisiae* in which wss1 was identified as a protease that is involved in the repair of DNA-crosslinked topoisomerase 1 [117]. Later, SPRTN , a mammalian homolog of wss1, was identified as a mammalian DNA-dependent protease responsible for the removal of DPCs formed in response to cell treatment with formaldehyde, etoposide, and camptothecin [118]. It has been reported that there is a second DPC-specific protease family known as GCNA (Germ Cell Nuclear Antigen), also known as Acidic Repeat Containing Protein (ACRC), which is a SprT domain-containing metalloprotease that promotes the survival of *C. elegans* following treatment with formaldehyde and is recruited to DNA damage foci [119].

There is also evidence of a role for the proteasome in the processing of DPCs formed in response to 5′azadC treatment [84] as well as DPCs transfected into mammalian cells [78]. Additionally, it has been shown that the proteasome, as well as SPRTN, is involved in the debulking of topoisomerase DPCS prior to their removal by

tyrosyl-DNA phosphodiesterase or the MRN complex [120, 121]. Studies completed in formaldehyde and 5′azadC treated bacteria [76] as well as in *Xenopus* extracts [122], suggest that DPC repair is not proteasome-dependent. These discrepancies could be explained by genetic redundancy (i.e., an ability for the proteasome, SPRTN, or another protease to interchangeably proteolyze DPCs) or due to the fact that the proteasomal inhibitors used in these studies also deplete free ubiquitin stores, resulting in an inability to independently study the roles of SPRTN and the proteasome in DPC repair [123].

IV. DPC UBIQUITINATION

Evidence suggests that NER and HR are mobilized independently for various types of DPC repair. As mentioned above, studies suggest that NER and HR differentially repair crosslinked proteins of different size ranges [76, 78]. Additionally, data generated in mammalian cells and in *Xenopus laevis* extracts suggest that HR can be tightly coupled to DNA replication [63, 64, 77, 124-127]. Finally, while both NER and HR repair DPCS formed during transcription, tc-NER (see above) is dedicated to the repair of DPCs encountered by RNA polymerase II during transcription [91, 128]. Mitotic recombination has been shown to be stimulated by transcription due to the induction of strand breaks, however the mechanism by which this form of HR is regulated is not fully understood [129-131].

There is increasing evidence to suggest that DPC repair is regulated by ubiquitin signaling. At one level, this is known to occur through ubiquitination of DNA repair proteins and would impact other types of DNA repair as well. For example, it has been

shown that both XPC and the UV-damaged DNA binding protein known as UV-DDB (two key NER proteins) undergo reversible ubiquitination following UV irradiation of cells, and this ubiquitination enhanced the ability of these two proteins to bind to DNA and to each other [132]. SPRTN, a DPC specific protease, must be deubiquitinated in order to bind to chromatin [133]. Additionally, ubiquitination of RAD51, CtBP-interacting protein (CtIP), and numerous other DNA repair proteins has been shown to affect their ability to engage in DNA repair following treatment of mammalian cells with DPC-forming drugs [134-136].

More notably, studies have shown that DNA crosslinked proteins are ubiquitinated following their formation as a result of cellular treatment with drugs 5-azadeoxycytidine, formaldehyde, and the topoisomerase poisons etoposide and camptothecin- and that this ubiquitination plays a role in their repair [66].

. Ruggiano *et al.,* showed that treatment of HeLa cells with formaldehyde resulted in a concentration-dependent accumulation of ubiquitinated DPCs. Sun *et al.,* showed that topoisomerase 1 and 2 -DPCs formed following treatment with camptothecin and etoposide, respectively, were ubiquitinated, and that co-treatment of cells with a ubiquitin ligase inhibitor and topoisomerase inhibitor resulted in the accumulation of topoisomerase-DPCs [137].

Additionally, Liu *et al.,* showed that 5-azadC treatment resulted in the ubiquitination of DNMT1 DPCs, and, furthermore, DNMT1 repair was impaired in cells that had been treated with siRNA targeting the SUMO Targeted Ubiquitin Ligase

(StubL), which they also used to show that DPC SUMOylation was required for DPC ubiquitination [66, 137, 138].

While the precise mechanism by which ubiquitination modulates DPC repair is unclear, studies in *Xenopus* extracts have demonstrated that, in a replication-dependent context, crosslinked protein ubiquitination was associated with the recruitment of both SPRTN and the proteasome to DPCs [128]. Additionally, *Ruggiano et al.,* showed that ubiquitinated proteins were co-purified with SPRTN that was recovered from formaldehyde treated cells [138]. Additionally, an investigation of camptothecin and etoposide induced DPCs showed that top-1 and top-2 DPCs were modified with K11, K48, and K63-linked polyubiquitin chains [66]. K11-linked and K48-linked polyubiquitin chains are known to trigger proteasomal recruitment, which is consistent with other findings that the proteasome is involved in DPC repair. K63-linked polyubiquitin chains, however, are known to trigger various protein-protein interactions that result in the regulation of proteasome-independent pathways such as signal transduction, endocytosis, and modulation of the DNA-damage response [139-142]. Together, these findings are consistent with the interpretation that ubiquitin signaling modulates DPC repair via proteasome dependent and proteasome independent mechanisms.

V. OBSTACLES IN STUDYING DPC REPAIR

As discussed above, the majority of studies investigating mechanisms of DPC repair in bacteria, yeast, and higher eukaryotes are performed using DPC forming drugs,

such as formaldehyde, cisplatin, 5′aza-2’-deoxycytidine and the topoisomerase inhibitors camptothecin and etoposide. The genetic requirements for DPC repair by NER and by HR were first identified by studying the extent to which inactivating mutations in DNA repair genes sensitized cells to DPC forming drugs [89, 100, 105]. A limitation of this strategy is that DPC-forming drugs also cause other forms of DNA damage. For example, in addition to DPCs, formaldehyde treatment results in the formation of protein-protein crosslinks, DNA monoadducts, DNA-DNA crosslinks and DNA strand breaks [143, 144]. Cisplatin is able to form mono adducts, DNA-protein crosslinks, protein-protein crosslinks, intrastrand and interstrand DNA-DNA crosslinks [145] and indirectly induces the formation of double-strand breaks as a result of aberrant processing of the DNA-DNA crosslinks [146, 147]. Additionally, as camptothecin or etoposide induced top-DPCs form following the formation of a single-strand or double-strand break in the DNA backbone by topoisomerase 1 or topoisomerase 2, respectively, the top-DPC is covalently bound to the DNA breaks. [148]. Hence, studies that measure the survival of repair mutants in response to these drugs cannot account for the possibility that the observed effect is due to impaired repair of a non-DPC lesion. Additionally, as is the case with any pharmacological treatment, it cannot be guaranteed that any observed effect of drug-treatment is not a result of non-specific drug effects.

The inherent heterogeneity of xenobiotic induced DPC structure results in additional obstacles in research surrounding the repair of these lesions. DPCs consist of three main structural components: DNA, proteins, and crosslinks, which may form between the protein and the DNA, or with a chemical linker joining the protein and DNA

components of the lesion. Some DPCs are formed by trapping to the deoxyribose backbone of DNA, while others are formed by covalent interaction with the nitrogenous bases of DNA, and the identity of the trapping agent affects the chemical identity of the crosslink. Additionally, each component of the DPC lesion is highly variable and dependent on the conditions preceding trapping. Studies have identified numerous proteins that become crosslinked to DNA following exposure to therapeutic anticancer agents [28, 38, 149-152]. This diversity in the identity of crosslinked proteins is reflected by the heterogeneity in the size and structure of crosslinked proteins. Therefore, DPC adducts are far more structurally diverse than DNA monoadducts, double-strand breaks, ultraviolet radiation-induced DNA photoproducts, and other DNA lesions classically associated with single repair pathways.

I am interested in understanding the mechanisms by which mammalian DNA protein crosslink recognition and repair is orchestrated. As discussed above, utilizing a platform of drug-treated cells to study these mechanisms is associated with several obstacles that limit the ability to query the orchestration of DPC repair. To address these limitations, I used a site-specific, chemically homogenous model DPC substrate which is generated by crosslinking a recombinant OGG1 protein to double stranded M13. This DPC substrate can be manipulated at the level of the protein, the crosslink, or the DNA to allow for independent study of different kinds of DPCs. These DPC substrates are transfected into mammalian cells, purified mitochondria, or nuclei, or nuclear protein extracts and assayed utilizing a variety of assays, including qPCR-based assays and non-qPCR-based assays. Together, these tools that I have developed allow us to study the role

of post-translational modifications in the orchestration of mammalian DPC recognition and repair.

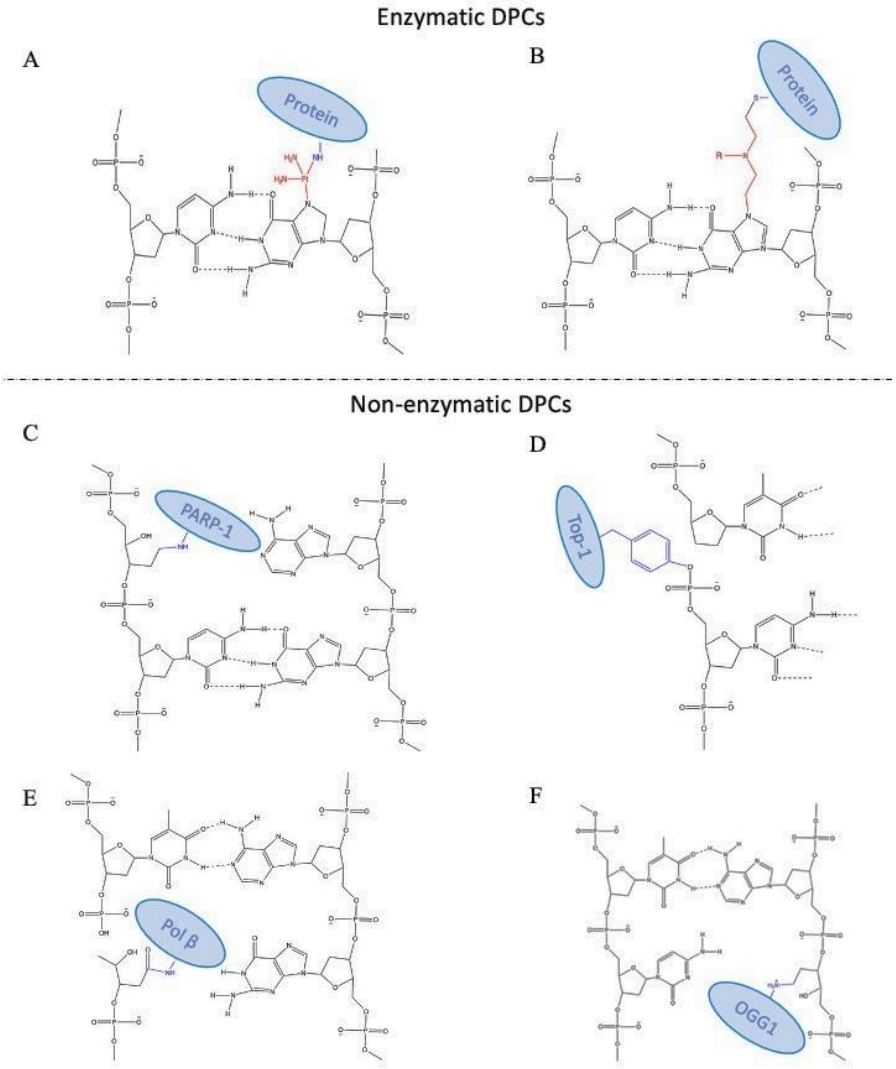

Figure 1.1 Structure of non-enzymatic and enzymatic DPCs. DPC formation can be non-enzymatic or enzymatic in origin. In theory, any protein in the vicinity of genomic DNA can nonspecifically be trapped onto DNA by DPC forming endogenous or exogenous agents (non-enzymatic DPCs). Additionally, enzymes that catalyze DNA-

related reactions during which transient interactions form between the enzyme and DNA can be trapped onto DNA due to aberrant activity and/or by DPC-forming endogenous or exogenous agents (enzymatic DPCS).

A

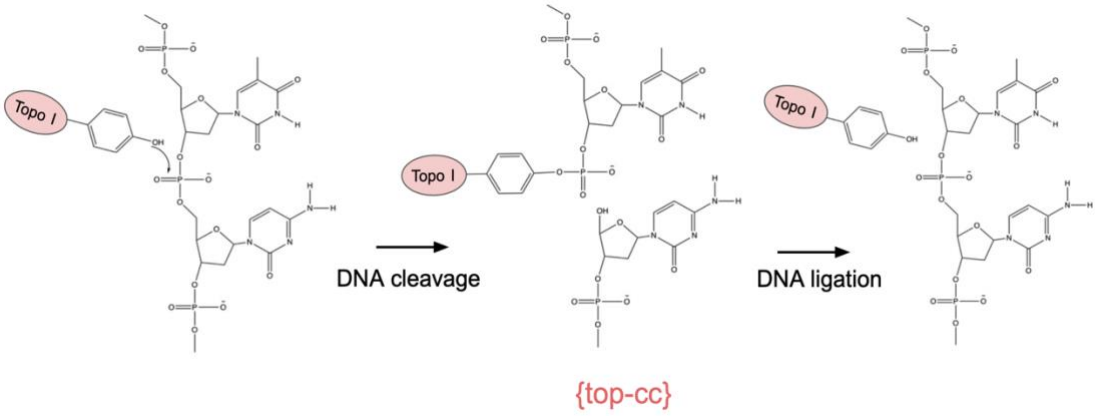

B

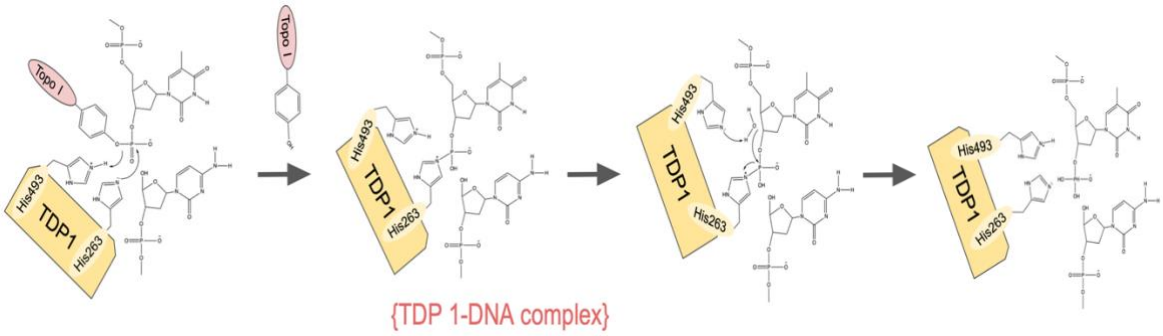

Figure 1.2 Topoisomerase 1 and Tyrosyl-DNA-Phosphodiesterase 1 reaction mechanisms. A) Reaction mechanism of topoisomerase 1 cleavage and religation of DNA B) Reaction mechanism of TDP 1 hydrolysis of Top-1 DPC

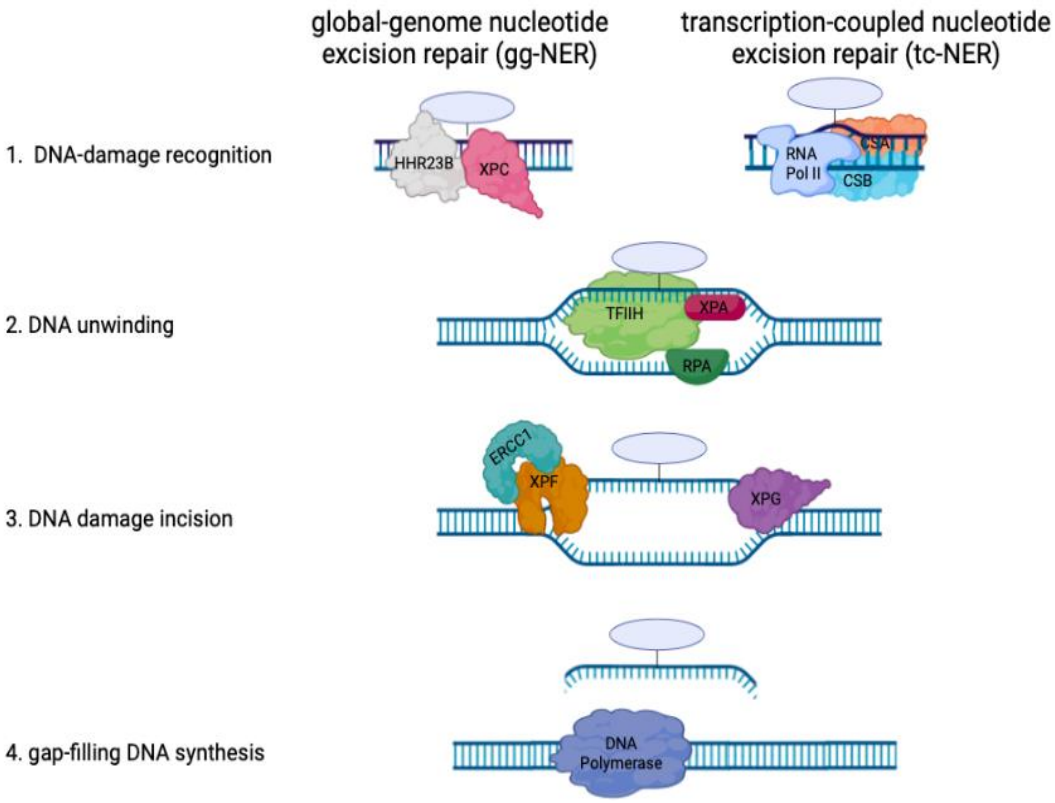

Figure 1.3 Eukaryotic Subpathways of NER. NER can be divided into two sub-pathways, global genomic NER (gg-NER, left) or transcription-coupled NER (TC-NER, right). As gg-NER is not dependent on transcription, damage-sensing occurs via the XPC-HHR23B complex, whereas in tc-NER, damage-sensing occurs by RNA Polymerase II.

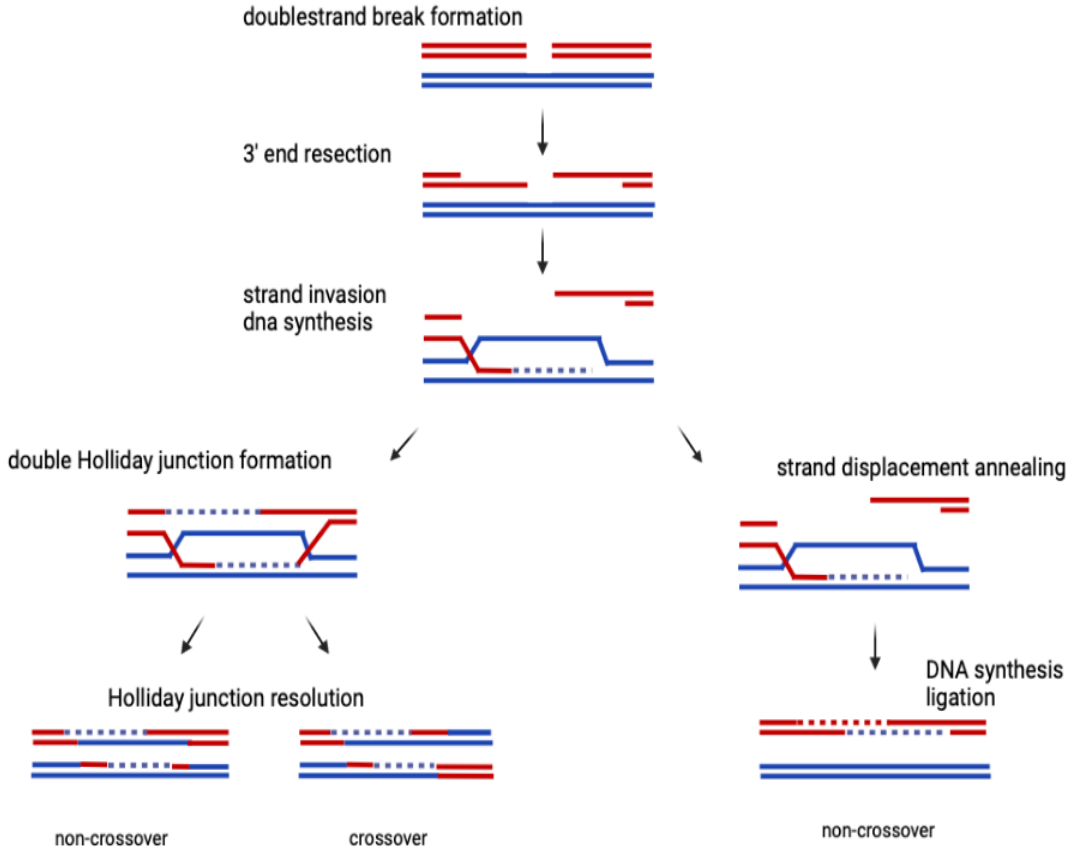

Figure 1.4 Eukaryotic Subpathways of HR. Homologous recombination can occur by various subpathways with various genetic outcomes. Depicted are two major pathways. Pathways characterized by the formation of double Holliday junctions can result in non-crossover or crossover repair outcomes, while pathways characterized by Strand Displacement Annealing (SDA) only result in non-crossover outcomes.

Chapter 2

Ubiquitin signaling and the proteasome drive human DNA-protein crosslink repair

I. INTRODUCTION

DPCs form when proteins become irreversibly trapped onto DNA. DPCs can be formed by a variety of exogenous factors (e.g., ionizing or ultraviolet radiation and toxins found in cigarette smoke), and endogenous factors (e.g., non-enzymatic or enzymatic protein trapping) [1, 2]. These DNA lesions are large and bulky, and thus sterically hinder essential cellular processes like replication and transcription [153-155]. Unrepaired DPCs lead to the induction of programmed cell death, hence, are highly toxic, particularly towards highly proliferating cells, such as cancer cells. DPC forming drugs, including topoisomerase poisons and nitrogen mustard agents and platinum derivatives, comprise a highly effective class of antineoplastic drugs [1, 11, 149, 156-158]. Cancer cells can become resistant to these drugs through a variety of mechanisms, representing a critical obstacle that limits the success of this class of drugs in cancer therapy [159-161].

Because enhanced DNA repair capability represents a potential avenue through which cancer cells become drug-resistant, there has been great interest in identifying the major mechanisms of DPC repair. However, the inherent heterogeneity of this type of DNA lesion represents a major challenge to gaining this insight. In principle, all nuclear proteins can potentially become crosslinked to genomic DNA. Indeed, studies have identified numerous proteins that become crosslinked to DNA following exposure to therapeutic anticancer agents [149]. In addition to the heterogeneity in size and structure of the crosslinked proteins, there is also variation in the types of

chemical bonds linking the DNA and protein molecules. Some DPCs form by trapping to the deoxyribose backbone of DNA, while others form by covalent interaction with the nitrogenous bases of DNA. It is therefore clear that DPC adducts are far more structurally diverse than DNA double-strand breaks and ultraviolet radiation-induced DNA photoproducts classically associated with single repair pathways. To protect the integrity of their genome, bacteria, yeast, and higher eukaryotes have evolved multiple repair mechanisms that can be mobilized for the removal of these diverse DNA lesions. Genetic and biochemical studies have established that some commonly formed DPCs, notably topoisomerase 1/2-DPCs and spo11 DPCs are subject to specialized repair mechanisms. Other studies have shown that DPCs formed in response to formaldehyde, platinum-derived drugs, and even topoisomerase poisons are subject to repair by NER and HR [162-164].

Whether a regulatory mechanism(s) exist(s) to orchestrate the cellular response to, and repair of DPCs by these pathways, is not clear. There is evidence to suggest that NER and HR are mobilized independently for various types of DPC repair. For example, various studies suggest that DPCs that are larger than 10-14 kDa in size are not amenable to NER, while HR machinery preferentially repairs DPCs comprised of larger proteins [76-78]. Additionally, data generated in mammalian cells and in *Xenopus laevis* extracts suggest that HR can be tightly coupled to DNA replication, while NER is active at all phases of the cell cycle [63, 64, 124-128]. Finally, while both NER and HR are capable of repairing DPCS formed during transcription, NER encompasses two major sub-pathways, global genomic NER and transcription-

coupled NER, the latter which is dedicated to the repair of DPCs that block the elongating RNA polymerase II complex [91, 92]**.** Undoubtedly, there are cases in which DPCs are amenable for repair by NER and HR. Thus there is interest in understanding the events following recognition that determine the cellular fate of DPCs (i.e., repair by NER or HR).

There is increasing evidence to suggest that DPC repair is regulated by ubiquitin signaling. It has been shown that the ubiquitination of numerous repair proteins impacts their ability to carry out DNA repair [132, 134-136]. More notably, studies have shown that xenobiotic induced DPCs are ubiquitinated shortly following their formation [66, 137, 138]. Sun *et al*., showed that co-treatment of mammalian cells with a ubiquitin ligase inhibitor and topoisomerase inhibitor resulted in an accumulation of topoisomerase-DPCs [66]. Additionally, Liu *et al*., showed that 5-azadC treatment in cells that had been treated with siRNA targeting the Sumo Targeted Ubiquitin Ligase (StubL) RNF4 resulted in impaired ability to repair DNA Methyltransferase I DPCs [137]. Additional studies in *Xenopus* oocyte extracts have demonstrated that in a replication-dependent context, ubiquitination was associated with the recruitment of SPRTN and the proteasome to DPCs [128]. Together, these findings are consistent with the interpretation that ubiquitin signaling modulates DPC repair *via* proteasome dependent and proteasome independent mechanisms.

I generate a homogenous, chemically defined, and site-specific DPC substrate formed on a non-replicating M13 molecule to query the role of ubiquitination in replication and transcription independent DPC repair. Herein, DPC transfection

conditions are manipulated to shuttle the DPCs into an NER or HR-mediated repair pathway to query the role of DPC ubiquitination in each of these pathways independently of one another. The SSPE-qPCR assay described previously [77] is used to measure DPC repair, an antibody-based immunoprecipitation followed by qPCR to detect post translational modifications to the DPC, and a KCl-SDS based precipitation followed by qPCR to measure crosslinked protein removal.

II. RESULTS

DPCs are subject to repair by HR. The Campbell lab and others [77, 78] have previously shown that substrates containing DPC lesions are efficiently repaired following introduction into mammalian cells, and that the efficiency of repair is substantially lower in cells deficient in NER activity. Reports have shown that bacterial, yeast and mammalian cells harboring defective HR enzymes display an impaired tolerance for DPCs [76, 104, 105], suggesting that the DPC repair defect observed in NER-deficient cells could be reversed if an undamaged homologous donor molecule were co-transfected with the DPC-containing substrate. To test this hypothesis, I transfected a DPC substrate containing a single human oxoguanine glycosylase I (OGG1) protein molecule crosslinked to double-stranded M13 (see reference [77]) into an immortalized NER-deficient cell line (GM08207 [38]) derived from a human donor harboring inactivating mutations in the XPD gene. The DPC was transfected in the presence of either un-lesioned M13 (a homologous donor) or a plasmid with no sequence similarity to M13 (a heterologous donor). Low molecular weight DNA was recovered from the NER-deficient cells (hereafter referred to as XPD) three-hours post-transfection, and the percentage of repaired substrates present determined using a strand-specific primer extension/quantitative real-time PCR assay (termed SSPE-qPCR, described in reference [77]). I observed that 73% of DPCs were repaired in XPD cells co-transfected with the homologous donor, whereas only 14% repair was observed when these cells were co-transfected with the heterologous donor molecule **(Figure 2.1A)**. These results

convincingly argue that the OGG1-crosslinked lesion is capable of being repaired *via* HR. During HR repair, 5′ ends of DNA are subject to endonucleolytic digestion to generate 3′ single-stranded DNA ends [165, 166]. This single-stranded DNA is initially coated by DNA replication protein A (RPA) and activates the ATR (Ataxia Telangiectasia and Rad3-related protein) response [167]. A RAD51 nucleofilament is then assembled and replaces the RPA coat to initiate the search for a homologous donor [168-170]. I therefore reasoned the NER-independent repair depicted in Figure 1A would be lost in cells that have impaired RAD51 activity. To test this prediction, XPD cells were pre-treated for one-hour in the presence or absence of 5 uM B02 [133], a pharmacological inhibitor of RAD51. Following B02 pretreatment, DPCs were transfected into the cells in the presence of homologous donor, and collected 3 hours following transfection, then DPC repair assayed as outlined above. The results presented in **Figure 2.1B** indicate that pretreatment with B02 resulted in a two-fold reduction in DPC repair in XPD cells. Together, the results presented in Figure 1, combined with our previous results [20] indicate that human cells can efficiently repair a DPC lesion *via* either the NER or HR pathways**.**

DPC removal in NER deficient cells, but not NER proficient cells, is donor dependent. This finding raises the fundamental question of how cells determine which repair pathway, e.g., HR or NER, is recruited to repair a DPC lesion. On the one hand, the context in which a particular lesion is detected may dictate the outcome. For example, DPC lesions encountered at the replication fork are likely to be subjected to HR-mediated repair [63, 64], whereas lesions detected during transcription are likely to be targeted for

transcription-coupled NER [77, 92]. However, the repair substrate utilized in the experiments depicted in Figure 1 is subject to neither replication nor transcription. The observation that this one substrate can be repaired *via* either mechanism led me to ask whether examining early repair intermediates could provide insight into the decision-making process.

The repair assay described above is unsuitable to address this question, because it only detects the fully repaired product. I therefore employed a KCl/SDS technique [171] which selectively precipitates protein-crosslinked DNA, to examine removal as the DPC substrate undergoes either recombination or NER-mediated repair. In this way I was able to quantitatively assess the extent to which the cross- linked OGG1 protein has been removed from the M13 molecule (See **Figure 2.2A**). Briefly, low molecular weight DNA recovered from transfected cells is digested with *Hha* I restriction endonuclease and subsequently subjected to KCl/SDS precipitation. The supernatant material is then subjected to parallel qPCR analyses using, in one instance, a primer pair specific for a restriction fragment (denoted 'b' in Figure 2A) that includes the protein crosslink site, and a second primer pair specific for a restriction fragment (denoted as 'c' in Figure 2A) from a different region of M13. The cycle thresholds (Ct) of these respective qPCRs can be used to calculate the relative abundance of these two restriction fragments, which can, in turn, be used to calculate the percentage of recovered molecules from which the DPC has been removed, which I depict as '% Removal' (see methods section for details). Based on the results presented in Figure 1**,** I predicted that DPC removal in NER proficient cells would occur in the absence of homologous donor, whereas removal of the

crosslinked protein in NER-deficient clones would require the presence of a homologous donor. To test this hypothesis, DPCs were transfected in the presence or absence of homologous donor into XPD cells, as well as into a gene-corrected derivative of this line (GM15877, referred to hereafter as XPDC), and a second NER-proficient cell line, HEK293T. Low molecular weight DNA was recovered one-hour post-transfection, and DPC removal was quantified as described above. The results presented in **Figure 2.2B** show that DPCs transfected into NER proficient cells were removed efficiently in both the presence and absence of a homologous donor. In contrast, DPC removal in the XPD cells co-transfected with the heterologous donor were significantly lower than those observed in XPDC and HEK cells. In contrast, co-transfection of homologous donor with the DPC substrate led to protein removal at levels indistinguishable from those observed in the NER-proficient cells.

Ubiquitination is required for efficient DPC removal in both NER and HR pathways. It has been shown that xenobiotic induced chromosomal DPCs are subject to ubiquitin conjugation shortly following their formation [66, 137, 138]. To examine the role of ubiquitination in removal of M13-crosslinked OGG1 protein I used the IP-qPCR assay outlined in **Figure 2.3A**. This assay resembles the KCl/SDS-qPCR assay in that the assay is initiated by restriction endonuclease digestion of low molecular weight DNA recovered from cells transfected with the DPC substrate.

However, rather than using KCl/SDS based precipitation to deplete DPC containing fragments, an anti-ubiquitin antibody is used to selectively *enrich* for ubiquitinated DPC-containing fragments. Immuno-affinity purified material is recovered

from protein G beads by digestion with proteinase K and qPCR amplification is performed using the same primer pairs depicted in figure 1 (see in the methods section for details). The antibody-based capture results in selective enrichment of ubiquitin-conjugated material, and subsequent qPCR analysis allows for the quantitative detection of recovered DNA. In these experiments, data are expressed as 'Fold Enrichment', which indicates the relative abundance of the DPC-containing fragment compared to the control fragment. I used this assay to measure DPC ubiquitination levels under conditions when the substrate is subject to primarily NER-mediated repair (when DPC substrate is transfected into HEK293T or XPDC cells in the absence of homologous donor) or HR-mediated repair (when substrate is transfected into XPD cells in the presence of homologous donor DNA). The results presented in **Figure 2.3B** indicate that DNA-crosslinked OGG1 becomes ubiquitinated following transfection into NER-proficient cells in both the presence and absence of homologous donor. In contrast, in the NER-deficient XPD cells, substantial levels of OGG1 ubiquitination were only observed when an undamaged homologous donor molecule was present. The observation that DPC ubiquitination only occurred in the cellular conditions that facilitated DPC repair was striking, and consistent with the interpretation that DPC ubiquitination is an intermediate step in DPC removal/repair.

As OGG1 has been shown to be targeted for ubiquitination by NEDD4L, a HECT domain containing E3 ligase [172], I predicted that a pharmacological inhibitor of HECT domain containing E3 ligases (Heclin) would impair DPC ubiquitination. To test this hypothesis, DPCs were transfected into HEK293T cells in the absence of

homologous donor (to monitor NER mediated ubiquitination) or into XPD cells in the presence of homologous donor (to monitor HR mediated ubiquitination). Prior to transfection, HEK293T or XPD cells were pretreated for one hour with 0 uM or 50 uM Heclin. One hour following transfection, low molecular weight DNA was recovered from transfected cells and subjected to anti-ubiquitin IP-qPCR. As seen in **Figure 2.4A**, pretreatment with Heclin resulted in complete loss of NER mediated DPC ubiquitination, but had no effect on HR-mediated ubiquitination, suggesting that the E3 ubiquitin ligase employed by the cell to catalyze DPC ubiquitination varies in NER mediated and HR mediated DPC ubiquitination.

To block DPC ubiquitination, irrespective of whether the DPC has been shuttled into an NER or HR mediated repair pathway, I expressed and purified a recombinant OGG1 mutant that contains a lysine to arginine polymorphism at lysine 341 (K341). This residue was chosen for modification because it has been shown that variation of this residue suppressed OGG1 ubiquitination *in vitro* [172]. Utilizing this strategy (i.e., blocking DPC ubiquitination by K-R substitution of a known ubiquitination site on the crosslinked protein) rather than using a pharmacological inhibitor of ubiquitination would allow us to directly query the role of *ubiquitination of the DNA-crosslinked protein,* and not of global cellular ubiquitination, in DPC repair. DPC substrates comprised of either unmodified (K341) OGG1 or modified (R341) OGG1 were transfected into HEK293T cells in the absence of homologous donor (to monitor NER-mediated DPC repair), or into XPD cells in the presence of homologous donor (to monitor HR-mediated DPC repair), and low molecular weight DNA recovered one hour later. This material was subjected to

anti-ubiquitin IP-qPCR, and as shown in **Figure 2.4B**, this substrate level modification resulted in a two-fold decrease in both NER-mediated and HR-mediated DPC ubiquitination. To then test the hypothesis that DPC ubiquitination was required for DPC removal, the transfection experiment was repeated, but rather than IP-qPCR, the recovered material was subjected to KCl-SDS-qPCR to examine the effect of DPC ubiquitination on DPC removal. As depicted in **Figure 2.4C**, during NER-mediated repair, the R341 version of OGG1 was significantly less well removed (20% removal) than was the native, K341, OGG1 protein (45% removal). Similarly, during HR-mediated repair R341 protein variant was less efficiently removed than K341 (20% and 40% removal, respectively) one-hour post-transfection into XPD cells in the presence of homologous donor, indicating that DPC removal by both NER and HR is at least partially dependent on ubiquitination of the DNA-crosslinked protein.

DPC removal by NER, but not HR, is proteasome dependent. The results presented in Figure 2.4 suggest that ubiquitination may trigger proteasomal degradation of DNA-crosslinked OGG1 as part of the repair mechanism. The available evidence suggests that the NER machinery is only capable of repairing DPC comprised of relatively small peptides or proteins, however no such limitation has been associated with HR-mediated DPC (see Introduction). I therefore predicted that pre-treatment with the proteasome inhibitor MG132 [142] would differentially impact DPC removal, dependent on which repair pathway was responsible for the repair. To test this hypothesis cells were pre-treated for one hour in the presence or absence of MG132 prior to transfection. As depicted in **Figure 2.5**, DPC removal mediated *via* NER (DPC transfected into XPDC

cells with heterologous donor) was decreased two-fold in MG132-treated cells relative to non-treated cells. In contrast, during HR-mediated repair (DPC transfected into XPD cells with homologous donor) proteasome inhibition had no effect on the efficiency of DPC removal.

DPCs are differentially polyubiquitinated in NER vs HR repair backgrounds. In addition to triggering proteasomal degradation, ubiquitination can serve as a signal for several additional fates. While post-translational modification of proteins with a single ubiquitin protein (monoubiquitin) is known to serve several signaling purposes in cells including protein sorting and trafficking [142, 173, 174], ubiquitin can also be conjugated through one of its seven lysine residues to form polyubiquitin chains [139]. Interestingly, it has been previously shown that topoisomerase-1 and topoisomerase-2 DPCs formed following treatment of mammalian cells with camptothecin or etoposide are modified with these chains [66]. K48-linked polyubiquitin chains trigger proteasomal degradation of cellular proteins [140], while K63-linked polyubiquitin chains trigger a variety of processes, including the recruitment of DNA damage response proteins [141, 175]. Therefore, I predicted that during NER repair, DPCs would undergo K48-linked polyubiquitination, and that in contrast, during recombinational repair DPCs would undergo K63-linked polyubiquitination. To test this hypothesis, DPCs were transfected into NER-deficient or proficient cells and low molecular weight DNA recovered one-hour post-transfection. Following recovery, DPCs were subjected to anti-K48 or anti-K63 polyubiquitin-specific IP-qPCR. As **Figure 2.6A** illustrates, during NER-mediated repair the DNA-crosslinked OGG1 protein is subject to both K48 and K63 polyubiquitination.

In contrast, when the DPC substrate was introduced into XPD cells in the presence of a homologous donor molecule neither K48 nor K63 polyubiquitination was detected **(Figure 2.6B)**. Interestingly, replacement of the homologous donor with a heterologous molecule resulted in robust levels of K63 polyubiquitination (Figure 5B). Notably, in this latter instance, I still failed to detect K48 polyubiquitination of the DNA-crosslinked OGG1 protein.

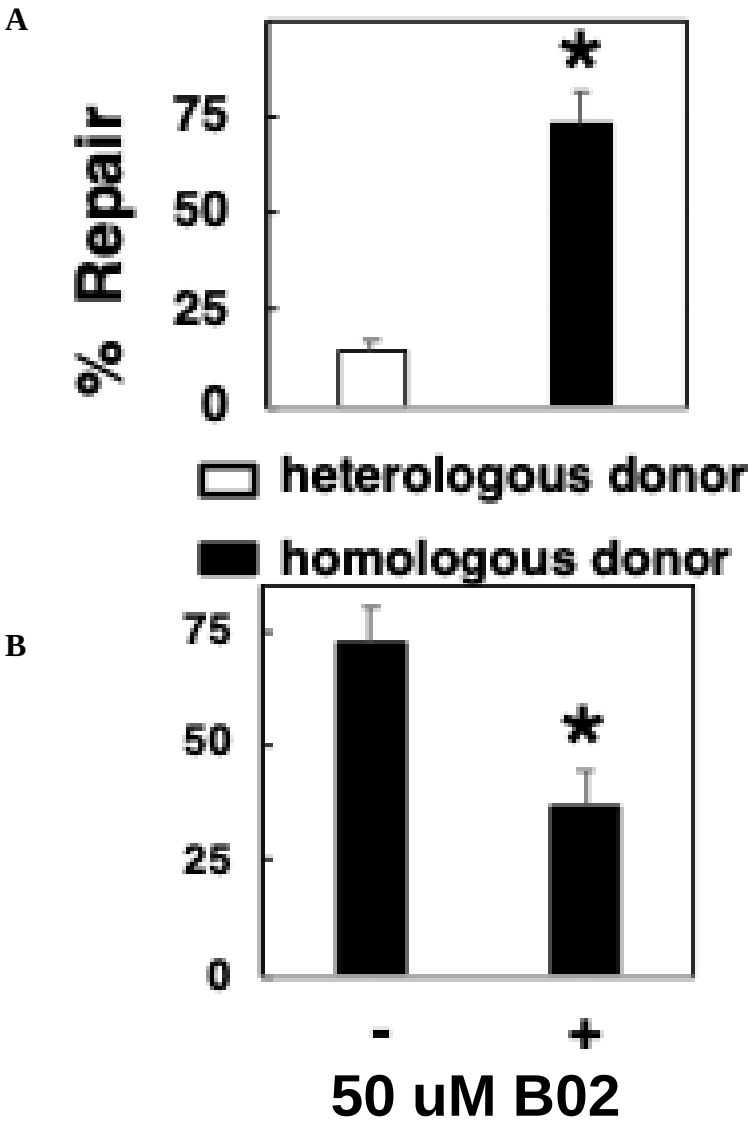

Figure 2.1 DPCs are subject to repair by HR (A) DPCs were transfected into NER deficient cells (XPD), in the presence of a heterologous or homologous donor molecule. Low molecular weight DNA was recovered three-hours post-transfection and subjected to the SSPE-qPCR repair assay. *; P=0.01. (B) DPCs were transfected into untreated (-) or B02 pre-treated (+) XPD cells. Low molecular weight DNA was recovered 3 hours following transfection and subjected to the SSPE-qPCR repair assay. *; P=0.04

- LC was responsible for performing SSPEqPCR assays.

A

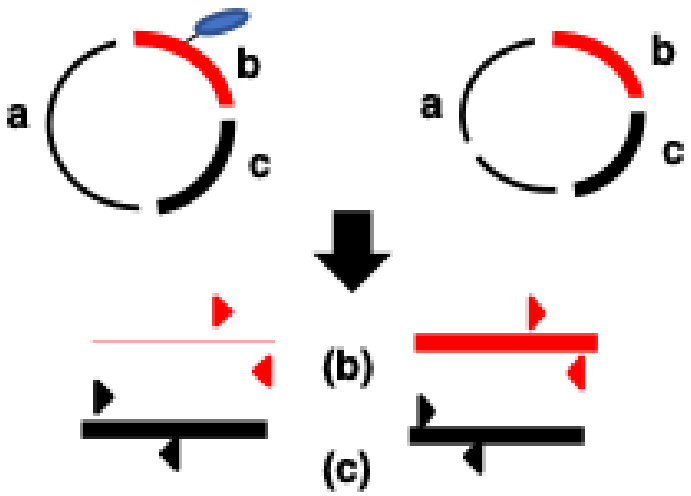

B

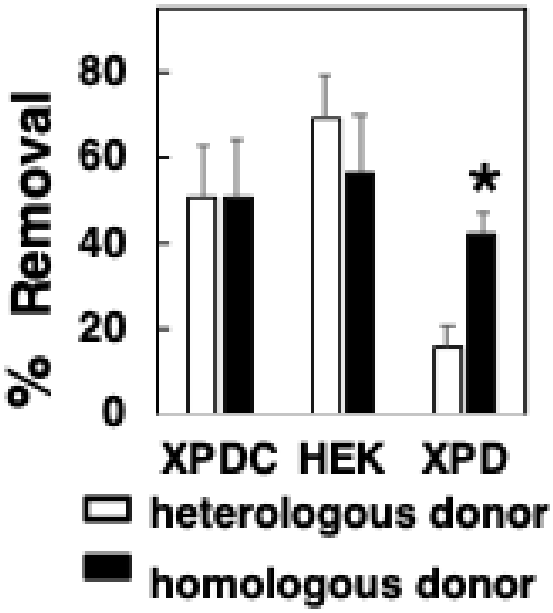

Figure 2.2 Removal of DNA-linked protein during DPC repair *via* NER and HR. (A) Schematic of KCl-SDS-qPCR assay. See *Methods* for details. (B) DPCs were transfected into XPDC, HEK293T or XPD cells, in the presence of a heterologous or homologous donor plasmid. DPCs were recovered one- hour post-transfection and subjected to KCl-SDS-qPCR. *; P=0.003

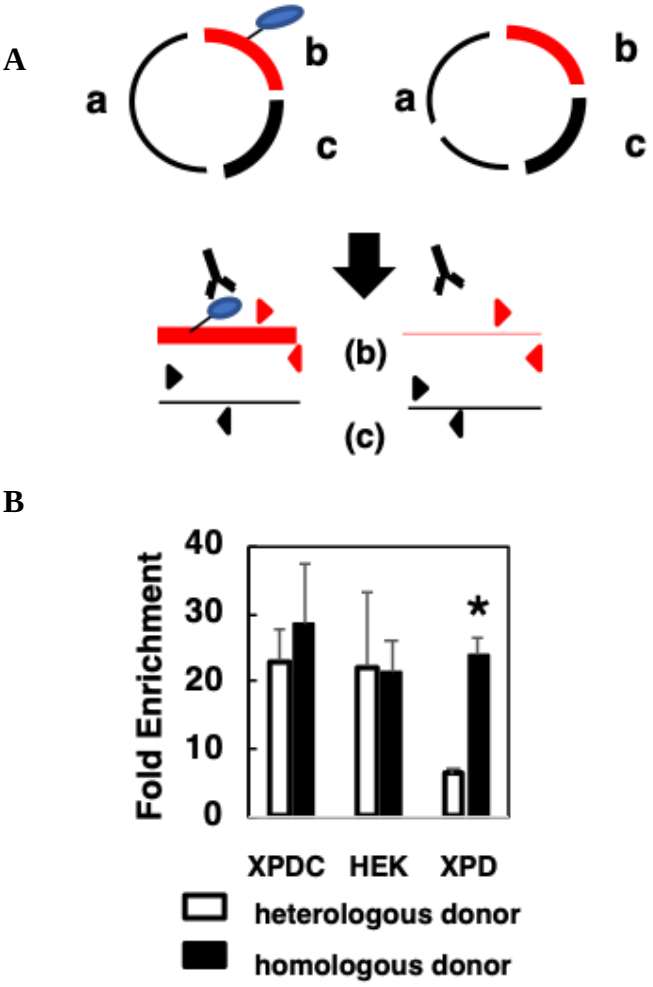

Figure 2.3 DPCs are ubiquitinated in NER and HR-mediated repair. (A) Schematic of anti-ubiquitin IP-qPCR; see *Methods* for details. (B) DPCs were transfected into cells proficient for NER (XPDC, HEK) or deficient for NER (XPD). Low molecular weight DNA was recovered from cells one-hour post transfection and subjected to anti-ubiquitin IP-qPCR. Results depict fold-enrichment, *; P= 0.01. (C) DPC substrates produced by crosslinking the wild-type OGG1 protein (K341) or arginine for lysine-substituted version (R341) were transfected into HEK293T cells in the absence of homologous donor (NER) or transfected into XPD cells in the presence of homologous donor (HR) cells and recovered 1 hour following transfection. DPCs were then subjected to KCl-SDS-qPCR, as described above, to determine the percentage of crosslinked protein removed (% Removal), *; P= 0.05.

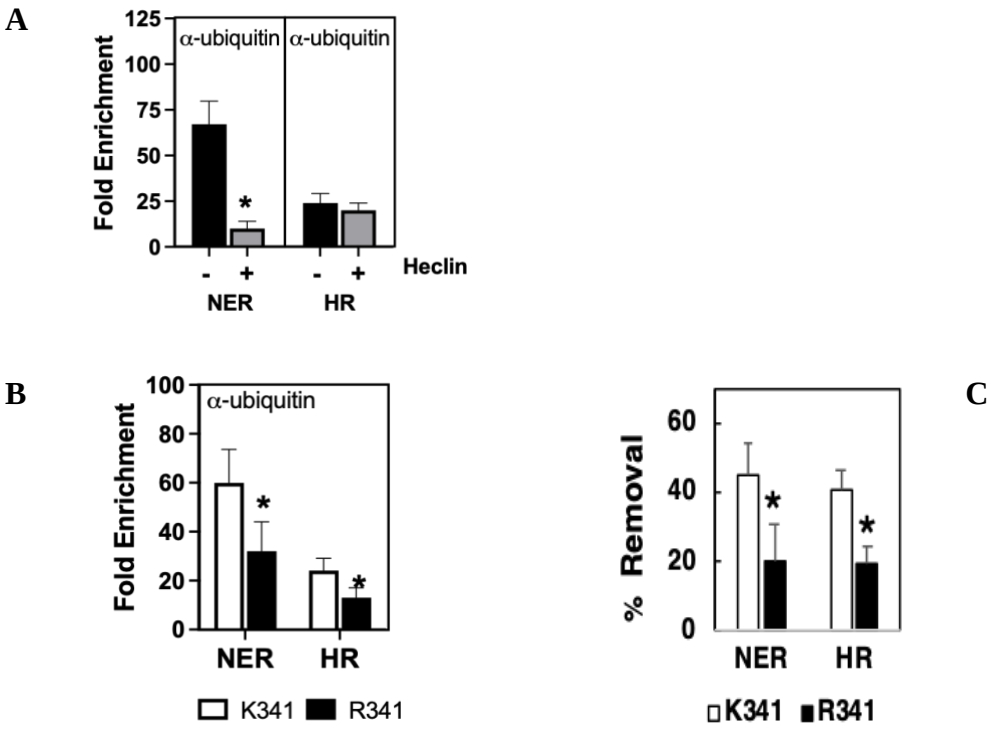

Figure 2.4 Requirements for NER and HR mediated OGG1-DPC ubiquitination

(A) DPCs were transfected into cells proficient for NER in the absence of homologous donor or deficient for NER in the presence of homologous donor (XPD) following pretreatment with 0 uM Heclin (-) or 50 uM Heclin (+). Low molecular weight DNA was recovered from cells one-hour post transfection and subjected to anti-ubiquitin IP-qPCR. *; P= 0.05. (B) K341 or R341 DPCs were transfected into HEK293T cells in the absence of homologous donor (NER) or transfected into XPD cells in the presence of homologous donor (HR) cells and recovered 1 hour following transfection. DPCs were then subjected to anti-ubiquitin IP-qPCR, as described above, to determine the percentage of crosslinked protein removed (Fold Enrichment), *; $P \leq 0.05$. . (C) K341 or R341 DPCs were transfected into HEK293T cells in the absence of homologous donor (NER) or transfected into XPD cells in the presence of homologous donor (HR) cells and recovered 1 hour following transfection. DPCs were then subjected to KCl-SDS-qPCR, as described above, to determine the percentage of crosslinked protein removed (% Removal), *; $P \leq 0.05$.

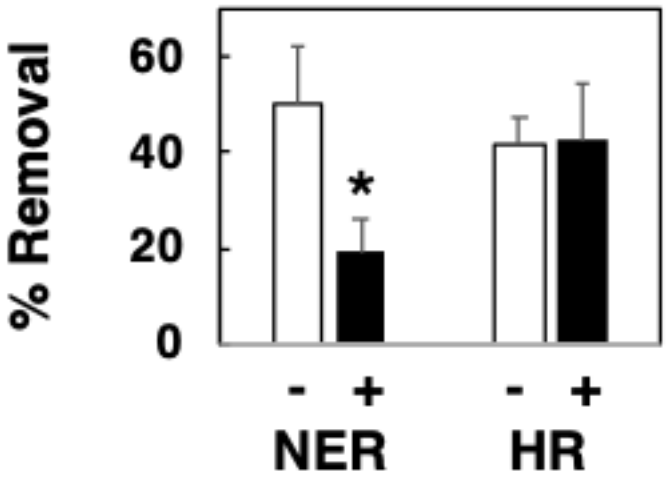

Figure 2.5 Effect of proteasome inhibition on DPC removal mediated *via* NER and HR. NER-mediated removal was measured by transfecting DPC substrate into XPDC cells in the absence of a homologous donor, and HR-mediated removal was measured by transfecting DPC substrate into XPD cells in the presence of a homologous donor. Transfections were performed on cells that had been pre-treated for one-hour in the absence (-, white bars) or presence (+, black bars) of 10 uM MG132. Low molecular weight DNA was recovered one-hour post-transfection, subjected to KCl-SDS-qPCR and % removal of DPC determined as described in the legend to Figure 2. *; P =0.02

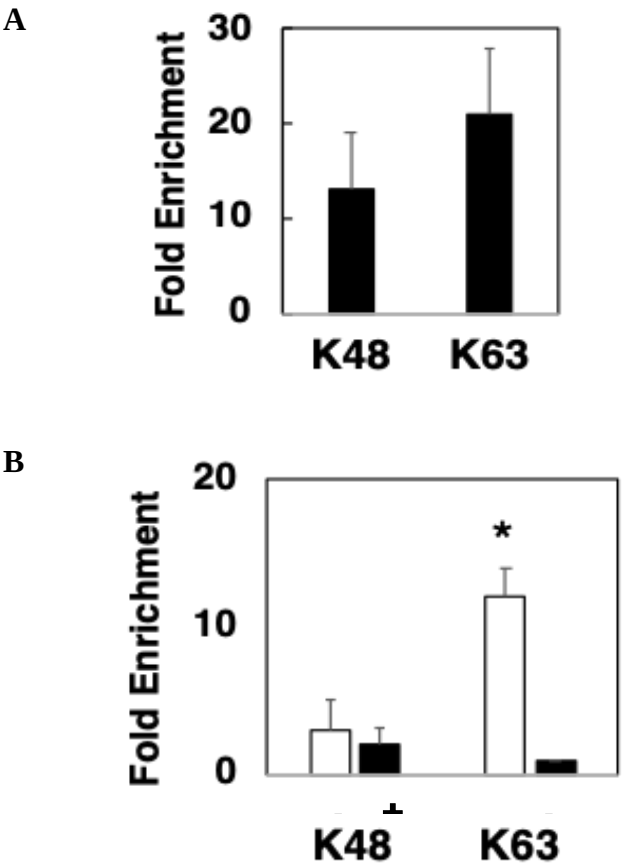

Figure 2.6 Differential polyubiquitination patterns during NER and HR mediated repair. (A) DPCs were transfected into NER-proficient HEK293T cells and low molecular weight DNA recovered one-hour post-transfection, then subjected to IP-qPCR using anti-K48 or K63 polyubiquitin -selective antibodies. (B) DPCs were transfected into NER-deficient XPD cells along with a non-homologous (-, white bars) or homologous (+, black bars) undamaged donor molecule and IP-qPCR performed as described above.

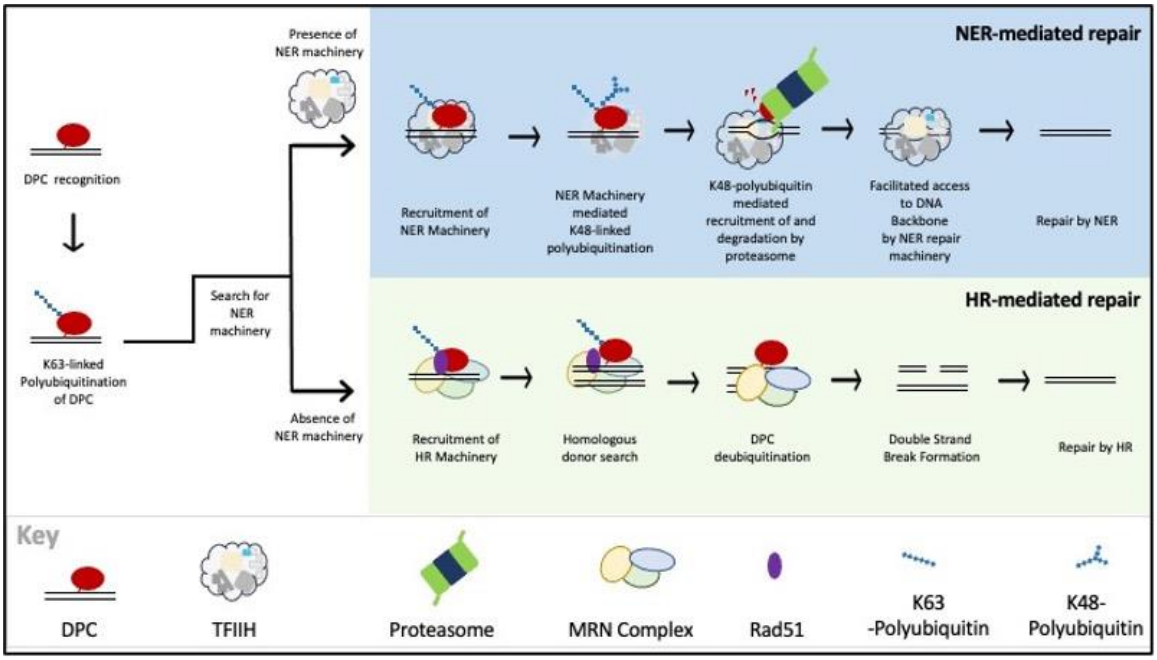

Figure 2.7 Proposed model of DPC ubiquitination and repair. Following recognition of a DPC lesion by NER machinery, DPCs are modified with K48- linked polyubiquitin chains. K48-polyubiquitination of DPC triggers proteasomal recruitment to and degradation of the crosslinked protein, eliminating steric hindrance by the DPC and allowing access to the DNA backbone by NER machinery. In the absence of NER machinery, DPCs are K63-polyubiquitinated. HR machinery are recruited to K63-polyubiquitinated DPCs and initiate a homologous donor search resulting in nucleolytic DPC repair by HR.

III. DISCUSSION

Cells utilize both NER and HR to repair DPCs, however considerable uncertainty exists regarding how one or the other pathway is selected to target individual lesions. To address this issue, I used a simplified system in which a model DPC molecule is transfected into human cells, recovered, and subjected to analysis. I show that while the substrate can be efficiently repaired by either pathway, manipulation of the system can dramatically influence the mechanism though which DPC repair occurs. In this way, I identified repair pathway-selective covalent modifications to the DNA-crosslinked protein. Our results lead me to propose a model (depicted in **Figure 2.7**) that summarizes these findings, presenting a framework for how the cell determines the repair fate of a DPC.

In our model, initial DPC recognition leads to ubiquitination of the DNA-crosslinked protein. This initial ubiquitination, which includes a K63 polyubiquitin chain, is an essential step, since converting one of the key residues involved (lysine 341) to an arginine dramatically reduces the efficiency of both NER and recombinational repair. This finding builds on previous reports showing that pharmacological inhibition of cellular ubiquitination impairs xenobiotic-induced DPC repair [134, 176-179], and demonstrates that the DNA-crosslinked protein must be ubiquitin-modified to ensure efficient removal.

The model proposes that K63 polyubiquitin chain leads to recruitment of additional cellular factors that result in subsequent K48 polyubiquitination of the DNA-crosslinked protein. The absence of this latter process in NER-deficient XPD cells led us to propose a role for the TFIIH complex, a multiprotein complex that facilitates the opening of DNA around an NER substrate via an XPD and XPB-dependent mechanism [93, 94]. It is conceivable that p44, one of the 5 non-helicase subunits of TFIIH acts as an E3 ubiquitin ligase for DPCs [93, 94]. Although no E3 ubiquitin ligase activity is currently attributed to p44, analyses of Ssl1, the yeast homolog of p44, have shown that it possesses E3 ligase activity [180].

Addition of the K48 polyubiquitin chain is postulated to recruit the proteasome, leading to proteolytic processing, converting the DPC to a DNA-crosslinked peptide that is subsequently repaired by the cellular NER machinery. This feature of the model is consistent with reports that repair of xenobiotic-induced chromosomal DPCs and DPCs generated in vitro are proteasome-dependent, and that only DPCs <10-14 kDa are amenable to repair by NER [78, 80]. The relatively large size of the DNA-crosslinked OGG1 (~37 kDa) is proposed to sterically hinder initiation of NER by incision of the DNA around the damage site, necessitating lesion pre-processing by the proteasome.

In NER-deficient cells where no undamaged homologous donor is present, the DPC recognition/processing steps stall at the stage of initial K63 linked polyubiquitin-modified protein. However, in the presence of a homologous donor, the DNA-crosslinked protein

is removed, and the lesion is subsequently repaired in a proteasome-independent process. I propose that during recombinational repair nucleolytic processing at the DPC site results in the creation of a DNA double strand break [75, 181]. It is conceivable that pre-processing by a protease such as SPRTN [118] is required. However, Desphande *et al.*, demonstrated that addition of purified recombinant MRN complex to a DNA-crosslinked protein substrate (generated by binding streptavidin to a biotin-labelled oligonucleotide) led to protein removal via sequential endonuclease and exonuclease processing [181]. Our model therefore proposes that DPCs that are tagged with a K63-polyubiquitin chain–but which lack the K48 chain recruit elements of the cellular recombinational repair machinery. These findings are consistent with literature reports that K63-linked polyubiquitin chains are key to the recruitment of HR machinery to DSBs [135, 182, 183].

Interestingly, our results indicate that the DPC lesion processing in NER-deficient clones stalls at a step prior to removal of the DNA-crosslinked protein–and that this block is relieved only when a homologous donor is present. Since it appears that DPC removal is mediated by nucleolytic cleavage and creation of a DNA double-strand break, it seems likely that the purpose of the blockade is to ensure that the potentially mutagenic and cytotoxic DNA double strand break is only created in a context where a homologous donor and the HR machinery have already been co-localized at the site of the DPC lesion.

The results described herein, coupled with the model presented in Figure 6 provide a potential explanation for how cells hierarchically orchestrate DPC repair. It is important to note that this model of DPC repair is likely to be relevant to lesions in loci that are not currently undergoing active replication or transcription. I hypothesize that specialized sub-pathways of DPC repair are likely to be involved in the processing of lesions detected under these circumstances. The model proposes that under these conditions, NER is the 'default' mechanism for DPC repair and that a multi-subunit complex, minimally comprised of TFIIH, is recruited to lesions following their initial recognition and 'tagging' with a K63 polyubiquitin chain. Whereas the subsequent K48 polyubiquitination 'commits' the lesion to a NER-mediated repair fate, our model proposes that lesions that retain the K63 polyubiquitin chain but lack the K48 chain are instead recognized by a different complex, that leads to subsequent formation of a DNA double-strand break formation and RAD51-dependent recombinational repair.

IV. MATERIALS AND METHODS

Chemicals and enzymes. 8-oxo-2′-deoxyguanosine (8-oxo-dG) containing oligonucleotides were purchased from Midland Certified Reagent (Midland, TX). All other oligonucleotides were purchased from the University of Minnesota Genomic Center. Human Oxoguanine glycosylase 1 (OGG1) was expressed and purified from BL21(DE3) competent E. coli using a pET-28a expression vector. OGG1 K341R mutant was generated by restriction cloning of the OGG1 K341R cDNA sequence to replace the wildtype OGG1 cDNA sequence in this pET-28a expression vector. OGG1 K341R was then expressed and purified from BL21-Gold (DE3) competent cells. Rabbit monoclonal anti-ubiquitin antibody was purchased from Abcam (Cat. #: ab134953, Lot #: GR3367020-2). 0.7 ug antibody was used in each ubiquitin pulldown. Rabbit polyclonal K48 linkage specific polyubiquitin antibody was purchased from Cell Signaling (Cat. #: 4289S, Lot #: 2). 1 ug antibody was used in each K48 linkage specific polyubiquitin pulldown. Mouse monoclonal K63 linkage specific polyubiquitin antibody was purchased from Biolegend (Cat. #: 932201, Lot #: B319879) 1 uL antibody was used in each K63 linkage specific polyubiquitin pulldown. Protein G beads were purchased from Invitrogen (Cat. #: 10003D), 5 uL beads were used for each IP. MG132 was purchased from Abcam (Cat. #: ab14707, Lot #: APN17146-2-1-S).

ODN	Sequence (5′→3′)	Use
M13-8oxo	AGCCACCCCTCACCCACTA(8-oxo-dG)GAT	Primer Extension
EcoRI-8oxo	CCGGGTACCGAGCTC(8-oxo-dG)AATTCGTAATCTTGGTCATAGCTG	Primer Extension
Fragment b L	CACCCCAGGCTTTACACTT	qPCR of M13
Fragment b R	GTAAAACGACGGCCAGTG	qPCR of M13
Fragment c L	CTGGGTGCAAAATAGCAACT	qPCR of M13
Fragment c R	CCCAATAGCAAGCAAATCA	qPCR of M13
DPC F	GCTGCAAGGCGATTAAGT	SSPEqPCR of M13 Plasmid
DPC R	CGGCTCGTATGTTGTGTG	SSPEqPCR of M13 Plasmid

Table 2.1 Oligonucleotides (ODNs) used in this study

Cell lines. HEK293T cells were purchased from the American Type Culture Collection (ATCC) and cultured in Dulbecco's modified eagle medium (DMEM) supplemented with 9% fetal bovine serum (FBS). The XPD cell line is an immortalized dermal fibroblast cell line with a primary defect in the XPD gene, first isolated from a patient with complementation group D xeroderma pigmentosum. The XPD-C cell line is the gene-corrected derivative of the XPD cell line. Both cell lines (GM08207 and GM15877, respectively) were purchased from the Coriell institute and cultured in DMEM supplemented with 9% FBS.

Construction of plasmid DNA repair substrates. Synthetic, 8-oxo-dG containing oligodeoxynucleotide (100 pmol) (M13-8oxo, or EcoRI-8oxo, Table 1.1) was phosphorylated with T4 PNK (40 units) in 1X DNA Ligase buffer for 30 minutes at 37°C. Phosphorylated oligonucleotide was then annealed to single-stranded M13 viral DNA (13.4 pmol) and extended with Taq polymerase (100 units), in a solution containing 1X Thermopol Reaction Buffer, 1X NEB Buffer 2, 10 mM ATP, 1 mM dNTPs, and 20 μg bovine serum albumin and incubated for 15 minutes at 75°C. The sample was cooled on ice, T4 DNA Polymerase (60 units) and T4 DNA Ligase (8000 units) were added, and the sample was incubated at 37°C overnight for complete extension and ligation of the new double stranded M13 DNA containing an 8-oxo-dG residue. Following overnight incubation, 8-oxo-dG containing DNA was purified by phenol-chloroform extraction and ethanol precipitation. To make plasmid DPC, 8-

oxodG containing M13 DNA was crosslinked to OGG1 in 200X or 250X protein: DNA molar excess (for crosslinking of recombinant wild type OGG1, or recombinant OGG1 K341R, respectively) in buffer containing 100 mM NaCl, 1 mM MgCl2, 20 mM Tris-HCl pH 7.0, and 10 mM sodium cyanoborohydride. Sodium cyanoborohydride stock solution was made fresh, and added immediately before OGG1, which was added last to the reaction mixture. Crosslinking was carried out at 37°C for 1 hour. During the crosslinking reaction, lysine residue 249 of OGG1 nucleophilically attacks C1, the attachment site of the deoxyribose sugar in the DNA backbone to 8-oxo-dG. This attack causes removal of 8-oxo-dG and the creation of an apurinic site in the DNA. The presence of sodium cyanoborohydride in the reaction causes the reduction of the Schiff base intermediate formed by OGG1 during this reaction, covalently trapping OGG1 to C1 of the deoxyribose.

Transfection of DPC into cells. 16 hours before transfection, cells were counted and plated into 6-well plates at a density of 600,000 cells per well. In the case of drug pretreatment, culture media was removed from the well by gentle aspiration and replaced with 4 mL serum-free media (SFM) +/- drug. MG132 was used at 10 uM concentration for one hour prior to transfection. BO2 was used at 5 uM concentration for 1 hour prior to transfection. Following drug pretreatment, drug containing media was removed by gentle aspiration and replaced with DMEM containing 9% FBS. For DPC transfection, 1 ug of plasmid DPC was added to each well in combination with lipofectamine, following manufacturer instructions. Plates were incubated at 37° C.

30 minutes following the beginning of transfection, media and lipofection mixture were removed from the well by gentle aspiration and replaced with 4 mL DMEM supplemented with 9% FBS, and plates resumed incubation at 37° C until cell collection at predetermined time points. At these time points, cells were lysed, and transfected DNA was collected by a modified HIRT procedure. Briefly, in each well, media was removed by gentle aspiration and replaced with 1 mL of lysis buffer containing 0.6% SDS and 0.01 M EDTA. Plates were incubated for 10 minutes at room temperature, then cells were scraped by rubber policeman and transferred into a 1.5 mL Eppendorf tube. NaCl was added to a final concentration of 1M, tubes were closed and inverted sharply 10 times, and incubated at 4° C overnight. The next day, tubes were spun in a tabletop centrifuge at 21,000 X G at 4° C for 30 minutes. Pellets were discarded and DNA was collected from supernatant by ethanol precipitation.

Immunoprecipitation and PCR analysis. DNA recovered from transfected cells by HIRT procedure was digested with 40 units *Hha* I at 37° C for 1 hour. Following *Hha* I restriction digest, samples were mixed with 200 uL IP Buffer (25 mM Tris-HCl pH 8.0, 150 mM NaCl, 1 mM EDTA, 1 % NP-40, 2.5 % (w/w) BSA 250 pmol of recombinant OGG1). 40 uL of this mixture was removed and saved as “input control”. To the remaining 200 uL, antibody for pulldown was added, and samples were placed on a tube inverter at 4° C for 3 hours. For each antibody pulldown, 5 uL of protein G Magnetic beads were incubated with 200 uL Blocking Buffer (25 mM Tris-HCl, pH 8.0, 150 mM NaCl, 1 mM EDTA, 1 % NP-40, 5 % (w/w) BSA, 250

pmol recombinant OGG1), and inverted at 4° C for 3hours. Following 3-hour incubation, protein G solution was combined and incubated with DNA/antibody/IP buffer containing sample at 4° C for 1 hour. To collect protein G bound material, tubes were placed on a magnetic separation rack and protein G beads were washed 3x with Washing Buffer 1 (25 mM Tris-HCl, pH 8.0, 150 mM NaCl, 1 mM EDTA, 1 % NP-40 and 2.5 % (w/w) BSA), 2X with Washing Buffer 2 (25 mM Tris-HCl, pH 8.0, 150 mM NaCl, 1 mM EDTA), and 2X with 1X TE buffer. DNA was recovered from beads by incubation with Proteinase K (8 units) in Proteinase K Buffer (10 mM Tris-HCl, pH 8.0, 1 mM EDTA, 0.5 % SDS), for 1 hour at 37° C, and finally by QIAquick PCR purification kit (following manufacturer protocol). 1 uL of PCR purified DNA was then added to 27 uL DI H2O, 30 uL 2X SYBR Green Master Mix, and 100 pmoles of each primer. (DNA was amplified by two different primer sets in parallel: for detection of DPC containing fragment, primer pair Fragment b L and Fragment b R (Table 1.1) were used, and for detection of control fragment, primer pair Fragment c L and Fragment c R (Table 1.1) were used. All samples were loaded in duplicate onto a 96 well plate and Real time PCR was performed using the Applied Biosystems StepOnePlus Real Time PCR System under the following conditions: 10 min denaturing at 95° C (1X), then 30 seconds denaturing at 95° C, 30 seconds primer annealing at 57° C, and 30 seconds for Taq polymerase extension at 72° C (40X).

KCl-SDS precipitation. Following *Hha* I restriction digest, SDS was added at a final concentration of 0.5% to DNA recovered from transfected cells, then the samples were heated at 65° C for 10 minutes. KCl was then added to 100 mM final

concentration, and tubes were chilled on ice for 5 minutes. Next, tubes were centrifuged at 21,000 X G, for 5 minutes at 4°C. Supernatants were carefully transferred to another tube using a gel loading pipette tip, and centrifugation was repeated. Supernatants were again transferred to a new tube using a gel loading pipette tip, diluted, and analyzed by qPCR, under the same primer and amplification conditions used for qPCR analysis of IP samples.

SSPE-qPCR. DNA recovered from transfected cells by HIRT prep then subjected to SSPE-qPCR as described previously. Briefly, DNA was added to 22.5 uL DI H2O, 30 uL 2X SYBR Green Master Mix, and 100 pmoles DPC F primer (Table 1.1) into each of two tubes. One tube was placed on ice while the other tube was subjected to 8 rounds of strand specific PCR (utilizing 100 pmoles of DPC F primer). Next, 100 pmoles DPC R primer (Table 1.1) was added to the tube that underwent the 8 rounds of strand specific PCR, and to the tube that was incubated on ice. All samples were then loaded in duplicate onto a 96 well plate and Real time PCR was performed using the Applied Biosystems StepOnePlus Real Time PCR System under the following conditions: 10 min denaturing at 95° C (1X), then 30 seconds denaturing at 95° C, 30 seconds primer annealing and Taq polymerase extension at 60° C (30X). Cycle Threshold (Ct) values were determined by Applied Biosystem StepOnePlus Software. Delta Cts were determined by subtracting the Ct of the sample that underwent 8 cycles of Strand Specific PCR from the Ct of the same sample that, in parallel, did not undergo 8 cycles of Strand Specific PCR. Percent undamaged DNA was calculated

by using the formula (Percent undamaged = 2^Delta Ct/2^3*100) and percent repair was calculated using the formula [Percent Repair = (Percent Undamaged Tx) - (Percent Undamaged To)].

Chapter 3

Cell-based and cell-free systems can be used to investigate the role of post-translational modifications in promoting DNA-protein crosslink repair

I. INTRODUCTION

Several therapeutic agents are used to generate DPCs in cells, including 5-aza-dC, formaldehyde, cisplatin, and the topoisomerase I and II inhibitors camptothecin and etoposide [7, 157]. Methods for isolating total genomic DPCs include cellular fractionation, RADAR, phenol-chloroform extraction, and KCl-SDS precipitation [184-187]. Following isolation, DPCs are analyzed using multiple methods, including quantification using DNA-binding dyes and labels and identification of DNA-binding proteins using immunoprecipitation and proteomics [23, 152, 188, 189]. Additionally, colocalization studies of DNA repair machinery with DPC foci are conducted using fluorescent labeling of intact cells followed by microscopy [137, 190]. These studies have provided most of our understanding of DPC repair. However, these methods also have several limitations. First, total genomic DPC isolation is time consuming and technically challenging. Second, following cell treatment with DPC-forming drugs, the kinetics of DPC formation and repair are difficult to distinguish as some DPCs can still be formed after others have been repaired, or spontaneously removed, as is known to occur with formaldehyde-induced DPCs [191]. Third, because of the sheer size of the genome, total genomic DPC isolation does not facilitate the tracking of processing and repair events of individual, site-specific DPCs. As such, separating the signaling and processing events associated with multiple, redundant DPC repair pathways is challenging. Finally, all DNA-damaging drugs that induce the formation of DPCs also cause multiple other types of DNA damage, including double-strand breaks and DNA-DNA crosslinks or exert other forms of cytotoxicity [143, 192, 193]. This presents a challenge when analyzing the

genetic requirements for DPC repair by studying the sensitization of genetic mutants to DPC-forming drugs, as the observed sensitization can be a result of impaired repair of other types of DNA damage caused by these drugs.

Another system used to investigate DPC repair involves the incubation of DPC substrates formed *in vitro* with cell-free extracts [78, 128]. Proteins are chemically trapped onto plasmid molecules or short oligonucleotides, incubated with nuclear or whole-cell extracts, and early repair intermediates quantified and analyzed by gel electrophoresis. Immunoprecipitation analyses are often performed to identify the proteins that are recruited to the DPC following recognition. However, while studies in cell-free systems have provided insights into DPC repair and proteolysis, some limitations remain. One key limitation is that some of the activities that exist in intact cells cannot be recapitulated in cell-free extracts. Therefore, it is reasonable to conclude that some aspects of DPC repair cannot be detected in the cell-free extracts. One exception to this is the *Xenopus laevis* extract system, in which DNA replication can be fully recapitulated; thus, this system is highly effective for studying replication-dependent repair [194]. However, other forms of replication independent DPC repair cannot be investigated using this system. Finally, many DPC repair studies performed in extracts utilize radiolabeled DNA. This has allowed groups such as Baker *et al.,* to visualize changes made to DPC substrates using electromobility shift assays [78]. However, there are some safety concerns associated with this methodology that could be avoided.

To address these concerns, I used several approaches to study DPC recognition and repair. The cell-based approach was first introduced in *Chapter 2* and was used to show that DPC removal by NER and HR is ubiquitin-dependent, and that DPC removal by NER, but not HR, is proteasome-dependent. Furthermore, I showed that differential DPC polyubiquitination selectively triggers NER or HR-mediated repair pathways. These findings allowed me to propose a model of NER and HR-mediated DPC recognition and repair.

Herein, I describe additional investigations that I have conducted to study the role of post-translational modifications and proteolysis in DPC recognition and repair. Additionally, I have developed novel approaches that allow for the study of DPCs that were incubated in intact, purified nuclei or in nuclear protein extracts. Transfecting the same kind of DPC lesion into cell-based, nuclei-based, or extract-based systems will permit for more diverse investigations of the mammalian mechanisms that are mobilized following recognition of a DPC. This will allow for deeper investigations of my previously proposed model.

II. RESULTS

Generation of site-specific model DPC substrates. To continue to test the model described in *Chapter 2,* I developed an additional site-specific, DPC model substrate that can be generated *in vitro* (**Figure 3.1**). The first DPC substrate, designated "DPC 1" in Figure 3.1, was used in the studies described in *Chapter 2* and was generated by crosslinking recombinant oxoguanine glycosylase (OGG1) to an 8-oxoguanine-containing double-stranded M13 molecule. "DPC 2" was generated utilizing identical chemistry to that used to make "DPC 1" (See *Methods),* but rather than trapping OGG1 to a double-stranded, 8-oxoguanine containing M13 molecule, it is instead trapped to an 8-oxoguanine-containing 120mer DNA hairpin, labeled with a 5′ biotin and 3′ dideoxycytidine. Utilizing a smaller DPC substrate permits me to generate 10,000-fold more DPC to use in experiments and including a 5′biotin allows for selective recovery of the DPC from a cellular or protein mixture.

DPC repair systems. To study different aspects of the recognition and repair of the same type of DPC, I used three simplified systems. As mentioned in the *Introduction,* using cell-based or extract-based systems alone results in a limitation in the types of questions that can be asked regarding mechanisms of DPC recognition and repair. To address this problem, I study the DPC substrates depicted in Figure 1 in intact cells (top panel of **Figure 3.2**), isolated cellular organelles (middle panel of Figure 3.2), and nuclear or mitochondrial protein extracts (bottom panel of Figure 3.2). Purified mitochondria and nuclei are biochemically active for several hours following their removal, and thus DPC-containing organelles are incubated for up to 3 hours at 37° C. In

the extract-based system, the DPC substrates are incubated with protein extracts generated from purified mammalian nuclei or mitochondria. Extracts can then be incubated at a range of temperatures between 4° C - 37° C, then heat-inactivated and DPCs affinity purified. I show below that all three repair systems can be used to study different aspects of DPC recognition and repair and describe the use of these systems to perform experiments that continue to test the model of the orchestration of DPC recognition and repair that was first proposed in *Chapter 2*.

K48 and K63 polyubiquitination of OGG1 DPCs occur on lysine 341. I had shown in *Chapter* 2 that following transfection into cells, the unmodified DPC (K341) was modified with K48 and K63 polyubiquitin chains, and that the DPC carrying the R341 polymorphism on OGG1 was less efficiently ubiquitinated and repaired. Following these observations, I predicted that this decrease in repair efficiency was due to a loss of K48 and K63 polyubiquitination at lysine 341. To test this prediction, DPCs were transfected into HEK293T cells in the absence of homologous donor, recovered one hour following transfection and subjected to anti-K48 (**Figure 3.3A)** or anti-K63 (**Figure 3.3B)** polyubiquitin-specific IP-qPCR. Interestingly, the R341 variant was not modified with either K48 or K63 polyubiquitin chains, suggesting that lysine 341 modulates DPC removal by NER or by HR through the formation of poly-ubiquitin chains at that residue. Together, these findings indicate that both K48 and K63 polyubiquitin modifications made to modulate DPC repair occur at the same lysine residue of the crosslinked protein.

SPRTN plays a role in DPC ubiquitination. In Chapter 2, I showed that NER-mediated DPC removal was partially, but not fully impaired by proteasomal inhibition,

which suggests that another DPC protease, like SPRTN [118] could also be involved in DPC removal. However, as SPRTN is known to be a part of the replisome [66] I predicted that SPRTN is not involved in DPC proteolysis. To test this hypothesis, DPCs were transfected into NER proficient mouse embryonic fibroblasts, MEF5 and MEF7. MEF7 cells originated from SPRTN knockout mice that harbored a null SPRTN allele in their germline, generated by Cre-LoxP mediated gene inactivation [195]. Low molecular weight DNA was collected one hour following transfection and subjected to KCl-SDS-qPCR, which showed that SPRTN deficient cells did not exhibit impaired DPC removal (**Figure 3.4A**). Interestingly, *Ruggiano et al.,* showed that SPRTN impaired ubiquitination of DPCs formed following cellular treatment with formaldehyde [138]. To test the hypothesis that SPRTN is involved in modulating DPC ubiquitination, I transfected DPCs into MEF5 and MEF7 cells, in the presence and absence of a one-hour pre-treatment with 10 uM MG132 (pharmacological inhibitor of the 26S subunit of the proteasome). One hour following transfection, low molecular weight DNA was collected and subjected to anti-ubiquitin IP-qPCR. Surprisingly, SPRTN deficiency alone did not affect DPC ubiquitination, and MG132 pretreatment of wildtype cells did not affect DPC ubiquitination (**Figure 3.4B)**. However, MG132 pre-treatment of SPRTN deficient MEF7 cells resulted in decreased DPC ubiquitination.

DPCs are rapidly SUMOylated following their transfection into mammalian cells. As discussed in *Chapter 2*, DPC repair by NER and HR are mediated by DPC ubiquitination, and that differential polyubiquitination modulates DPC repair by either pathway. While K48-linked polyubiquitination only occurs in the presence of NER machinery, K63-

linked polyubiquitination occurs in the presence and absence of NER machinery, suggesting that K63 polyubiquitination of the DPC is a post-translational modification that occurs soon following DPC recognition, irrespective of the presence of DNA repair machinery, leaving the question: What is the mechanism that triggers DPC K63-polyubiquitination? Others have shown that top 1 and top 2 DPC ubiquitination occurs in a SUMO-dependent manner [66]. SUMO1 and SUMO2/3 are two major eukaryotic SUMO paralogs that play fundamental roles in many cellular processes [196]. To test the hypothesis that the ubiquitination of the DPC substrate used in this study occurs in a SUMO-dependent manner, I transfected DPCs into HEK293T cells for one hour and subjected untransfected and transfected DPCs to anti-SUMO1 or anti-SUMO2/3 IP-qPCR . As seen in **Figure 3.5A**, untransfected DPCs were not significantly enriched following pulldown by either antibody, however they showed ~75-fold enrichment following anti-SUMO1 IP-qPCR and 50-fold enrichment following anti-SUMO 2/3 IP-qPCR. To test whether DPC SUMOylation occurs on the same residue as DPC ubiquitination, DPC substrates comprised of either unmodified (K341) OGG1 or modified (R341) OGG1 were transfected into HEK293T cells in the absence of homologous donor and low molecular weight DNA recovered one hour later, then subjected to anti-SUMO1 IP-qPCR. As shown in **Figure 3.5B**, the R341 polymorphism did not affect DPC SUMOylation, suggesting that DPC SUMOylation does not occur on K341. While this does not eliminate the possibility that DPC ubiquitination and SUMOylation co-occur on another lysine residue, this finding shows that the loss of DPC removal observed in R341 (see Figure 2.4C) is not SUMO1-mediated. I next reasoned

that, if DPC SUMOylation is observed in the absence of DNA repair machinery (as observed with K48 polyubiquitination of the DPC, above), it is likely that DPC SUMOylation occurs prior to DPC ubiquitination. To test this hypothesis, DPCs generated by crosslinking K341 (**Figure 3.6A)** or R341 (**Figure 3.6B)** OGG1 onto M13 were transfected into the NER proficient cell line, XPDC or the NER deficient cell line, XPD, in the absence of homologous donor. Low molecular weight DNA was recovered one hour following each transfection, and the subjected to anti-SUMO1 IP-qPCR. Unlike DPC ubiquitination (see *Chapter 2*) DPC SUMOylation was not affected following transfection into NER-deficient cells, suggesting that DPC SUMOylation occurs in the absence of DNA repair machinery, and is likely to occur prior to DPC ubiquitination.

DPC SUMOylation occurs with faster kinetics than DPC ubiquitination. To test the hypothesis that DPC SUMOylation occurs prior to DPC ubiquitination, DPCs were transfected into HEK293T cells in the absence of homologous donor, and recovered 2.5 or 6 hours following transfection. Recovered low molecular weight DNA was recovered and subjected to anti-ubiquitin (**Figure 3.7A**) or anti-SUMO1 IP-qPCR (**Figure 3.7B**). Interestingly, the levels of anti-ubiquitin induced enrichment of the DPC observed at one hour did not substantially differ 2.5 or even 6 hours following transfection. Levels of anti-SUMO1 induced enrichment of the DPC, however, were about 75-fold at one hour, were reduced drastically at 2.5 hours (about 20-fold enrichment) and, by 6 hours, dropped to levels that were indistinguishable from those observed in untransfected DPC samples, showing that DPC SUMOylation does indeed occur with faster kinetics than DPC ubiquitination. These findings demonstrate that DPC SUMOylation is more

transient than DPC ubiquitination, and is consistent with other studies that show that DPC SUMOylation modulates DPC ubiquitination [66].

DPC ubiquitination and SUMOylation are interdependent. I was next interested in testing the hypothesis that DPC ubiquitination was modulated by DPC SUMOylation. I reasoned that, since the R341 OGG1 variant did not impair DPC ubiquitination, a pharmacological inhibitor of SUMOylation could be used to test this hypothesis. I first showed that DPC SUMOylation was inhibited using ML-792, a pharmacological inhibitor of the SUMO Activating Enzyme (SAE) following transfection into HEK293T cells in the absence of homologous donor. As seen in **Figure 3.8A**, pre-treatment with ML-792 resulted in complete abolishment of DPC SUMOylation. To test the hypothesis that DPC SUMOylated modulated DPC ubiquitination, anti-ubiquitin IP-qPCR was performed on DPCs recovered from HEK293T cells that had been pretreated with ML-792 (**Figure 3.8B,** left panel), and it was observed that DPC ubiquitination was also fully abolished in the presence of ML-792, indicating that DPC ubiquitination is SUMO-dependent. I next reasoned that, if DPC SUMOylation modulated DPC ubiquitination, DPC ubiquitination would not modulate DPC SUMOylation. I tested this hypothesis by performing anti-SUMO1 IP-qPCR on DPCs that had been recovered from HEK293T cells that were pretreated with the HECT Domain Containing E3 ligase inhibitor Heclin, which I showed in *Chapter 2* to impair NER mediated DPC ubiquitination. Interestingly, DPC SUMOylation was fully impaired in Heclin-treated cells, indicating that DPC SUMOylation also occurs in a ubiquitin-dependent manner.

SSPEqPCR assay quantifies DPC repair in intact cells and in purified cellular organelles. Our lab has previously shown the utility of the SSPEqPCR assay for the quantification of the repair of the "DPC 1" substrate in various mammalian cell lines, as well as in isolated mammalian mitochondria [77, 82]. I was interested in testing the hypothesis that DPC substrates would be subject to repair in purified nuclei. Validation of this methodology was started by Lisa Chesner, and thus her SSPEqPCR analyses of DPC repair are included in the *Supplemental Figures* portion of this chapter. Briefly, 8-oxoguanine containing M13 (8-oxo-dG) or M13 that has been crosslinked to OGG1 (DPC 1) was electroporated into nuclei isolated from V79 cells or mitochondria isolated from HEK293T cells, recovered 2 hours following electroporation, and then subjected to analysis by SSPEqPCR. As 8-oxoguanine is not a Taq polymerase blocking lesion, 8-oxoguanine repair was measured by first treating recovered plasmids with an excess of OGG1 (to remove any unrepaired 8-oxoguanine lesions) prior to SSPEqPCR. As shown in **Supplemental Figure 3.1**, both 8-oxoguanine lesions and DPCs were repaired with similar efficiency in both isolated nuclei and mitochondria (note, DPCs were electroporated into mitochondria in the presence of an undamaged, homologous donor plasmid, as I have shown previously [82] that DPCs are not subject to repair in mitochondria in the absence of a homologous donor). Together, these results indicate that, for at least 2 hours, electroporated mammalian nuclei are viable for DPC repair, and can be used to study mammalian mechanisms of DPC recognition and repair.

KCl-SDS-qPCR assay quantifies DPC removal in purified nuclei. I next tested the prediction that KCl-SDS-qPCR can be used to quantify DPC removal in electroporated

nuclei. As these experiments are method validation experiments, rather than directly quantifying DPC removal in the figures, I instead quantify and depict the "Percent Soluble DPC" value on the y-axis of the figure. This allows for the visualization of the percentage of KCl-SDS soluble DPC (see *methods* for a detailed explanation of the method used to calculate this value*)* before and after incubation in purified nuclei. As seen in **Figure 3.9**, 0% soluble DPC was observed in the electroporated DPC substrate prior to transfection, while 13% and 15% soluble DPC was observed 10- and 60-minutes following electroporation, respectively, showing that DPC removal occurs as a mechanism of nuclear DPC repair.

IP-qPCR assay detects DPC ubiquitination in purified nuclei. Next, the DPC substrate was electroporated into nuclei purified from HEK293T cells and incubated for 10 or 60 minutes. Following recovery, DPCS were subjected to anti-ubiquitin IP-qPCR, and while no enrichment was observed in the non-electroporated DPC substrate (**Figure 3.10**) 21- and 13-fold enrichment was observed 10- and 60-minutes following electroporation, respectively, demonstrating that DPCs are transiently ubiquitinated in purified mammalian nuclei.

DPCs are ubiquitinated in mammalian nuclear protein extracts. One limitation of the transfection and electroporation systems described in this report is that femtomolar amounts of DPC are recovered from transfected cells or nuclei, rendering it virtually impossible to analyze repair intermediates using non-qPCR-based methods. To overcome this limitation, I developed a nuclear protein extract-based system to examine the role that DPC ubiquitination plays in DPC repair in vitro. I prepared nuclear protein extracts

from nuclei isolated from HEK293T cells, then tested the hypothesis that DPCs would be ubiquitinated in these extracts by incubating 1 ug of AP or DPC substrate with 10 ug of HEK293T nuclear proteins at 37° C for 10, 30, or 90 minutes. AP substrate was generated by incubating 8-oxoguanine containing M13 with OGG1, in the absence of $NaCNBH_3$. As $NaCNBH_3$ is required for the trapping of OGG1 onto M13, the AP substrate is used as a negative control for ubiquitination and removal assays. Following the incubation, the sample was heat inactivated and then subjected to anti-ubiquitin IP-qPCR (**Figure 3.11A)** or anti-K48- polyubiquitin IP-qPCR (**Figure 3.11B)**. In both cases, AP plasmid showed no enrichment following incubation in the nuclear extract. Following anti-ubiquitin IP-qPCR, DPCs showed ~30-fold enrichment as early as 10 minutes and as long as 90 minutes following incubation in the nuclear extract. Following anti-K48 polyubiquitin IP-qPCR, DPCs showed 15-20-fold enrichment following incubation in the nuclear protein extract. These results show that DPC ubiquitination can be recapitulated in mammalian nuclear protein extracts. I was next interested in asking whether repair pathway selective posttranslational modifications of DNA crosslinked protein seen in intact cells is also observed in purified nuclear extracts. To test this hypothesis, nuclei were isolated from the NER-deficient XPD cell line, and soluble nuclear proteins were collected. I have previously shown that HR-mediated DPC repair was dependent on the presence of an undamaged homologous donor molecule that would act as a template for recombinational repair. DPCs were thus incubated with the NER-deficient nuclear extract in the presence of an undamaged plasmid with no sequence similarity to M13 (heterologous donor) or an undamaged M13 molecule (homologous

donor) for 90 minutes, then heat-inactivated the extract to end the reaction. Next, OGG1-DPCs were subjected to anti-ubiquitin IP-qPCR. As seen in **Figure 3.11C**, there was no observed enrichment of the DPC sample that was incubated with the extract in the presence of heterologous donor, while, interestingly, there was ~5-fold enrichment of in the DPC sample that was incubated in XPD extracts in the presence of homologous donor. This homology-dependent ubiquitination pattern of DNA crosslinked protein in NER-deficient systems is identical to the cell-based outcome observed in *Figure 2.3*, indicating that early events regulating DPC ubiquitination in cells also occur in purified nuclear extracts. Thus, these extracts can be used for studies of HR-mediated recognition and repair of DPCs. To diversify the types of questions that can be asked about DPC recognition and repair in nuclear extracts, I proceeded to employ the extracts to assay DPC ubiquitination using a non-qPCR-based method. To do this, DPCs were incubated in HEK293T extracts for one hour, and then subjected to IP-western analysis. Immunoprecipitation of the sample was done with an anti-ubiquitin antibody; the western blot was performed utilizing an anti-OGG1antibody. As seen in **Figure 3.11D**, there were two faint signals in the lane containing DPC alone, and these signals intensified in the lane containing DPC that had been incubated with the nuclear protein extract. The bottom panel represents the band that migrates at a molecular weight of 37 kDa (the molecular weight of unmodified OGG1 is 37 kDa) while the top panel represents the band corresponding to a molecular weight of ~55 kDa (corresponding with ubiquitinated OGG1). As both signals were enhanced following incubation of the DPC sample in the nuclear extracts, the data depicted in Figure 3.11 together show that DPCs are

ubiquitinated in nuclear extracts, and that this ubiquitination can be detected using q-PCR-based and non-qPCR-based methods.

Using a biotinylated hairpin DPC to study DPC ubiquitination in mammalian nucleus-based systems. To better detect DPC ubiquitination in nuclear extracts, I designed a biotinylated hairpin DPC substrate (See DPC 2 in Figure 2.1). Because of the relatively small size of the biotinylated hairpin, it is easier to synthesize and use large amounts of the hairpin for crosslinking and incubation in cells than it is of the M13 molecule. The 5′ biotin tag allows for the specific recovery of the biotinylated hairpin from the system it has been incubated in, and the 3′ ddC and the hairpin loop provide protection against nucleolytic degradation of otherwise free DNA ends. 100 picomoles of AP or DPC hairpin were electroporated into nuclei purified from HEK293T cells or incubated with 1 mg of HEK293T nuclear protein extract for 30 minutes, and then recovered by streptavidin capture (see **Figure 3.12**). Briefly, following heat inactivation of the nuclear protein extract or HIRT recovery of electroporated nuclei, samples were incubated with streptavidin-coated magnetic beads, and then a magnetic microcentrifuge holder was used to selectively recover streptavidin-bound material. This material was then resolved by gel electrophoresis, transferred to a PVDF membrane, and western blotting was performed using a ubiquitin antibody. As shown in Figure 2.12, neither DPC nor AP hairpins showed evidence of ubiquitination in the absence of nuclear material, and only the DPC hairpin was ubiquitinated following electroporation in purified nuclei (**Figure 3.13A**) or following incubation in a nuclear extract (**Figure 3.13B**),

demonstrating that the hairpin DPC is subject to ubiquitination in mammalian cell-free systems and that this ubiquitination is crosslink-dependent.

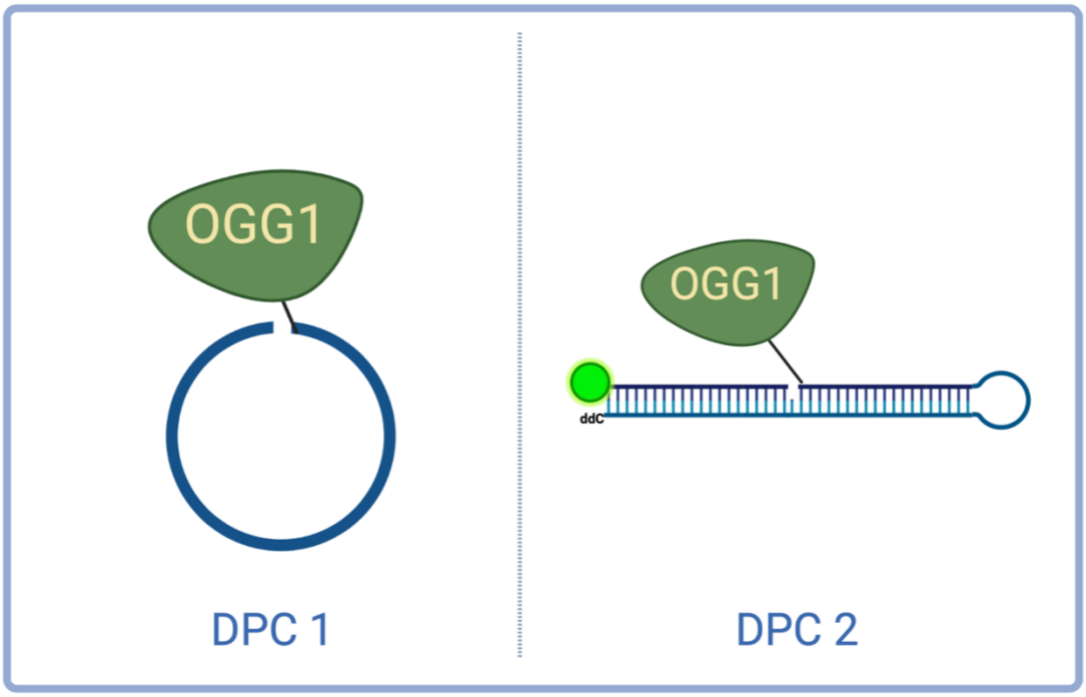

Figure 3.1 Substrates designed for mammalian DPC recognition and repair studies. **(**DPC 1) OGG1 protein is crosslinked to an AP site on M13 following the expulsion of a site-specific 8-oxoguanine residue on M13 (DPC 2) OGG1 protein is crosslinked to an AP site following the expulsion of a site-specific 8-oxoguanine residue on a 120mer biotinylated hairpin

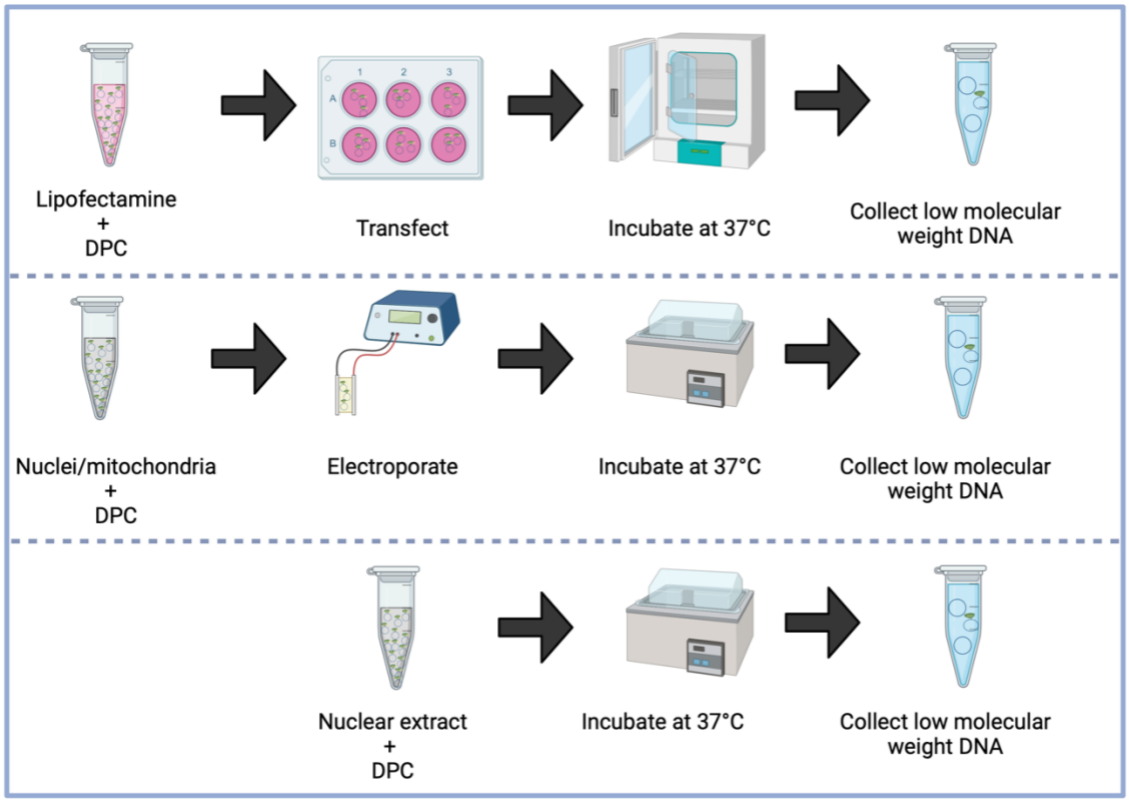

Figure 3.2 Repair systems developed to study mammalian mechanisms of DPC recognition and repair. (Top panel) DPCs are transfected into cells *via* lipofection, incubated at 37° C for designated time period, and recovered by HIRT prep (Middle panel) DPCs are electroporated into isolated mammalian nuclei or mitochondria, incubated at 37° C in the presence of ATP and dNTPs, and recovered by HIRT prep. (Lower panel) DPCs are incubated with nuclear protein extracts, incubated at 37° C for designated time period, then recovered *via* DPC selective-capture methodology

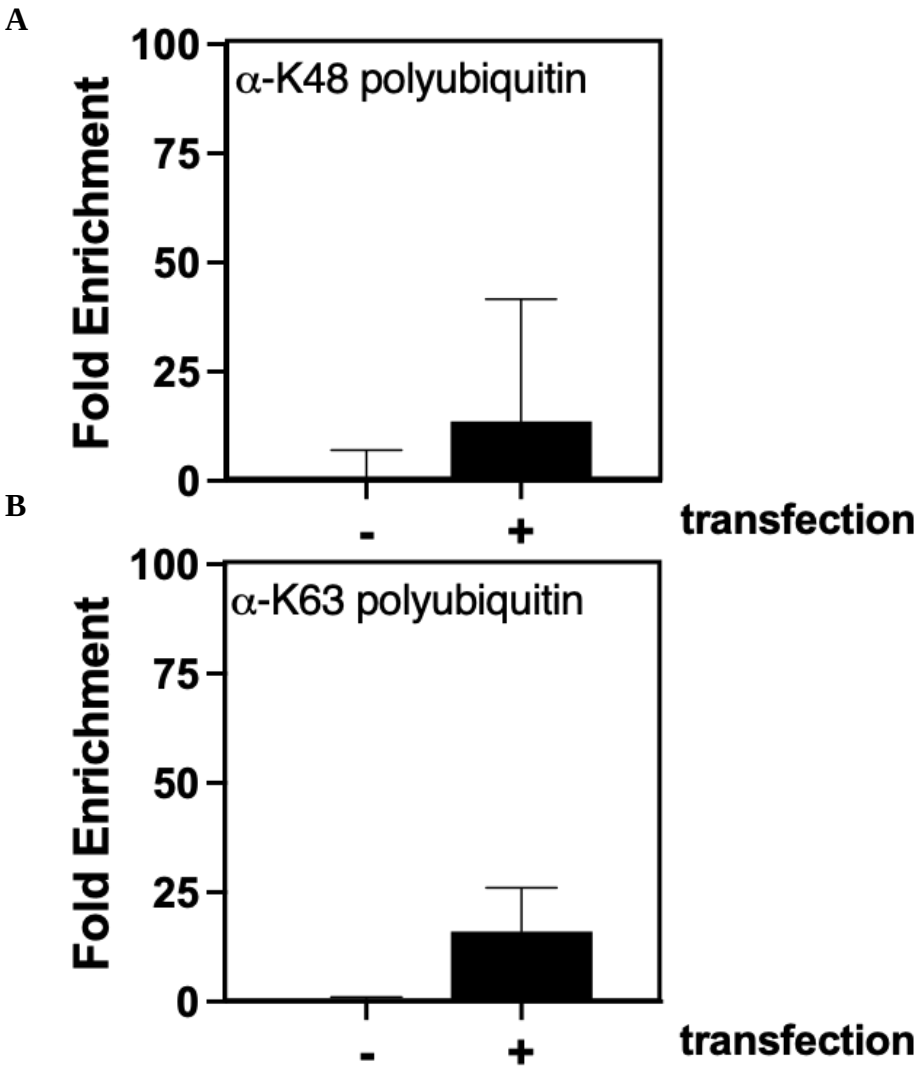

Figure 3.3 R341 OGG1 DPCs are not K48 or K63 polyubiquitinated. (A) DPC substrates comprised of modified (R341) OGG1 were transfected into HEK293T cells in the absence of homologous donor, recovered one hour following transfection and subjected to anti-K48 polyubiquitin IP-qPCR (difference not statistically significant, $p > 0.05$) (B) DPC substrates comprised of modified (R341) OGG1 were transfected into HEK293T cells in the absence of homologous donor, recovered one hour following transfection and subjected to anti-K63 polyubiquitin IP-qPCR (difference not statistically significant, $p > 0.05$)

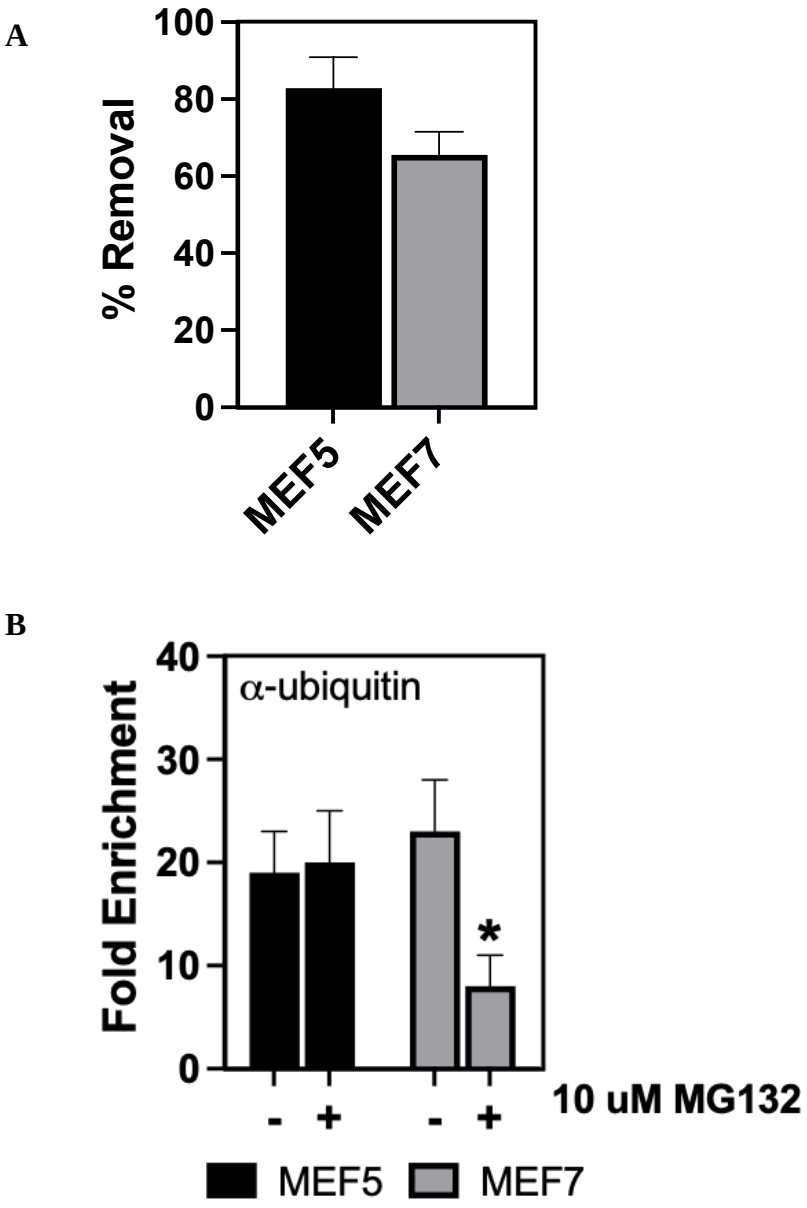

Figure 3.4 SPRTN and the proteasome play independent roles in DPC ubiquitination and repair. (A) DPCs were transfected for one-hour (in the absence of homologous donor) into MEF5 and MEF7 cells. Following recovery DPCs were subjected to KCl-SDS-qPCR *; P =0.02 (B) DPCs recovered from identical transfection conditions as depicted in A were subjected to anti-ubiquitin IP-qPCR *; P =0.04

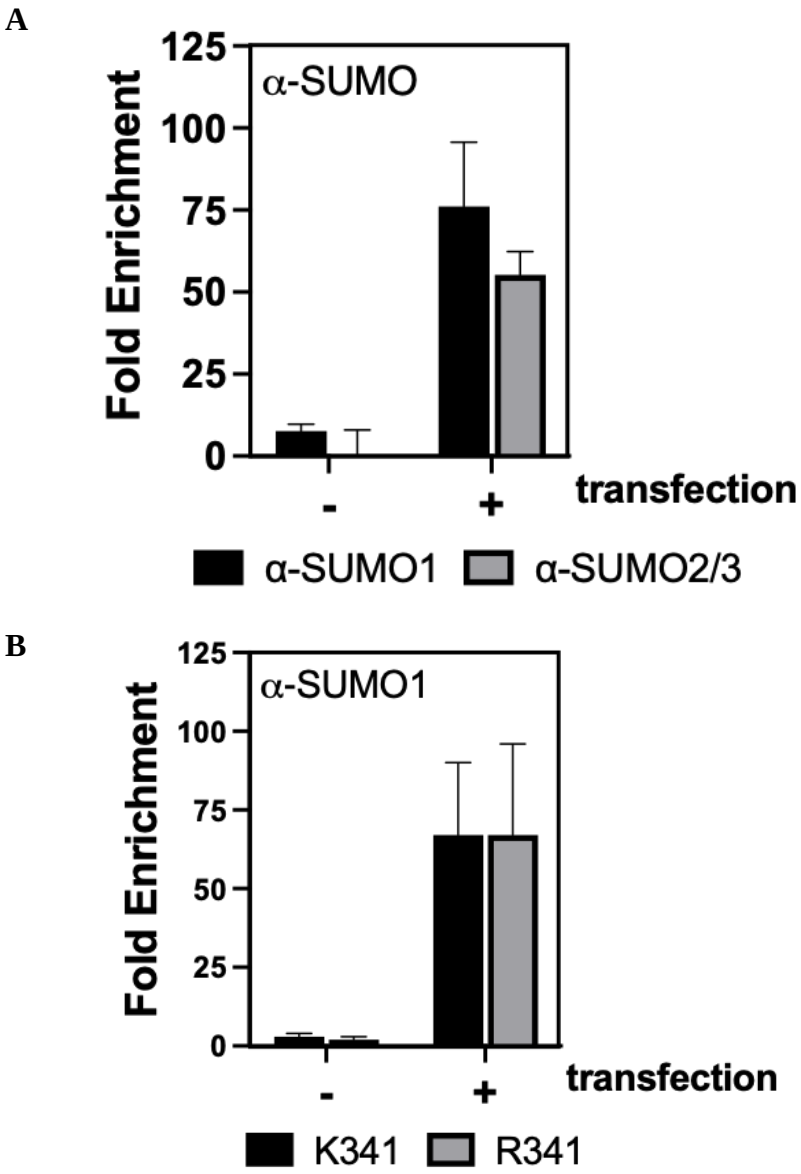

Figure 3.5 DPCs are SUMOylated following transfection into mammalian cells. (A) DPCs were transfected into HEK293T cells in the absence of homologous donor, recovered one hour following transfection and subjected to anti-SUMO1 or anti-SUMO2/3 IP-qPCR (B) DPC substrates comprised of unmodified (K341) or modified (R341) OGG1 were transfected into HEK293T cells in the absence of homologous donor, recovered one hour following transfection and subjected to anti-SUMO1 IP-qPCR

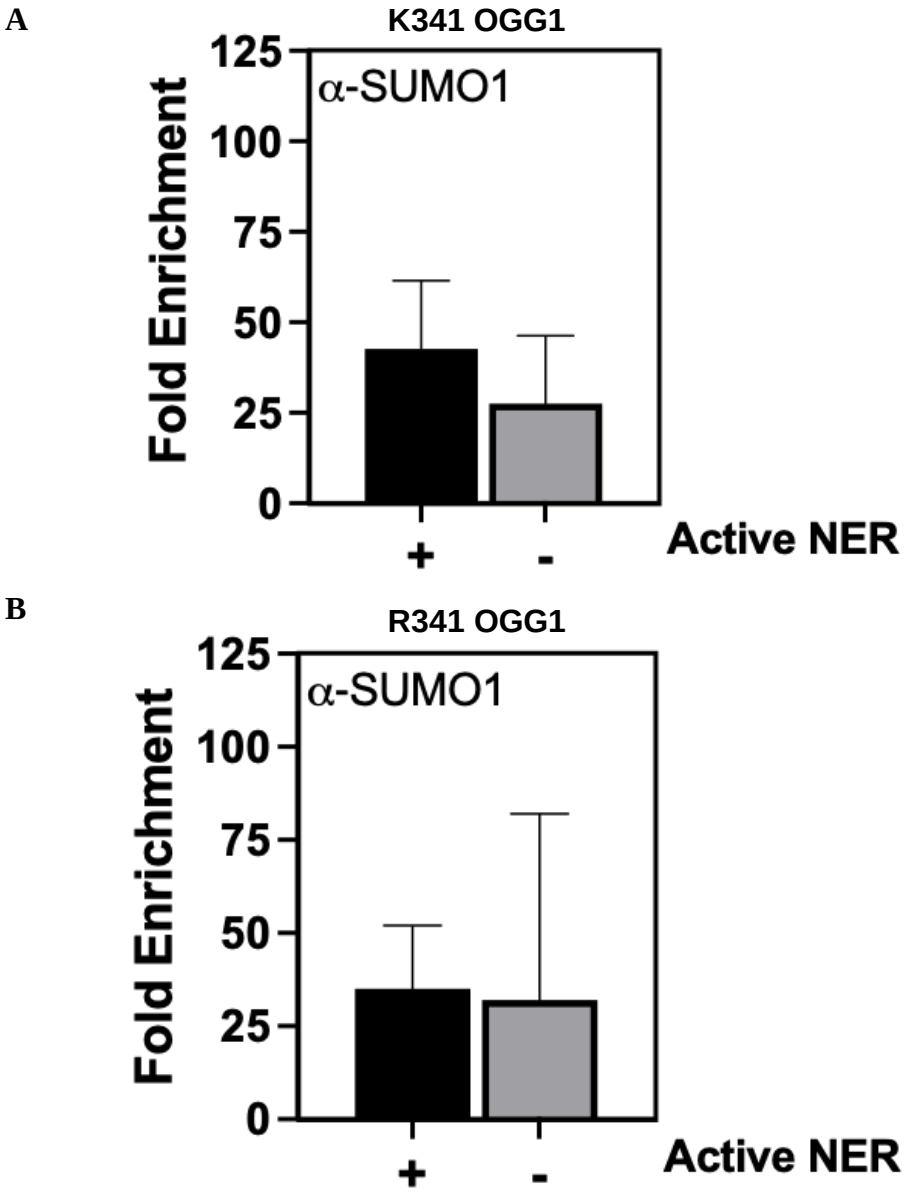

Figure 3.6 DPC SUMOylation is not dependent on the presence of NER machinery. (A) DPC substrates comprised of unmodified (K341) OGG1 were transfected into NER proficient (+) or deficient (-) cells in the absence of homologous donor, recovered one hour following transfection and subjected to anti-SUMO1 IP-qPCR (B) DPC substrates comprised of modified (R341) OGG1 were transfected into NER proficient (+) or deficient (-) cells in the absence of homologous donor, recovered one hour following transfection and subjected to anti-SUMO1 IP-qPCR

A

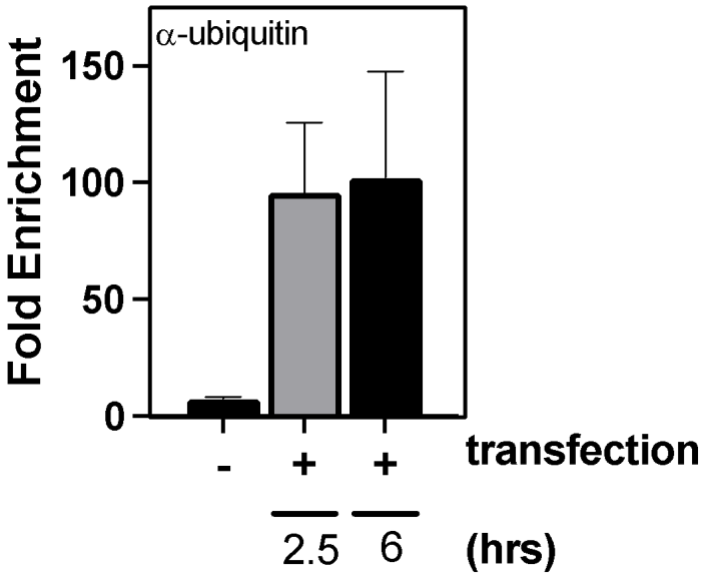

B

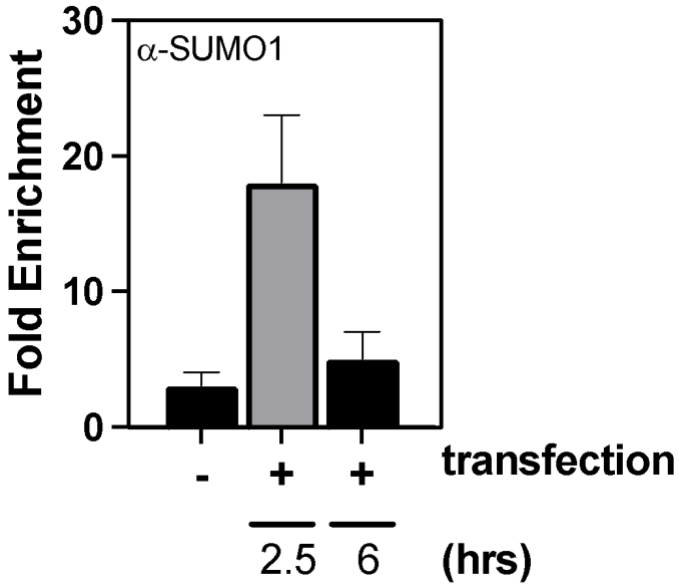

Figure 3.7 DPC SUMOylation occurs with faster kinetics than DPC ubiquitination. DPCs were transfected into HEK293T cells and recovered 2.5 hours or 6 hours following transfection. Untransfected and transfected DPCs were subjected to anti-ubiquitin (A) or anti-SUMO1 (B) IP-qPCR to sensitively detect DPC containing fragments that have been selectively enriched following immunoprecipitation

A

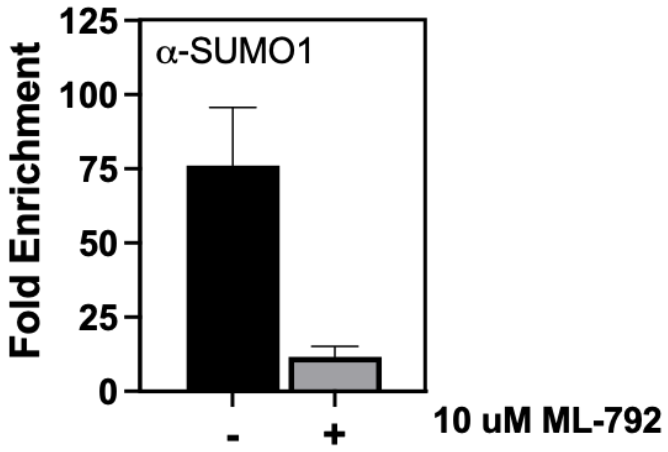

B

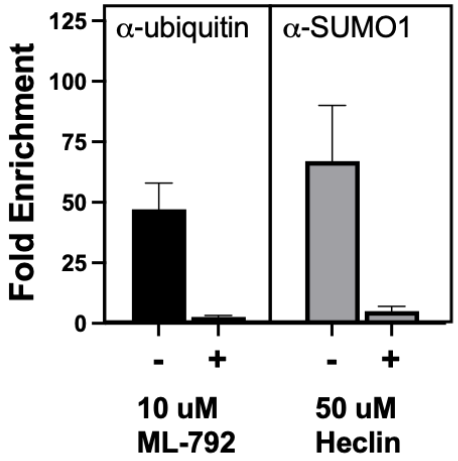

Figure 3.8 DPC ubiquitination and SUMOylation are interdependent. (A) DPCs were transfected (in the absence of homologous donor) into HEK293T cells that had been pretreated with 0 uM or 10 uM ML-792. DPCs were recovered one hour following transfection and subjected to anti-SUMO1 IP-qPCR. (B) Left panel: DPCs were transfected (in the absence of homologous donor) into HEK293T cells that had been pretreated with 0 uM or 10 uM ML-792. DPCs were recovered one hour following transfection and subjected to anti-SUMO1 IP-qPCR. Right panel: DPCs were transfected (in the absence of homologous donor) into HEK293T cells that had been pretreated with 0 uM or 50 uM Heclin. DPCs were recovered one hour following transfection and subjected to anti-ubiquitin IP-qPCR.

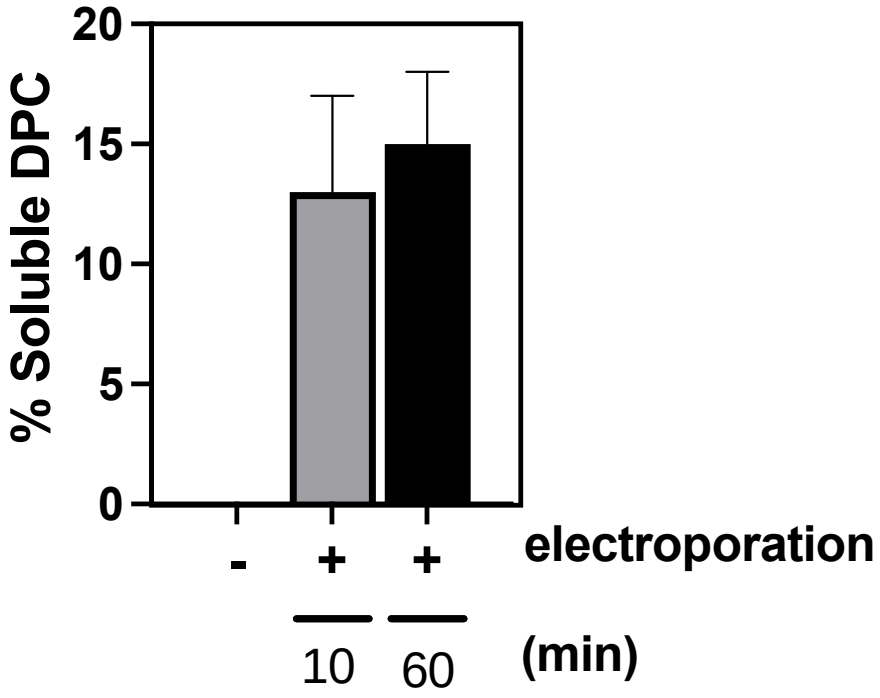

Figure 3.9 Quantification of DPC removal in purified nuclei. DPC substrates electroporated into purified nuclei and recovered 10- or 60-minutes following electroporation then were subjected to KCl-SDS-qPCR to quantify the percentage of KCl-SDS soluble DPC.

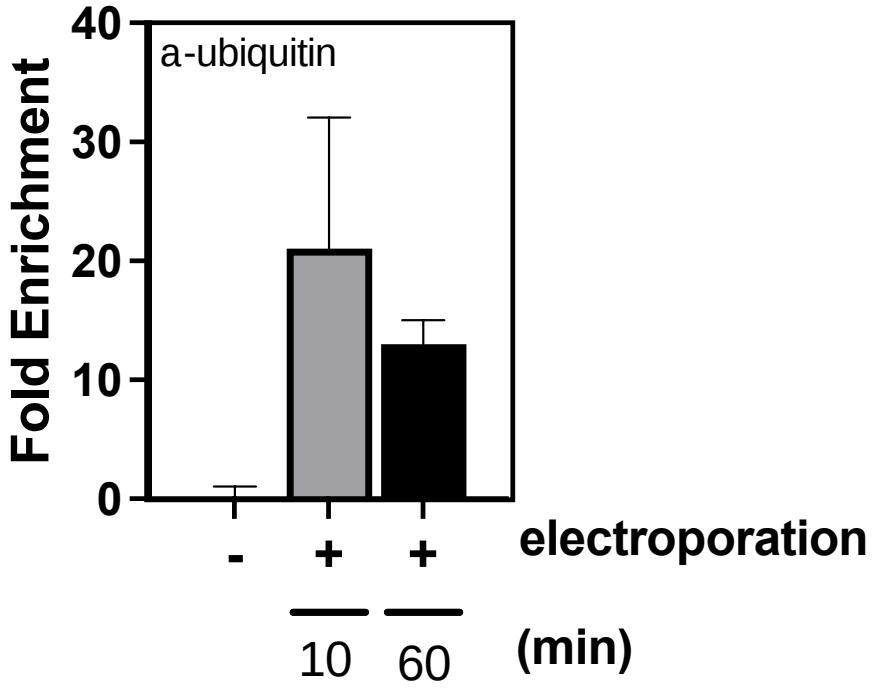

Figure 3.10 Quantification of DPC ubiquitination in purified nuclei. DPC substrates were electroporated into purified nuclei and recovered 10- or 60-minutes following electroporation. Electroporated (+) and unelectroporated (-) DPCS were subjected to anti-ubiquitin IP-qPCR to sensitively detect DPC containing fragments that have been selectively enriched following immunoprecipitation

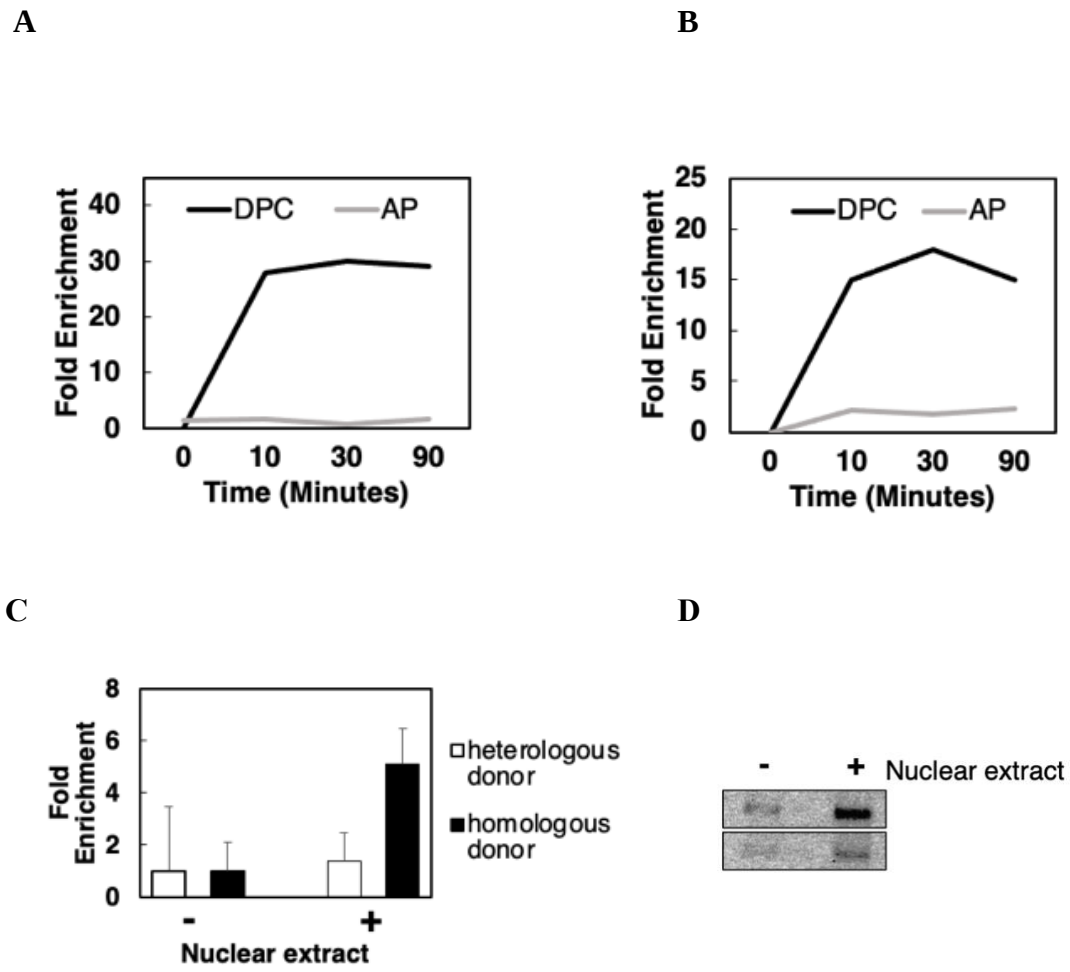

Figure 3.11 DPCs are ubiquitinated in vitro. (A) 1 µg DPC or AP plasmids were incubated with 10 µg of nuclear protein extract prepared from HEK293T cells for 10, 30, or 90 minutes then subjected to anti-ubiquitin IP-qPCR as described above. (B) DPC or AP plasmids were incubated with nuclear protein extract as in 3.11A then subjected to anti-K48 polyubiquitin IP-qPCR. (C) 1 µg DPC was incubated in the absence (-), or presence (+), of 10 µg of nuclear protein extract prepared from XPD along with 3 µg of heterologous or homologous donor for 90 minutes, then subjected to anti-ubiquitin IP-qPCR. P= 0.05 (D) 5 µg DPC was incubated with 20 µg of nuclear protein extract from HEK293T cells for 60 minutes, then subjected to anti-ubiquitin IP. IP material was resolved on an SDS-page gel, transferred to a PVDF membrane then probed with an anti-OGG1 antibody.

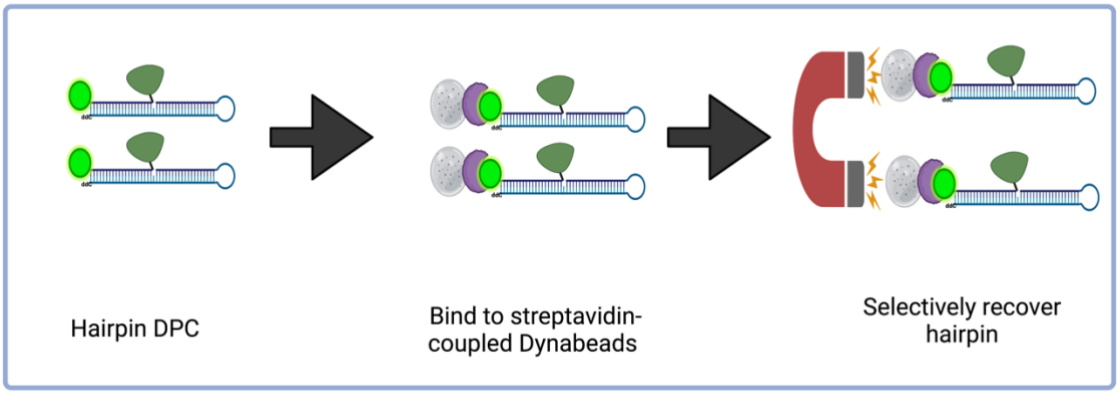

Figure 3.12 Biotinylated hairpin capture schematic. Following recovery from isolated nuclei or nuclear protein extracts, biotinylated hairpin is recovery by selective binding to streptavidin coupled Dynabeads and separated from cellular material using magnetic microcentrifuge holder. Following washes, biotinylated hairpin is eluted by boiling samples at 95°C in 0.4% SDS-containing buffer.

A

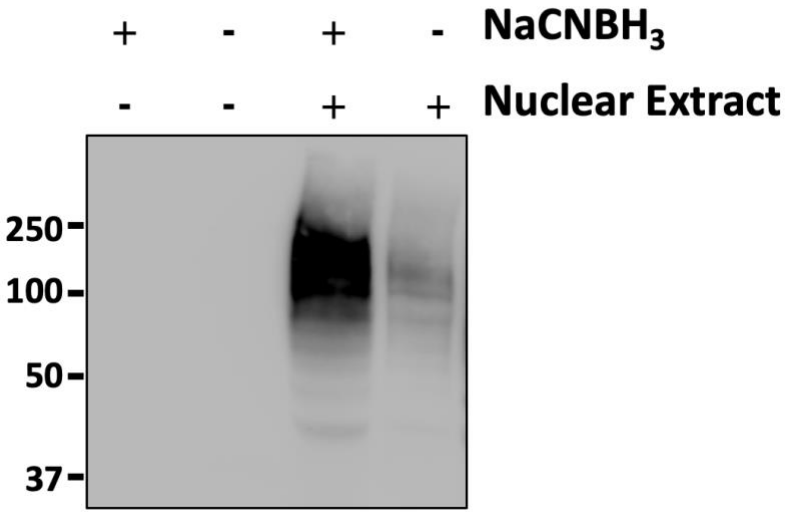

B

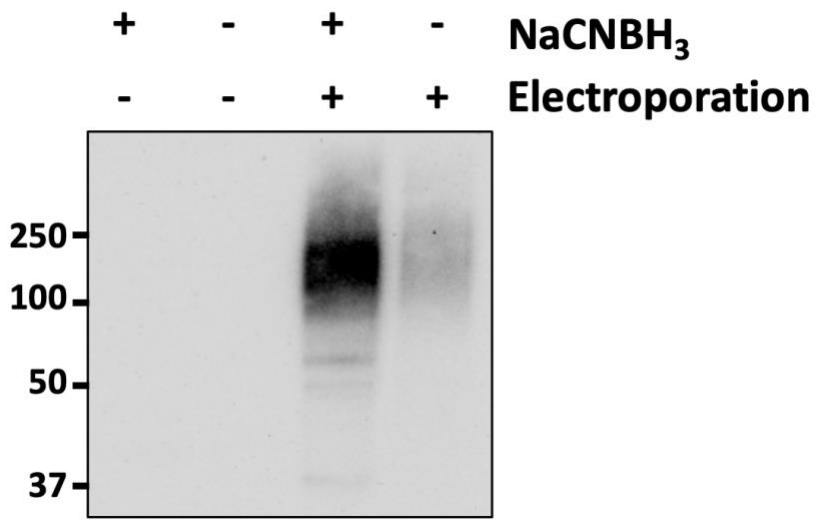

Figure 3.13 Hairpin DPC substrate is ubiquitinated *in vitro.* Biotinylated hairpin DPC was incubated in nuclear protein extract recovered from HEK293T cells (A) or electroporated into purified HEK293T nuclei following incubation with OGG1 in the presence or absence of $NaCNBH_3$, recovered by streptavidin-mediated capture, and resolved on an SDS-PAGE gel. Electrophoresed material was transferred to a PVDF membrane and anti-ubiquitin western blotting was performed

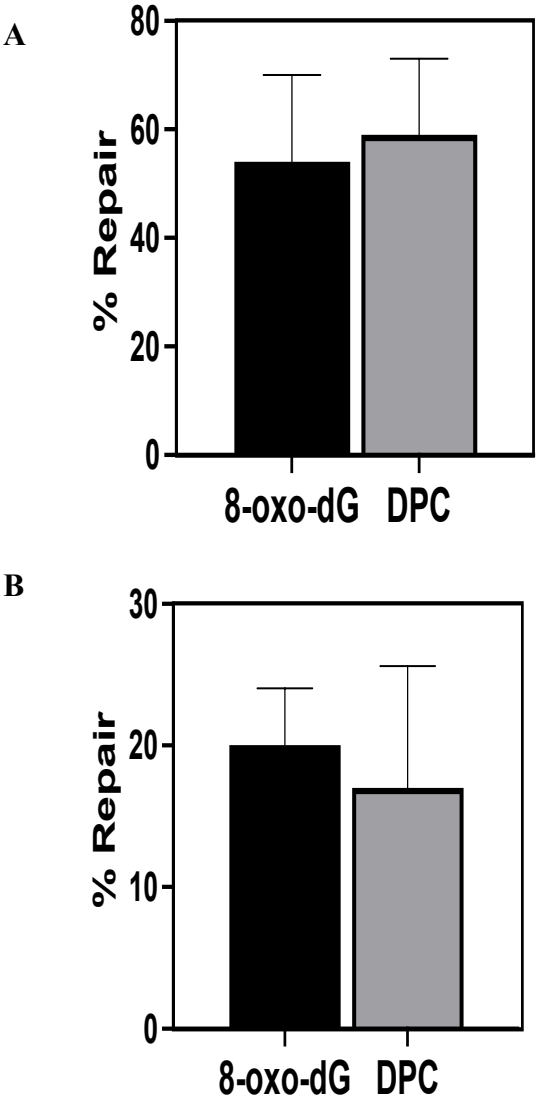

Supplemental Figure 3.1 DNA repair in isolated mammalian nuclei. 8-oxoguanine containing or DPC containing M13 was electroporated into nuclei purified from HEK293T cells (A) or mitochondria isolated from V79 cells (B). Low molecular weight DNA was recovered 2 hours following electroporation and repair was quantified using SSPEqPCR

- LC was responsible for performing SSPEqPCR assays.

III. DISCUSSION

The work described in this chapter was done to achieve two goals, first to continue examination of the model first proposed in *Chapter 2*, and second to develop and validate novel systems for the study of the role of DPC post-translational modifications in DPC repair. The model proposed in *Chapter 2* shows that differential polyubiquitination of a DNA-crosslinked protein selectively triggers repair-pathway specific removal of the DPC, that NER mediated removal is K48 polyubiquitin and proteasome-dependent, and that K48 polyubiquitination of the DPC is triggered by the presence of NER machinery. Furthermore, the model proposes that K63 polyubiquitination occurs rapidly following DPC recognition. The mechanisms that modulate this form of DPC ubiquitination are unknown, and the data shown in this chapter were designed to address this question.

I showed that, in the presence of proteasomal inhibitor, DPCs were less efficiently ubiquitinated in SPRTN deficient cells. These data indicate that proteasomal inhibition enhanced the effect of SPRTN inactivation on DPC ubiquitination. DPC ubiquitination was unaffected in SPRTN deficient cells that were not treated with proteasomal inhibitor, thus the precise mechanism by which SPRTN and the proteasome work together to modulate total ubiquitinated DPC levels is unclear. I speculate that SPRTN enhances DPC ubiquitination, and that 1) in the absence of proteasomal inhibitor, the proteasome degrades ubiquitinated proteins and thus SPRTN-enhanced DPC ubiquitination cannot be detected and 2) in the presence of proteasomal inhibitor, free ubiquitin levels are depleted

and thus the effect of decreased SPRTN levels is compounded. Further studies are required to better understand the mechanism by which SPRTN modulates DPC ubiquitination and whether the form of ubiquitination modulated by SRPTN is monoubiquitination or polyubiquitination.

I also showed that DPCs are modified with SUMO1 and SUMO2/3 chains. While investigating the hypothesis that DPC SUMOylation triggers DPC ubiquitination, I showed that DPC SUMOylation occurs in the presence or absence of NER repair machinery. As K63 polyubiquitination also occurs in the presence and absence of NER repair machinery (see *Chapter 2)*, these data suggest that, like K63 polyubiquitination, DPC SUMOylation occurs early following DPC recognition. I next showed that DPC SUMOylation occurs with faster kinetics than DPC ubiquitination, and that pharmacological inhibition of SUMOylation abolished DPC ubiquitination, which is consistent with the interpretations that DPC SUMOylation modulates DPC regulation. This interpretation is supported by studies that showed that the pharmacological inhibition of SUMOylation impaired the ubiquitination of DPCs formed in response to cellular camptothecin, etoposide, and formaldehyde [66, 138]. Interestingly, I also found that pharmacological inhibition of ubiquitination abolished DPC SUMOylation, which shows that DPC ubiquitination and DPC SUMOylation are interdependent, however further studies are required to test this finding more thoroughly, to determine whether the observations regarding NER-mediated DPC SUMOylation are also true in an HR-mediated DPC repair context, and to identify the mechanism by which post-translational modifications trigger the recruitment of an E3 SUMO or ubiquitin ligase.

Next, I developed novel, nuclear based systems that allow for non-qPCR based DPC analyses to further investigate the mechanisms that modulate DPC recognition and repair. I first validated the nuclear electroporation-based and nuclear extract-based systems by showing that DPC ubiquitination patterns that were observed in transfected cells also can be observed in nuclear extracts. First, I showed that DPCs incubated in nuclear extracts collected from NER proficient cells are not only ubiquitinated, but also modified with K48-polyubiquitin chains. Second, I showed that (like transfected DPCs) DPCs incubated in nuclear extracts collected from NER deficient cells are only pulled down with anti-ubiquitin antibody following transfection into cells in the presence of homologous donor. It is important to note that, in transfected cells, this observation was reversed following K63-polyubiquitin IP-qPCR (i.e., K63 polyubiquitination occurred in NER deficient cells only in the *absence* of homologous donor), however we speculate that this discrepancy is due to decreased selectivity of the anti-ubiquitin antibody to K63 polyubiquitin chains. Finally, I showed using IP-western and using streptavidin-based capture of a biotinylated DPC substrate that DPC ubiquitination in electroporated nuclei and in nuclear protein extract can be detected by western blot. The validation of the nuclear systems using qPCR-based and non-qPCR-based methods demonstrates that they can be used to test hypotheses regarding the role of DPC ubiquitination in DPC repair that cannot be tested using transfected cells. I have found that the “DPC 1” substrate cannot be recovered from formaldehyde trapped cells. In the extract-based system, formaldehyde can be used to trap elements of the repair machinery that have been recruited to the DPC, which can then be analyzed by western blot or by proteomics

(following selective recovery of the DPC). Hypotheses I am interested in investigating using the extract system include the role of DPC ubiquitination in the recruitment of the proteasome and of the HR repair machinery. Other studies that I am interested in performing to study and optimize my proposed model are more deeply discussed in the *Future Directions* portion of this thesis.

IV. MATERIALS AND METHODS

Chemicals and enzymes. Oligonucleotides containing 8-oxo-2′-deoxyguanosine (8-oxo-dG) (see **Table 3.1)** were purchased from Midland Certified Reagent (Midland, TX). Remaining oligonucleotides were purchased from the University of Minnesota Genomic Center (Table 3.1). Human Oxoguanine glycosylase 1 (OGG1) was expressed and isolated from BL21(DE3)-competent E. coli using a pET-28a expression vector. Protein G-beads were purchased from Invitrogen (Cat. #:10003D), 5 µL of beads was used for each immunoprecipitation. Streptavidin-coupled Dynabeads were purchased from Invitrogen (Cat. # 65001), 45 uL of beads were used for each immunoprecipitation. Antibodies used for immunoprecipitations are listed in **Table 3.2.**

Cell lines. HEK293T cells were obtained from the American Type Culture Collection (ATCC) and cultured in Dulbecco's modified eagle medium (DMEM) augmented with 9% fetal bovine serum (FBS). The XPD cell line is an SV40 transformed, immortalized dermal fibroblast cell line with a deleterious mutation in the XPD gene, first isolated from a patient with complementation group D xeroderma pigmentosum. XPD cells were purchased from the Coriell Institute for Medical Research and cultured in DMEM augmented with 9% FBS. The Chinese hamster lung fibroblast cell lines, V79 (GM16136) and V-H1 (GM16141), were purchased from the Coriell Institute for Medical Research (Camden, NJ, USA). The V79 cell line is a wild-type hamster lung fibroblast cell line derived from Chinese hamsters, which was established following spontaneous transformation. V-H1 clones were derived from V79 cells using

an ethyl nitrosourea-induced mutagenesis screen (39-41). V-H1 cells belong to nucleotide excision repair complementation group 2 and lack a functional XPD gene (42). Chinese hamster lung fibroblast cells were cultured in Ham's F-12 modified essential Eagle's media (Life Technologies, Grand Island, NY) augmented with 9% fetal bovine serum (Atlanta Biologics, Atlanta, GA).

ODN	**Sequence (5′→3′)**	**Use**
M13-8oxo	AGCCACCCCTCACCCACTA(8-oxo-dG)GAT	Primer Extension
EcoRI-8oxo	CCGGGTACCGAGCTC(8-oxo-dG)AATTCGTAATCTTGGTCATAGCTG	Primer Extension
Biotinylated Hairpin	(Biotin)ATCGAATTCTCTTGGGTCTAAGTCG(8-oxo-dG)ATCCATTTACCGTGGTCATAAGCTTGCGGAT CAACGATCCGCAAGCTTATGACCACGGTAAATG GATCCGACTTAGACCCAAGAGAATTCGAT	DPC formation
Fragment b L	CACCCCAGGCTTTACACTT	qPCR of M13
Fragment b R	GTAAAACGACGGCCAGTG	qPCR of M13
Fragment c L	CTGGGTGCAAAATAGCAACT	qPCR of M13
Fragment c R	CCCAATAGCAAGCAAATCA	qPCR of M13
DPC F	GCTGCAAGGCGATTAAGT	SSPEqPCR of M13 Plasmid
DPC R	CGGCTCGTATGTTGTGTG	SSPEqPCR of M13 Plasmid

Table 3.1 Oligodeoxynucleotides (ODNs) used in this study

Antibody	Assay	Vendor	Catalog Number	Lot Number	Amount used
anti-OGG1 (Rabbit, polyclonal)	IP-qPCR	Novus	NB100-106AF350	S-041421-AF350	0.7 ug/IP
anti-OGG1 (Mouse, polyclonal)	IP-Western	Sigma	SAB1400189	CC181	1:2000 dil. (WB)
anti-ubiquitin (Rabbit, polyclonal)	IP-qPCR	Abcam	ab134953	GR3367020-2	0.7 ug/IP 1:2000 dil. (WB)
anti-SUMO1 (Rabbit, polyclonal)	IP-qPCR	Boster Bio	PA2220	0221312c012088	0.5 ug/ IP
Goat anti-rabbit IgG (H+L) (HRP conjugated)	IP-qPCR, Western blot	Invitrogen	31460	WE323493	1:10000 dil. (WB)
Horse anti-mouse IgG (H+L) (Peroxidase-labeled)	Western blot	Vector	PI-2000	X0328	1:10000 dil. (WB)

Table 0.2

Table 3.2 Antibodies used in this study

Construction of plasmid DNA repair substrates. 100 picomoles of M13 8-oxo, or EcoRI 8-oxo (See Table 3.1) was phosphorylated using 40 units of T4 PNK in 1X DNA Ligase buffer for 30 minutes at 37°C. Phosphorylated oligonucleotide was then annealed to 13.4 picomoles of single-stranded M13 and extended using 100 units of Taq polymerase, in a solution containing 1X Thermopol Reaction Buffer, 1X NEB Buffer 2, 10 mM ATP, 1 mM dNTPs, and 20 μg bovine serum albumin. Primer annealing was carried out for 15 minutes at 75°C. Following cooling, 60 units of T4 DNA Polymerase and 8000 units of T4 DNA Ligase were added to the sample, which was then incubated at 37°C overnight for complete extension and ligation of the new double stranded M13 DNA containing a site-specific 8-oxo-dG lesion(8-oxo-PE).The following day, 8-oxo-PE was purified by phenol-chloroform extraction and ethanol precipitation. To make plasmid DPC, 8-oxo-PE was crosslinked to hOGG1 in 200X protein: DNA molar excess in buffer containing 100 mM NaCl, 1 mM MgCl2, 20 mM Tris-HCl pH 7.0, and 10 mM sodium cyanoborohydride. Sodium cyanoborohydride stock solution was made fresh, and added immediately before hOGG1, which was added last to the reaction mixture. Crosslinking was carried out at 37°C for 1 hour. To make hairpin DPC, 8-oxo-dG containing biotinylated hairpin was crosslinked to hOGG1 in 10X protein: DNA molar excess in otherwise identical conditions described above. *Note: The reaction catalyzed by OGG1 involves the expulsion of 8-oxoguanine bases from DNA when the active site lysine residue (K249) of the glycosylase attacks the C1 position of the deoxyribose bound to the 8-oxoguanine lesion [197]. This results in the formation of an abasic, or apurinic (AP) site, which, in cells, is followed by further enzymatic steps to complete repair [13].

In our OGG1 trapping reaction, however, sodium cyanoborohydride ($NaCNBH_3$) is added to reduce the intermediate Schiff base (reductive amination) formed during the OGG1 excision reaction, resulting in a covalent crosslink between OGG1 and the deoxyribose to which 8-oxoguanine was originally bound [13].

Transfection of DPC into cells. Sixteen hours before transfection, cells were counted and plated in 6-well plates at a density of 600,000 cells per well. For DPC transfection, 1 µg of plasmid DPC was added to each well in combination with Lipofectamine (a synthetic cationic lipid that allows for the transport of DNA into the nucleus via the endocytic pathway [198, 199]), according to the manufacturer's instructions, and incubated at 37° C. Thirty minutes after the beginning of transfection, the medium and lipofection mixture were removed from the well by gentle aspiration and replaced with 4 mL DMEM supplemented with 9% FBS. The plates were incubated at 37° C until collection at predetermined time points, at which point the cells were lysed, and the transfected DNA was collected using a modified HIRT procedure [200]. Plates were incubated for 10 minutes at room temperature, then cells were scraped and transferred into a 1.5 mL Eppendorf tube. NaCl was added to a final concentration of 1M, tubes were closed and inverted sharply 10 times, and incubated at 4° C overnight. The following day, samples were centrifuged at 21,000 X G for 30 minutes (4° C). Low-molecular-weight DNA was recovered from the supernatant via ethanol precipitation.

Purification of nuclei. Note: cells and reagents were always kept cold or on ice during purification. Four 15 cm dishes were plated with V79 or HEK23T cells which were grown to confluence, washed twice with 5mL of 1X PBS and resuspended in 2mL of Buffer A (10mM Tris-HCl pH 7.4, 10mM MgCl2, 10mM KCl, and 1mM DTT). Resuspended cells were lysed by incubation at 0° C for 10-15 minutes followed with 20 strokes of a Dounce homogenizer (utilizing a 'loose' pestle). Broken cells were centrifuged at 1150 x G for 8 minutes at 4°C and washed with 0.5mL of NIB-250 Buffer (15mM Tris-HCl pH 7.5, 60mM KCl, 15mM NaCl, 5mM MgCl2, 1mM CaCl2, 250mM sucrose, and 1mM DTT) (x). The supernatant was discarded, and the wash and centrifugation were repeated one time. For electroporation of purified nuclei, nuclear pellet was resuspended in 400 uL NIB-250 Buffer (see "Electroporation of purified nuclei" section below). For generation of nuclear protein extract, the nuclear pellet was resuspended in 2 mL modified Buffer A (see "Nuclear protein extract" section below). *Nuclear Protein Extract.* Nuclear pellet was resuspended in 2 mL Buffer A containing 350 mM NaCl, 0.70 mug/mL Pepstatin, 0.1 ug/mL Leupeptin, 0.1 ug/mL aprotinin, and 1 mM PMSF, then incubated at 0° C for 1 hour. Sample was then centrifuged at 70,000 RPM for 30 min at 2° C, in a Beckman TL-100.3 rotor. Pellet was adjusted to 10% glycerol and frozen immediately or analyzed by BCA (see "BCA" section below).

Electroporation of purified nuclei. Nuclear pellet was resuspended in 400μL NIB-250 Buffer and mixed with 100ng of 8-oxo-guanine containing M13, 100 ng of DPC-containing M13 or 100 picomoles of hairpin DPC. Samples were then transferred to a

chilled, 4mm gap cuvette (Fisher Scientific, Waltham, MA) and electroporated using an ECM 630 Electro Cell Manipulator (BTX, Molliston, MA) at a field strength of 300V/cm, resistance of 25Ω, and 950μF capacitance. Following electroporation, samples centrifuged using the same conditions as above, and resuspended in 400μL Incubation Buffer (40mM Tris-HCl pH 7.4, 25mM NaCl, 5mM MgCl2, 10% glycerol, 1mM pyruvate, 1mM ATP (Teknova), 1 mg/mL BSA (New England Biolabs), and 10μM dNTPs (Thermo Scientific))216. Nuclei were incubated in a 37°C water bath for the designated time points described in the Results section of this report. Following incubation, nuclei were lysed by adjusting the final concentrations of SDS and EDTA to 0.5% and 0.01M, respectively, and incubation at room temperature for 12 minutes. Chromosomal DNA was precipitated by adding NaCl to a 1M final concentration and incubated at 4°C overnight. The following day, samples were centrifuged at 21130 X G for 30 minutes at 4°C. Low molecular weight DNA was recovered from the supernatant by ethanol precipitation.

Nuclear extract Incubation. 5 ug of plasmid DPC was incubated with 5 ug of HEK293T nuclear extract or 100 pmoles of biotinylated hairpin DPC was incubated with 1 mg of HEK293T nuclear extract in a buffer containing 75 mM Tris-HCl, pH 7.4, 10 mM $MgCl_2$, 10 mM DTT, 10 mM ATP, and 2 mM dNTPs. Extracts were incubated for one hour at 37° C then extract was heat inactivated by incubation at 95° C for 5 minutes.

Mitochondria purification. Note: cells and reagents were always kept cold or on ice during purification. V79 or HEK293T cells were grown to confluence in four 15 cm dishes and mitochondria purified as described in Yoon and Koob *et al*., [201] Briefly, cells were washed twice with 5mL of buffer containing 1mM Tris-HCl pH 7.0, 0.13M NaCl, 5mM KCl, and 7.5mM MgCl2 in a table-top centrifuge at 1000 X G for 5 minutes at room temperature. The cell pellet was resuspended in half the cell volume in 0.1X incubation buffer (IB buffer) (4mM Tris-HCl pH 7.4, 2.5mM NaCl, and 0.5mM MgCl2) and broken with 10 strokes of a Dounce homogenizer. 10X IB buffer (400mM Tris-HCl pH 7.4, 250mM NaCl, and 50mM MgCl2) was then added in a volume equivalent to 11% of the volume of the original cell pellet to reach a final concentration of ~1X. This sample was then centrifuged at 376 x G for 5 minutes at 4°C. The supernatant was collected, and the centrifugation step was repeated one time. To isolate the mitochondrial fraction, the supernatant was then centrifuged at 21130 X G for 10 minutes at 4°C. The mitochondria (pellet) were then washed with 0.5mL of 1X IB buffer (40mM Tris-HCl pH 7.4, 25mM NaCl, and 5mM MgCl2) two times. Purified mitochondria were then resuspended in the electroporation buffer described below.

Electroporation of purified mitochondria. Purified mitochondria were resuspended in 50µL 0.33M sucrose/10% glycerol and mixed with 100ng of an 8-oxo-guanine or DPC-containing plasmid (15µL)). Note: 1µL of the DNA mixture was saved and diluted in 500µL of water to be used as a 'Time 0' sample for SSPE-qPCR (see section below). Samples were then transferred to a chilled, 1mm gap cuvette (Fisher Scientific, Waltham,

MA) and electroporated using an ECM 630 Electro Cell Manipulator (BTX, Molliston, MA) at a field strength of 1000V/cm, resistance of 400Ω, and 25μF capacitance. Following electroporation, cuvettes were rinsed with 100μL of 1X IB buffer + 10% glycerol (40mM Tris-HCl pH 7.4, 25mM NaCl, 5mM MgCl2, and 10% glycerol). An additional 900μL of 1X IB buffer + 10% glycerol was then added to electroporated mitochondria, which were then centrifuged at 21130 X G for 10 minutes at 4°C. Supernatant was discarded, and pellet washed three times in 200μL of 1X IB buffer + 10% glycerol. The final pellet was resuspended in 50μL of a solution containing 40mM Tris-HCl pH 7.4, 25mM NaCl, 5mM MgCl2, 10% glycerol, 1mM pyruvate, 1mM ATP (Teknova), 1 mg/mL BSA (New England Biolabs), and 10μM dNTPs (Thermo Scientific) and incubated in a 37°C water bath for 2 hours. Following incubation, mitochondria were resuspended in 300 μL lysis buffer (0.5 % SDS, 10 mM TRIS−HCl pH 7.4, 150 mM NaCl, 1 mM EDTA containing 100 μg proteinase K (New England Biolabs) and incubated at 37 °C for 15 min. 300 μL of a 1:1 phenol: chloroform solution prepared as described previously in *Chesner at al.,* was then added to the mitochondrial sample which was then shaken vigorously and centrifuged at 21130 x g for 5 min at room temperature. The top layer was then transferred to a new microcentrifuge tube and low molecular weight DNA was recovered by ethanol precipitation.

Bicinchoninic acid assay (BCA). Nuclear protein extract concentration was calculated using the BCA assay. Briefly, glycerol adjusted nuclear protein extract was serially diluted in Buffer A containing 350 mM NaCl, 0.70 mug/mL Pepstatin, 0.1 ug/mL

Leupeptin, 0.1 ug/mL aprotinin, and 1 mM PMSF and 10% glycerol. (BSA) standards were then prepared in identical buffer according to the manufacturer's protocol (23225, Thermo Scientific) and 25µL of each diluted standard was added to a 96-well plate (3595, Costar) along with 25µL of each sample in lysis solution (loaded in triplicate). Absorbance values were determined by TECAN Infinite M100 Pro Microplate reader and protein concentration was determined according to the manufacturer's protocol.

Immunoprecipitation and PCR analysis. DNA recovered from transfected cells, extracts, or electroporated nuclei was treated with 40 units of *Hha* I endonuclease and incubated at 37° C for 1 hour. Following restriction digest, samples were mixed with 200 uL IP Buffer (25 mM Tris-HCl pH 8.0, 150 mM NaCl, 1 mM EDTA, 1 % NP-40, 2.5 % (w/w) BSA 250 pmol of recombinant hOGG1). 10% of this mixture was transferred to a new microcentrifuge tube and saved as "input control". To the remaining sample, antibody for pulldown was added (in the amounts described in Table 3.2), and samples were placed on a tube inverter at 4° C for 3 hours. For each pulldown, 5 uL of protein G-coupled Dynabeads were incubated with 200 uL Blocking Buffer (25 mM Tris-HCl, pH 8.0, 150 mM NaCl, 1 mM EDTA, 1 % NP-40, 5 % (w/w) BSA, 250 pmol recombinant hOGG1), and inverted at 4° C for 3 hours. Protein g-containing mixture and DNA/antibody containing-mixture were combined and incubated at 4° C for 1 hour. Microcentrifuge tubes containing the protein G-antibody-DNA mixture were then placed on a magnetic separation rack and protein G beads were washed 3x with Washing Buffer 1 (25 mM Tris-HCl, pH 8.0, 150 mM NaCl, 1 mM EDTA, 1 % NP-40 and 2.5 % (w/w)

BSA), 2X with Washing Buffer 2 (25 mM Tris-HCl, pH 8.0, 150 mM NaCl, 1 mM EDTA), and 2X with 1X TE buffer. Antibody-bound material was recovered from protein G beads by incubation with 8 units of proteinase K in 200 uL buffer containing 10 mM Tris-HCl, pH 8.0, 1 mM EDTA, 0.5 % SDS. Proteinase K-treated samples were incubated for 1 hour at 37° C and recovered by QIAquick PCR purification kit (following manufacturer protocol). 1 uL of PCR purified DNA was then added to 27 uL DI H2O, 30 uL 2X SYBR Green Master Mix, and 100 pmoles of each primer. (DNA was amplified by two different primer sets in parallel: for detection of DPC containing fragment, primer pair Fragment a L and Fragment a R (Table 3.1) were used, and for detection of control fragment, primer pair Fragment b L and Fragment b R (Table 3.1) were used. All samples were loaded in duplicate onto a 96 well plate and Real time PCR was performed using the Applied Biosystems StepOnePlus Real Time PCR System under the following conditions: 10 min denaturing at 95° C (1X), then 30 seconds denaturing at 95° C, 30 seconds primer annealing at 57° C, and 30 seconds for Taq polymerase extension at 72° C (40X).

KCl-SDS precipitation. DNA recovered from transfected cells by HIRT prep and ethanol precipitation was then treated with *Hha* I restriction enzyme and SDS added at a concentration of 0.5%. Samples were incubated at 65° C for 10 minutes, then KCl added to a final concentration of 100 mM. Samples were chilled on ice for 5 minutes, then centrifuged at 21,000 X G for 5 minutes at 4° C. Supernatants were carefully transferred to a new microcentrifuge tube and centrifugation was repeated. Supernatants

were again transferred to a new microcentrifuge tube and analyzed by qPCR, under the same primer and amplification conditions used for qPCR analysis of IP samples.

SSPEqPCR. DNA recovered from transfected cells by HIRT prep and ethanol precipitation was then subjected to analysis by SSPEqPCR as described previously. Briefly, DNA was mixed with DI H2O, 2X SYBR Green Master Mix, and DPC F primer (Table 3.1). One half of the sample was chilled on ice while the other half was subjected to 8 rounds of strand specific PCR. Next, DPC R primer (Table 3.1) was added to all samples which were then loaded in duplicate onto a 96 well plate and Real time PCR was performed using the Applied Biosystems StepOnePlus Real Time PCR System under the following conditions: 10 min denaturing at 95° C (1X), followed by 30 seconds denaturing at 95° C, 30 seconds primer annealing and Taq polymerase extension at 60° C (30X). Delta Cts were calculated by subtracting the Ct of the sample that underwent 8 cycles of Strand Specific PCR from the Ct of its respective sample that, in parallel, did not undergo 8 cycles of Strand Specific PCR. Percent undamaged DNA was calculated by using the formula (Percent undamaged = 2^Delta Ct/2^3*100) and percent repair was calculated using the formula [Percent Repair = (Percent Undamaged Tx) - (Percent Undamaged To)].

Biotin hairpin capture. Streptavidin-coupled Dynabeads were washed per manufacturer's recommendation, then combined with biotinylated-hairpin recovered from electroporated nuclei or nuclear extract. Samples were incubated with rotation for 15 minutes at room temperature, placed on a magnetic microcentrifuge rack and washed

two times with 1X B&W Buffer (10 mM Tris-HCl, pH 7.4, 1 mM EDTA, 2M NaCl) containing 0.1% SDS. Biotinylated hairpin was eluted from Dynabeads by incubation at 95° C for 5 minutes in 0.4% SDS solution.

Western Blot analysis. AP hairpin, DPC hairpin, or DPC plasmid were recovered from nuclear fractions as described above then boiled for 5 min in 5X protein loading dye (Quality Biological, 351-334-021) and run at 110V on a Bolt 10% Bis-Tris gel (ThermoFisher Scientific NW04120BOX). Proteins were transferred to a PVDF membrane for 60 minutes at 10V in 1X Bolt Transfer Buffer (Novex BT00061) utilizing the Mini Blot Module transfer system (ThermoFisher Scientific B1000). After blocking, blots were probed with primary antibodies at 4° C overnight, and secondary antibodies for one hour at room temperature in the dilutions described in Table 2.2. The Western blots were developed using the Pierce ECL Western Blotting Substrate (ThermoFisher Scientific 32209) and images were captured using a Bio-Rad ChemiDoc MP imaging system.

Chapter 4

Discussion

I. DISCUSSION OF THE MODEL

My lab has shown that one site-specific, chemically homogenous DPC substrate generated *in vitro* can be transfected into cells, and that manipulation of transfection conditions results in the shuttling of the DPC substrate into primarily NER-mediated or HR-mediated repair pathways. In *Chapter 2* and *Chapter 3* of this dissertation, I described the use of two novel qPCR-based assays to study pathway-specific DPC post-translational modifications and removal. Using IP-qPCR, post-translational modifications of the DNA crosslinked protein can be detected, while using KCl-SDS-qPCR, early DPC repair events leading to crosslinked protein removal can be quantified. As I am interested in understanding the mechanisms by which mammalian cells orchestrate the initiation of DPC repair by NER or HR, these two methods of DPC analysis provide an advantage over the SSPEqPCR assay previously used by my lab. SSPEqPCR is used to sensitively quantify *complete* DPC repair, and thus is blind to the processes that mediate the early modifications made to the DPC following its recognition.

Using these systems, I showed that DPC removal by NER and by HR is ubiquitin-dependent, and that only DPC removal by NER is proteasome-dependent. I showed that DPCs are only modified with K48 polyubiquitin chains in the presence of NER machinery and are modified with K63 polyubiquitin chains in the presence and absence of NER machinery. Interestingly, in the absence of NER machinery, K63 polyubiquitination of the crosslinked protein was ablated in the presence of homologous donor. Together, these findings allowed me to propose a model in which differential DPC polyubiquitination modulates NER and HR mediated DPC repair. K48polyubiquitination

of the crosslinked protein triggers proteasomal degradation of the oversized crosslinked protein to facilitate its repair by NER, while, in the absence of NER machinery, K63 polyubiquitination triggers the recruitment of HR machinery and the homologous donor search. The predictions made by this model are consistent with studies that have reported that oversized DPCs are subject to repair by HR, while only DPCs <14 kDa are amenable to repair by NER [76, 78] as well as reports that DPCs formed in response to cellular treatment with topoisomerase poisons are K48 and K63 polyubiquitinated [66]. While K48 polyubiquitination is known to trigger proteasomal degradation of the target protein, K63 polyubiquitin chains are known to trigger multiple signaling pathways [139-142]. While others have not studied the signaling role of K63 polyubiquitination of DPCs these findings are consistent with literature reports that K63-polyubiquitin chains trigger the recruitment of repair machinery to DSBs to promote repair by HR [135, 182, 183]. Finally, the model that I have proposed explains a discrepancy in DPC repair research, i.e., that some studies report a role for the proteasome in DPC repair while others report no role for the proteasome in DPC repair research (See *Introduction)*.

In *Chapter 3* I expanded on the findings of *Chapter 2* by showing that: 1) DPC SUMOylation occurs on a different lysine residue on the crosslinked protein than the one on which DPC polyubiquitination occurs, 2) DPC SUMOylation occurs with faster kinetics than DPC ubiquitination, and 3) DPC SUMOylation does not require the presence of DNA repair machinery to occur. Additionally, I found that pharmacological inhibition of SUMOylation resulted in the abolishment of DPC ubiquitination. These findings show that DPC SUMOylation occurs prior to DPC ubiquitination and suggest

that SUMOylation may trigger DPC ubiquitination. While these findings require further investigation, they are supported by other studies that show that xenobiotic induced DPC ubiquitination is SUMO dependent [66, 138], and provide a mechanistic explanation for the first DPC ubiquitination event in my proposed model (K63 polyubiquitination).

To further expand our understanding of the mechanisms that modulate DPC recognition and repair, I developed and validated a simplified, nuclear extract-based system in which DPC post-translational modification and recruitment studies can be conducted. Post-translational modification of proteins as well as recruitment of repair machinery are transient processes that may occur too rapidly for efficient detection in intact cells. As nuclear extracts are a more simplified system, these transient processes may occur more slowly, and thus early repair intermediates accumulate and are easier purify and subsequently analyze. To my knowledge, no other DPC repair studies have been carried out in electroporated nuclei, therefore this presents a novel, simpler approach to studying the mammalian DPC response.

While I have preliminarily shown that both DPCs formed on an M13 molecule and on a biotinylated hairpin molecule are ubiquitinated in extracts, I am interested in next completing a series of experiments (that will be discussed in the *Future Directions* section of this dissertation) that will allow a broader investigation of the role of ubiquitination SUMOylation in DPC repair.

II. CLINICAL IMPLICATIONS

An overarching goal of DPC repair research is to understand the mechanisms by which mammalian cells recognize and respond to DNA damage to identify therapeutic targets that can be used to sensitize cancer cells to DNA damaging drugs, and thus decrease the possibility of cancer cell resistance to these drugs. The work described above proposes several signaling events in NER and HR mediated DPC repair that, if targeted, could potentially achieve this goal. As NER mediated DPC repair is proteasome-dependent, I predict that blocking proteasomal activity in cancer cells that are treated with DPC forming drugs will impair their ability to repair DPCs and thus sensitize them to this DNA damaging treatment. This is supported by findings that co-treatment of cancer cells with the proteasome inhibitor bortezomib sensitized them to cisplatin treatment [202] and the proteasome inhibitor lactacystin enhanced cisplatin cytotoxicity in Hela cells [203]. Identification of the E3 ubiquitin ligase involved in K48 and K63 polyubiquitination of DPCs could thus result in the identification of an additional target for the prevention of cellular repair of DPCs formed in response to treatment by DPC forming drugs and thus sensitize these cells to these drugs. Similarly, identification of the enzymes involved in the nucleolytic incision of the DNA surrounding the DPC for the initiation of repair by HR could also impair the ability of the cells to repair DPCs by HR. More generally, as both NER and HR mediated DPC repair are ubiquitin dependent, I speculate that blocking DPC ubiquitination using pharmacological inhibitors of the involved E3 ubiquitin ligases could sensitize cells to DPC forming drugs. Additionally, as I found that the inhibition of DPC SUMOylation also impaired DPC ubiquitination, I

speculate that targeting of the SUMO pathway could also sensitize cells to treatment by DPC forming drugs.

Overall, the model presented in this presentation proposes a mechanistic explanation for the initiation of DPC repair by NER or HR. While aspects of this model remain to be expanded and tested, the model nevertheless offers a variety of signaling events that could potentially be therapeutically targeted for the sensitization of cancer cells to DPC forming drugs.

CHAPTER 5

Future Directions

I. TESTING THE MODEL

The work presented herein describes the development of multiple tools for the study of mammalian mechanisms of DPC recognition and repair, and the use of these tools to propose a model for the role of ubiquitin and the proteasome in DPC repair by NER and HR. While the majority of our studies have been conducted by using qPCR-based assays to analyze DPCs recovered from transfected cells, the extract-based systems will allow continued investigation of novel aspects of the mammalian DPC response and a fine-tuning of our understanding of ones that I have already studied.

All of the studies described in this dissertation were conducted utilizing a DPC substrate that was generated by crosslinking OGG1 to an abasic site in double stranded DNA. Utilizing a chemically homogenous lesion allows us to overcome some of the obstacles of DPC research discussed in *Chapter 1* (inability to differentiate mechanisms that modulate structurally different DPCs formed by the same DNA damaging drug) however, there is interest in generating additional DPC lesions that can be subjected to the same analyses discussed in this dissertation. DPC substrates I am interested in generating include site-specific topoisomerase-DPCs, PARP-1 DPCs, as well as DPCs crosslinked to a 5-formylcytosine or 7-deazaguanine residue. Generation of these DPC substrates will allow us carry out the natural next step of the work discussed herein, which is to query whether the mechanisms that orchestrate NER and HR mediated DPC repair vary in response to changes in the chemical linkage or crosslinked protein that form the structure of the DPC.

Another approach that can be used to study the orchestration of the DPC response is the extract-based system. In this way it is possible to incubate 10,000-fold more hairpin DPC substrate in the nuclear protein extracts relative to the plasmid DPC substrates. Using larger amounts of DPC substrates will allow for proteomics-based analyses of the DPCs following their incubation in nuclear extracts. Utilizing proteomics, I can conduct both hypothesis generating and hypothesis testing analyses of the mechanisms that modulate DPC recognition and repair. Examples of investigations that can be conducted utilizing proteomics include 1) identification of the first proteins recruited to the DPC in the extract and test the hypothesis that they are involved in triggering ubiquitination or SUMOylation of the DPC 2) identification of candidate E3 ubiquitin ligases that are involved in DPC ubiquitination 3) identification of the nucleolytic enzymes involved in HR mediated DPC repair 4) tests of the hypothesis that the proteasome is only recruited to the DPC for NER mediated repair and 5) tests of the hypothesis that K63-polyubiquitination triggers the recruitment of HR repair machinery.

Additional studies that I am interested in include using the transfection-based system to test predictions made by our proposed model that I have not yet been able to investigate. One topic I am interested in is the role of SPRTN in DPC recognition and repair. Additionally, I am interested in further understanding the role of SUMO in DPC ubiquitination and repair. While I have data to suggest that, in NER mediated DPC repair, pharmacologically blocking SUMOylation also results in the inhibition of DPC ubiquitination, the mechanism by which SUMOylation modulates DPC ubiquitination remains to be understood. The generation of OGG1 mutants with novel K-R substitutions

at OGG1 lysine residues may allow for the identification of the residue at which OGG1 is SUMOylated, and block SUMOylation at this residue to further understand the role of SUMO in DPC ubiquitination. Additionally, all of the studies that I have done to study DPC SUMOylation have been done in an NER-mediated context, yet I remain interested in also understanding the role of SUMO in HR-mediated DPC repair as well.

Next, I am interested in showing that, by blocking post-translational modification of DPCs, the formation of the repair intermediates depicted in the model is also impaired or even fully inhibited. Our model predicts that, in the case of an oversized crosslinked protein like OGG1, the NER excision product should contain a proteolytically degraded OGG1 molecule, while the HR excision product should contain an intact OGG1 molecule, and I am interested in conducting extract-based and cell-based studies that will allow for the to capture these repair intermediates and thereby test these hypotheses.

II. CLINICAL IMPLICATIONS

Finally, as mentioned in the *Discussion* section, the overarching goal of DPC repair research includes the discovery of therapeutic targets for the sensitization of cancer cells resistant to DNA-damaging drugs. Long-term goals of this work would revolve around testing that pharmacological inhibition of key enzymatic steps proposed by the model, including crosslinked protein ubiquitination and SUMOylation, proteasomal degradation, and even homologous donor search, will sensitize cancer cells to treatment by DPC forming drugs including cisplatin, camptothecin, etoposide, and 5-azadC.

BIBLIOGRAPHY

1. Barker, S., M. Weinfeld, and D. Murray, *DNA–protein crosslinks: their induction, repair, and biological consequences.* Mutation Research/Reviews in Mutation Research, 2005. **589**(2): p. 111-135.
2. Zhang, H., Y. Xiong, and J. Chen, *DNA–protein cross-link repair: what do we know now?* Cell & Bioscience, 2020. **10**(1): p. 3.
3. Lai, Y., et al., *Measurement of Endogenous versus Exogenous Formaldehyde–Induced DNA–Protein Crosslinks in Animal Tissues by Stable Isotope Labeling and Ultrasensitive Mass Spectrometry.* Cancer Research, 2016. **76**(9): p. 2652-2661.
4. Chatterjee, N. and G.C. Walker, *Mechanisms of DNA damage, repair, and mutagenesis.* Environ Mol Mutagen, 2017. **58**(5): p. 235-263.
5. Klages-Mundt, N.L. and L. Li, *Formation and repair of DNA-protein crosslink damage.* Science China. Life sciences, 2017. **60**(10): p. 1065-1076.
6. Nakamura, J. and M. Nakamura, *DNA-protein crosslink formation by endogenous aldehydes and AP sites.* DNA Repair (Amst), 2020. **88**: p. 102806.
7. Tretyakova, N.Y., A.I.V. Groehler, and S. Ji, *DNA–Protein Cross-Links: Formation, Structural Identities, and Biological Outcomes.* Accounts of Chemical Research, 2015. **48**(6): p. 1631-1644.
8. Quiñones, J.L., et al., *Enzyme mechanism-based, oxidative DNA–protein cross-links formed with DNA polymerase β in vivo.* Proceedings of the National Academy of Sciences, 2015. **112**(28): p. 8602-8607.

9. Prasad, R., et al., *Repair pathway for PARP-1 DNA-protein crosslinks.* DNA Repair (Amst), 2019. **73**: p. 71-77.
10. Regairaz, M., et al., *Mus81-mediated DNA cleavage resolves replication forks stalled by topoisomerase I-DNA complexes.* J Cell Biol, 2011. **195**(5): p. 739-49.
11. Pommier, Y., et al., *Tyrosyl-DNA-phosphodiesterases (TDP1 and TDP2).* DNA Repair, 2014. **19**: p. 114-129.
12. Brown, K.L., et al., *Binding of the human nucleotide excision repair proteins XPA and XPC/HR23B to the 5R-thymine glycol lesion and structure of the cis-(5R,6S) thymine glycol epimer in the 5'-GTgG-3' sequence: destabilization of two base pairs at the lesion site.* Nucleic Acids Res, 2010. **38**(2): p. 428-40.
13. Krokan, H.E. and M. Bjørås, *Base excision repair.* Cold Spring Harb Perspect Biol, 2013. **5**(4): p. a012583.
14. Kumar, A., et al., *Interlocking activities of DNA polymerase β in the base excision repair pathway.* Proceedings of the National Academy of Sciences, 2022. **119**(10): p. e2118940119.
15. Satoh, M.S., G.G. Poirier, and T. Lindahl, *Dual function for poly(ADP-ribose) synthesis in response to DNA strand breakage.* Biochemistry, 1994. **33**(23): p. 7099-106.
16. Langelier, M.F., et al., *Structural basis for DNA damage-dependent poly(ADP-ribosyl)ation by human PARP-1.* Science, 2012. **336**(6082): p. 728-32.
17. Alemasova, E.E. and O.I. Lavrik, *Poly(ADP-ribosyl)ation by PARP1: reaction mechanism and regulatory proteins.* Nucleic Acids Research, 2019. **47**(8): p. 3811-3827.

18. Wei, H. and X. Yu, *Functions of PARylation in DNA Damage Repair Pathways.* Genomics, Proteomics & Bioinformatics, 2016. **14**(3): p. 131-139.

19. Prasad, R., et al., *Suicidal cross-linking of PARP-1 to AP site intermediates in cells undergoing base excision repair.* Nucleic Acids Res, 2014. **42**(10): p. 6337-51.

20. Ji, S., et al., *5-Formylcytosine mediated DNA–protein cross-links block DNA replication and induce mutations in human cells.* Nucleic Acids Research, 2018. **46**(13): p. 6455-6469.

21. LoPachin, R.M. and T. Gavin, *Molecular Mechanisms of Aldehyde Toxicity: A Chemical Perspective.* Chemical Research in Toxicology, 2014. **27**(7): p. 1081-1091.

22. Stingele, J., et al., *Mechanism and Regulation of DNA-Protein Crosslink Repair by the DNA-Dependent Metalloprotease SPRTN.* Mol Cell, 2016. **64**(4): p. 688-703.

23. Groehler, A.t., et al., *Oxidative cross-linking of proteins to DNA following ischemia-reperfusion injury.* Free Radic Biol Med, 2018. **120**: p. 89-101.

24. Hawkins, C.L., D.I. Pattison, and M.J. Davies, *Reaction of protein chloramines with DNA and nucleosides: evidence for the formation of radicals, protein–DNA cross-links and DNA fragmentation.* Biochemical Journal, 2002. **365**(3): p. 605-615.

25. Greenberg, M.M., *Abasic and oxidized abasic site reactivity in DNA: enzyme inhibition, cross-linking, and nucleosome catalyzed reactions.* Acc Chem Res, 2014. **47**(2): p. 646-55.

26. Weng, L., C. Zhou, and M.M. Greenberg, *Probing interactions between lysine residues in histone tails and nucleosomal DNA via product and kinetic analysis.* ACS Chem Biol, 2015. **10**(2): p. 622-30.

27. Swenberg, J.A., et al., *Endogenous versus exogenous DNA adducts: their role in carcinogenesis, epidemiology, and risk assessment.* Toxicol Sci, 2011. **120 Suppl 1**(Suppl 1): p. S130-45.

28. Stützer, A., et al., *Analysis of protein-DNA interactions in chromatin by UV induced cross-linking and mass spectrometry.* Nature Communications, 2020. **11**(1): p. 5250.

29. Himmelstein, M.W., et al., *Toxicology and epidemiology of 1,3-butadiene.* Crit Rev Toxicol, 1997. **27**(1): p. 1-108.

30. Tretyakova, N., et al., *Identification and quantitation of DNA adducts from calf thymus DNA exposed to 3,4-epoxy-1-butene.* Carcinogenesis, 1997. **18**(1): p. 137-147.

31. Tretyakova, N.Y., et al., *Synthesis, Characterization, and in Vitro Quantitation of N-7-Guanine Adducts of Diepoxybutane.* Chemical Research in Toxicology, 1997. **10**(7): p. 779-785.

32. Wickramaratne, S., et al., *Base Excision Repair of N6-Deoxyadenosine Adducts of 1,3-Butadiene.* Biochemistry, 2016. **55**(43): p. 6070-6081.

33. Sangaraju, D., et al., *Capillary HPLC-Accurate Mass MS/MS Quantitation of N7-(2,3,4-Trihydroxybut-1-yl)-guanine Adducts of 1,3-Butadiene in Human Leukocyte DNA.* Chemical Research in Toxicology, 2013. **26**(10): p. 1486-1497.

34. Sangaraju, D., et al., *NanoHPLC-nanoESI+-MS/MS Quantitation of Bis-N7-Guanine DNA–DNA Cross-Links in Tissues of B6C3F1 Mice Exposed to subppm Levels of 1,3-Butadiene.* Analytical Chemistry, 2012. **84**(3): p. 1732-1739.

35. Goggin, M., et al., *Persistence and Repair of Bifunctional DNA Adducts in Tissues of Laboratory Animals Exposed to 1,3-Butadiene by Inhalation.* Chemical Research in Toxicology, 2011. **24**(6): p. 809-817.

36. Koc, H., et al., *Molecular Dosimetry of N-7 Guanine Adduct Formation in Mice and Rats Exposed to 1,3-Butadiene.* Chemical Research in Toxicology, 1999. **12**(7): p. 566-574.

37. Park, S. and N. Tretyakova, *Structural Characterization of the Major DNA−DNA Cross-Link of 1,2,3,4-Diepoxybutane.* Chemical Research in Toxicology, 2004. **17**(2): p. 129-136.

38. Groehler, A.t., A. Degner, and N.Y. Tretyakova, *Mass Spectrometry-Based Tools to Characterize DNA-Protein Cross-Linking by Bis-Electrophiles.* Basic Clin Pharmacol Toxicol, 2017. **121 Suppl 3**(Suppl 3): p. 63-77.

39. Chesner, L.N., et al. *Cellular Repair of DNA–DNA Cross-Links Induced by 1,2,3,4-Diepoxybutane*. International Journal of Molecular Sciences, 2017. **18**, DOI: 10.3390/ijms18051086.

40. Cao, P.R., et al., *The DNA minor groove-alkylating cyclopropylpyrroloindole drugs adozelesin and bizelesin induce different DNA damage response pathways in human colon carcinoma HCT116 cells.* Mol Cancer Ther, 2003. **2**(7): p. 651-9.

41. Begleiter, A., *Clinical applications of quinone-containing alkylating agents.* Front Biosci, 2000. **5**: p. E153-71.

42. He, Q., C.H. Liang, and S.J. Lippard, *Steroid hormones induce HMG1 overexpression and sensitize breast cancer cells to cisplatin and carboplatin.* Proceedings of the National Academy of Sciences, 2000. **97**(11): p. 5768-5772.

43. Tiek, D. and S.-Y. Cheng, *DNA damage and metabolic mechanisms of cancer drug resistance.* Cancer Drug Resistance, 2022. **5**(2): p. 368-379.

44. Pommier, Y., et al., *DNA topoisomerases and their poisoning by anticancer and antibacterial drugs.* Chem Biol, 2010. **17**(5): p. 421-33.

45. Polavarapu, A., et al., *The Mechanism of Guanine Alkylation by Nitrogen Mustards: A Computational Study.* The Journal of Organic Chemistry, 2012. **77**(14): p. 5914-5921.

46. Loeber, R.L., et al., *Proteomic Analysis of DNA−Protein Cross-Linking by Antitumor Nitrogen Mustards.* Chemical Research in Toxicology, 2009. **22**(6): p. 1151-1162.

47. Loeber, R., et al., *Cross-Linking of the DNA Repair Protein O6-Alkylguanine DNA Alkyltransferase to DNA in the Presence of Antitumor Nitrogen Mustards.* Chemical Research in Toxicology, 2008. **21**(4): p. 787-795.

48. Groehler, A.I.V., et al., *Covalent DNA–Protein Cross-Linking by Phosphoramide Mustard and Nornitrogen Mustard in Human Cells.* Chemical Research in Toxicology, 2016. **29**(2): p. 190-202.

49. Wickramaratne, S., et al., *Bypass of DNA-Protein Cross-links Conjugated to the 7-Deazaguanine Position of DNA by Translesion Synthesis Polymerases.* J Biol Chem, 2016. **291**(45): p. 23589-23603.

50. Thompson, V.R. and A.P. DeCaprio, *Covalent Adduction of Nitrogen Mustards to Model Protein Nucleophiles.* Chemical Research in Toxicology, 2013. **26**(8): p. 1263-1271.

51. Ji, S., et al., *Transcriptional Bypass of DNA–Protein and DNA–Peptide Conjugates by T7 RNA Polymerase.* ACS Chemical Biology, 2019. **14**(12): p. 2564-2575.

52. Pujari, S.S. and N. Tretyakova, *Chemical Biology of N5-Substituted Formamidopyrimidine DNA Adducts.* Chemical Research in Toxicology, 2017. **30**(1): p. 434-452.

53. Pande, P., et al., *Mutagenicity of a Model DNA-Peptide Cross-Link in Human Cells: Roles of Translesion Synthesis DNA Polymerases.* Chemical Research in Toxicology, 2017. **30**(2): p. 669-677.

54. Minko, I.G., C.J. Rizzo, and R.S. Lloyd, *Mutagenic potential of nitrogen mustard-induced formamidopyrimidine DNA adduct: Contribution of the non-canonical α-anomer.* Journal of Biological Chemistry, 2017. **292**(46): p. 18790-18799.

55. Gruppi, F., et al., *Characterization of nitrogen mustard formamidopyrimidine adduct formation of bis(2-chloroethyl)ethylamine with calf thymus DNA and a human mammary cancer cell line.* Chemical research in toxicology, 2015. **28**(9): p. 1850-1860.

56. Dasari, S. and P.B. Tchounwou, *Cisplatin in cancer therapy: molecular mechanisms of action.* Eur J Pharmacol, 2014. **740**: p. 364-78.

57. Cheung-Ong, K., G. Giaever, and C. Nislow, *DNA-Damaging Agents in Cancer Chemotherapy: Serendipity and Chemical Biology.* Chemistry & Biology, 2013. **20**(5): p. 648-659.

58. Jüttermann, R., E. Li, and R. Jaenisch, *Toxicity of 5-aza-2'-deoxycytidine to mammalian cells is mediated primarily by covalent trapping of DNA methyltransferase rather than DNA demethylation.* Proc Natl Acad Sci U S A, 1994. **91**(25): p. 11797-801.

59. Jackson-Grusby, L., et al., *Mutagenicity of 5-aza-2'-deoxycytidine is mediated by the mammalian DNA methyltransferase.* Proceedings of the National Academy of Sciences, 1997. **94**(9): p. 4681-4685.

60. Karran, P., *Mechanisms of tolerance to DNA damaging therapeutic drugs.* Carcinogenesis, 2001. **22**(12): p. 1931-1937.

61. Naldiga, S., et al., *Error-prone replication of a 5-formylcytosine-mediated DNA-peptide cross-link in human cells.* Journal of Biological Chemistry, 2019. **294**(27): p. 10619-10627.

62. Basu, A.K. and J.M. Essigmann, *Establishing Linkages Among DNA Damage, Mutagenesis, and Genetic Diseases.* Chemical Research in Toxicology, 2022. **35**(10): p. 1655-1675.

63. Ira, G., et al., *DNA end resection, homologous recombination and DNA damage checkpoint activation require CDK1.* Nature, 2004. **431**(7011): p. 1011-7.

64. Aylon, Y., B. Liefshitz, and M. Kupiec, *The CDK regulates repair of double-strand breaks by homologous recombination during the cell cycle.* Embo j, 2004. **23**(24): p. 4868-75.

65. Sun, Y., et al., *Excision repair of topoisomerase DNA-protein crosslinks (TOP-DPC).* DNA Repair (Amst), 2020. **89**: p. 102837.

66. Sun, Y., et al., *A conserved SUMO pathway repairs topoisomerase DNA-protein cross-links by engaging ubiquitin-mediated proteasomal degradation.* Science Advances. **6**(46): p. eaba6290.

67. Plo, I., et al., *Association of XRCC1 and tyrosyl DNA phosphodiesterase (Tdp1) for the repair of topoisomerase I-mediated DNA lesions.* DNA Repair (Amst), 2003. **2**(10): p. 1087-100.

68. Hartung, F. and H. Puchta, *Molecular characterization of homologues of both subunits A (SPO11) and B of the archaebacterial topoisomerase 6 in plants.* Gene, 2001. **271**(1): p. 81-6.

69. Hartung, F. and H. Puchta, *Molecular characterisation of two paralogous SPO11 homologues in Arabidopsis thaliana.* Nucleic acids research, 2000. **28**(7): p. 1548-1554.

70. Malik, S.B., et al., *Protist homologs of the meiotic Spo11 gene and topoisomerase VI reveal an evolutionary history of gene duplication and lineage-specific loss.* Mol Biol Evol, 2007. **24**(12): p. 2827-41.

71. Romanienko, P.J. and R.D. Camerini-Otero, *Cloning, Characterization, and Localization of Mouse and Human SPO11.* Genomics, 1999. **61**(2): p. 156-169.

72. Keeney, S., C.N. Giroux, and N. Kleckner, *Meiosis-Specific DNA Double-Strand Breaks Are Catalyzed by Spo11, a Member of a Widely Conserved Protein Family.* Cell, 1997. **88**(3): p. 375-384.

73. Cao, L., E. Alani, and N. Kleckner, *A pathway for generation and processing of double-strand breaks during meiotic recombination in S. cerevisiae.* Cell, 1990. **61**(6): p. 1089-1101.

74. Keeney, S., *Spo11 and the Formation of DNA Double-Strand Breaks in Meiosis.* Genome Dyn Stab, 2008. **2**: p. 81-123.

75. Neale, M.J., J. Pan, and S. Keeney, *Endonucleolytic processing of covalent protein-linked DNA double-strand breaks.* Nature, 2005. **436**(7053): p. 1053-1057.

76. Nakano, T., et al., *Nucleotide Excision Repair and Homologous Recombination Systems Commit Differentially to the Repair of DNA-Protein Crosslinks.* Molecular Cell, 2007. **28**(1): p. 147-158.

77. Chesner, L.N. and C. Campbell, *A quantitative PCR-based assay reveals that nucleotide excision repair plays a predominant role in the removal of DNA-protein crosslinks from plasmids transfected into mammalian cells.* DNA Repair, 2018. **62**: p. 18-27.

78. Baker, D.J., et al., *Nucleotide Excision Repair Eliminates Unique DNA-Protein Cross-links from Mammalian Cells *.* Journal of Biological Chemistry, 2007. **282**(31): p. 22592-22604.

79. Minko, I.G., Y. Zou, and R.S. Lloyd, *Incision of DNA-protein crosslinks by UvrABC nuclease suggests a potential repair pathway involving nucleotide excision repair.* Proc Natl Acad Sci U S A, 2002. **99**(4): p. 1905-9.

80. Reardon, J.T. and A. Sancar, *Repair of DNA–polypeptide crosslinks by human excision nuclease.* Proceedings of the National Academy of Sciences, 2006. **103**(11): p. 4056-4061.

81. Fang, Q., *DNA-protein crosslinks processed by nucleotide excision repair and homologous recombination with base and strand preference in E. coli model system.* Mutat Res, 2013. **741-742**: p. 1-10.

82. Chesner, L.N., et al., *DNA-protein crosslinks are repaired via homologous recombination in mammalian mitochondria.* DNA Repair (Amst), 2021. **97**: p. 103026.

83. Nishioka, H., *Lethal and mutagenic action of formaldehyde in Hcr+ and Hcr− strains of Escherichiacoli.* Mutation Research/Fundamental and Molecular Mechanisms of Mutagenesis, 1973. **17**(2): p. 261-265.

84. Orta, M.L., et al., *5-Aza-2'-deoxycytidine causes replication lesions that require Fanconi anemia-dependent homologous recombination for repair.* Nucleic Acids Res, 2013. **41**(11): p. 5827-36.

85. Setlow, R.B. and W.L. Carrier, *THE DISAPPEARANCE OF THYMINE DIMERS FROM DNA: AN ERROR-CORRECTING MECHANISM.* Proc Natl Acad Sci U S A, 1964. **51**(2): p. 226-31.

86. Boyce, R.P. and P. Howard-Flanders, *RELEASE OF ULTRAVIOLET LIGHT-INDUCED THYMINE DIMERS FROM DNA IN E. COLI K-12.* Proc Natl Acad Sci U S A, 1964. **51**(2): p. 293-300.

87. Pettijohn, D. and P. Hanawalt, *EVIDENCE FOR REPAIR-REPLICATION OF ULTRAVIOLET DAMAGED DNA IN BACTERIA.* J Mol Biol, 1964. **9**: p. 395-410.

88. Rasmussen, R.E. and R.B. Painter, *Evidence for Repair of Ultra-Violet Damaged Deoxyribonucleic Acid in Cultured Mammalian Cells.* Nature, 1964. **203**(4952): p. 1360-1362.

89. Cleaver, J.E., *Defective Repair Replication of DNA in Xeroderma Pigmentosum.* Nature, 1968. **218**(5142): p. 652-656.

90. Hess, M.T., et al., *Bipartite substrate discrimination by human nucleotide excision repair.* Proceedings of the National Academy of Sciences, 1997. **94**(13): p. 6664-6669.

91. Petruseva, I.O., A.N. Evdokimov, and O.I. Lavrik, *Molecular mechanism of global genome nucleotide excision repair.* Acta Naturae, 2014. **6**(1): p. 23-34.

92. Daniel, L., et al., *Mechanistic insights in transcription-coupled nucleotide excision repair of ribosomal DNA.* Proceedings of the National Academy of Sciences, 2018. **115**(29): p. E6770-E6779.

93. Compe, E. and J.-M. Egly, *TFIIH: when transcription met DNA repair.* Nature Reviews Molecular Cell Biology, 2012. **13**(6): p. 343-354.

94. Kuper, J., et al., *In TFIIH, XPD helicase is exclusively devoted to DNA repair.* PLoS Biol, 2014. **12**(9): p. e1001954.

95. Rüthemann, P., C. Balbo Pogliano, and H. Naegeli, *Global-genome Nucleotide Excision Repair Controlled by Ubiquitin/Sumo Modifiers.* Front Genet, 2016. **7**: p. 68.

96. Lederberg, J. and E.L. Tatum, *Gene Recombination in Escherichia Coli.* Nature, 1946. **158**(4016): p. 558-558.

97. Tatum, E.L. and J. Lederberg, *Gene Recombination in the Bacterium Escherichia coli.* J Bacteriol, 1947. **53**(6): p. 673-84.

98. Wildy, P., *Recombination with herpes simplex virus.* J Gen Microbiol, 1955. **13**(2): p. 346-60.

99. Holliday, R., *A mechanism for gene conversion in fungi.* Genetical Research, 1964. **5**(2): p. 282-304.

100. Clark, A.J. and A.D. Margulies, *ISOLATION AND CHARACTERIZATION OF RECOMBINATION-DEFICIENT MUTANTS OF ESCHERICHIA COLI K12*.* Proceedings of the National Academy of Sciences, 1965. **53**(2): p. 451-459.

101. Kuzminov, A., *Recombinational repair of DNA damage in Escherichia coli and bacteriophage lambda.* Microbiol Mol Biol Rev, 1999. **63**(4): p. 751-813, table of contents.

102. Michel, B., et al., *Rescue of arrested replication forks by homologous recombination.* Proc Natl Acad Sci U S A, 2001. **98**(15): p. 8181-8.

103. Shinohara, A., H. Ogawa, and T. Ogawa, *Rad51 protein involved in repair and recombination in S. cerevisiae is a RecA-like protein.* Cell, 1992. **69**(3): p. 457-70.

104. Nakano, T., et al., *Homologous Recombination but Not Nucleotide Excision Repair Plays a Pivotal Role in Tolerance of DNA-Protein Cross-links in Mammalian Cells *.* Journal of Biological Chemistry, 2009. **284**(40): p. 27065-27076.

105. de Graaf, B., A. Clore, and A.K. McCullough, *Cellular pathways for DNA repair and damage tolerance of formaldehyde-induced DNA-protein crosslinks.* DNA repair, 2009. **8**(10): p. 1207-1214.

106. Hoa, N.N., et al., *Mre11 Is Essential for the Removal of Lethal Topoisomerase 2 Covalent Cleavage Complexes.* Mol Cell, 2016. **64**(3): p. 580-592.

107. Michel, B., Z. Baharoglu, and R. Lestini, *Molecular genetics of recombination.* 2007.

108. Davis, L. and N. Maizels, *DNA nicks promote efficient and safe targeted gene correction.* PLoS One, 2011. **6**(9): p. e23981.

109. Kim, E., et al., *Precision genome engineering with programmable DNA-nicking enzymes.* Genome Res, 2012. **22**(7): p. 1327-33.

110. Ramirez, C.L., et al., *Engineered zinc finger nickases induce homology-directed repair with reduced mutagenic effects.* Nucleic Acids Res, 2012. **40**(12): p. 5560-8.

111. Jasin, M. and R. Rothstein, *Repair of strand breaks by homologous recombination.* Cold Spring Harb Perspect Biol, 2013. **5**(11): p. a012740.

112. Resnick, M.A., *The repair of double-strand breaks in DNA; a model involving recombination.* J Theor Biol, 1976. **59**(1): p. 97-106.

113. Orr-Weaver, T.L., J.W. Szostak, and R.J. Rothstein, *Yeast transformation: a model system for the study of recombination.* Proc Natl Acad Sci U S A, 1981. **78**(10): p. 6354-8.

114. Szostak, J.W., et al., *The double-strand-break repair model for recombination.* Cell, 1983. **33**(1): p. 25-35.

115. Li, X. and W.-D. Heyer, *Homologous recombination in DNA repair and DNA damage tolerance.* Cell Research, 2008. **18**(1): p. 99-113.

116. Bhargava, R., D.O. Onyango, and J.M. Stark, *Regulation of Single-Strand Annealing and its Role in Genome Maintenance.* Trends Genet, 2016. **32**(9): p. 566-575.

117. Stingele, J., et al., *A DNA-Dependent Protease Involved in DNA-Protein Crosslink Repair.* Cell, 2014. **158**(2): p. 327-338.

118. Lopez-Mosqueda, J., et al., *SPRTN is a mammalian DNA-binding metalloprotease that resolves DNA-protein crosslinks.* eLife, 2016. **5**: p. e21491.

119. Borgermann, N., et al., *SUMOylation promotes protective responses to DNA-protein crosslinks.* The EMBO Journal, 2019. **38**(8): p. e101496.

120. Sun, Y., et al., *Debulking of topoisomerase DNA-protein crosslinks (TOP-DPC) by the proteasome, non-proteasomal and non-proteolytic pathways.* DNA Repair (Amst), 2020. **94**: p. 102926.

121. Mao, Y., et al., *26 S proteasome-mediated degradation of topoisomerase II cleavable complexes.* J Biol Chem, 2001. **276**(44): p. 40652-8.

122. Duxin, Julien P., et al., *Repair of a DNA-Protein Crosslink by Replication-Coupled Proteolysis.* Cell, 2014. **159**(2): p. 346-357.

123. Takeshita, T., et al., *Perturbation of DNA repair pathways by proteasome inhibitors corresponds to enhanced chemosensitivity of cells to DNA damage-inducing agents.* Cancer Chemotherapy and Pharmacology, 2009. **64**(5): p. 1039-1046.

124. Trickey, M., M. Grimaldi, and H. Yamano, *The anaphase-promoting complex/cyclosome controls repair and recombination by ubiquitylating Rhp54 in fission yeast.* Mol Cell Biol, 2008. **28**(12): p. 3905-16.

125. Sarkar, S., et al., *DNA interstrand crosslink repair during G1 involves nucleotide excision repair and DNA polymerase zeta.* Embo j, 2006. **25**(6): p. 1285-94.

126. van Oosten, M., et al., *Differential role of transcription-coupled repair in UVB-induced G2 arrest and apoptosis in mouse epidermis.* Proc Natl Acad Sci U S A, 2000. **97**(21): p. 11268-73.

127. Marini, F., et al., *DNA nucleotide excision repair-dependent signaling to checkpoint activation.* Proceedings of the National Academy of Sciences, 2006. **103**(46): p. 17325-17330.

128. Larsen, N.B., et al., *Replication-Coupled DNA-Protein Crosslink Repair by SPRTN and the Proteasome in Xenopus Egg Extracts.* Mol Cell, 2019. **73**(3): p. 574-588.e7.

129. Aguilera, A. and H. Gaillard, *Transcription and recombination: when RNA meets DNA.* Cold Spring Harb Perspect Biol, 2014. **6**(8).

130. Ouyang, J., et al., *RNA transcripts stimulate homologous recombination by forming DR-loops.* Nature, 2021. **594**(7862): p. 283-288.

131. Nickoloff, J.A. and R.J. Reynolds, *Transcription stimulates homologous recombination in mammalian cells.* Mol Cell Biol, 1990. **10**(9): p. 4837-45.

132. Sugasawa, K., et al., *UV-Induced Ubiquitylation of XPC Protein Mediated by UV-DDB-Ubiquitin Ligase Complex.* Cell, 2005. **121**(3): p. 387-400.

133. Huang, F. and A.V. Mazin, *A Small Molecule Inhibitor of Human RAD51 Potentiates Breast Cancer Cell Killing by Therapeutic Agents in Mouse Xenografts.* PLOS ONE, 2014. **9**(6): p. e100993.

134. Orthwein, A., et al., *A mechanism for the suppression of homologous recombination in G1 cells.* Nature, 2015. **528**(7582): p. 422-6.

135. Luo, K., et al., *A phosphorylation-deubiquitination cascade regulates the BRCA2-RAD51 axis in homologous recombination.* Genes Dev, 2016. **30**(23): p. 2581-2595.

136. Yu, X., et al., *BRCA1 ubiquitinates its phosphorylation-dependent binding partner CtIP.* Genes & development, 2006. **20**(13): p. 1721-1726.

137. Liu, J.C.Y., et al., *Mechanism and function of DNA replication-independent DNA-protein crosslink repair via the SUMO-RNF4 pathway.* The EMBO Journal, 2021. **40**(18): p. e107413.

138. Ruggiano, A., et al., *The protease SPRTN and SUMOylation coordinate DNA-protein crosslink repair to prevent genome instability.* Cell Rep, 2021. **37**(10): p. 110080.

139. Yau, R. and M. Rape, *The increasing complexity of the ubiquitin code.* Nature Cell Biology, 2016. **18**(6): p. 579-586.

140. Chau, V., et al., *A multiubiquitin chain is confined to specific lysine in a targeted short-lived protein.* Science, 1989. **243**(4898): p. 1576-83.

141. Huen, M.S.Y., et al., *RNF8 Transduces the DNA-Damage Signal via Histone Ubiquitylation and Checkpoint Protein Assembly.* Cell, 2007. **131**(5): p. 901-914.

142. Strous, G.J., et al., *The ubiquitin conjugation system is required for ligand-induced endocytosis and degradation of the growth hormone receptor.* Embo j, 1996. **15**(15): p. 3806-12.

143. Grafstrom, R.C., et al., *Formaldehyde Damage to DNA and Inhibition of DNA Repair in Human Bronchial Cells.* Science, 1983. **220**(4593): p. 216-218.

144. Kawanishi, M., T. Matsuda, and T. Yagi, *Genotoxicity of formaldehyde: molecular basis of DNA damage and mutation.* Frontiers in Environmental Science, 2014. **2**.

145. Rocha, C.R.R., et al., *DNA repair pathways and cisplatin resistance: an intimate relationship.* Clinics (Sao Paulo), 2018. **73**(suppl 1): p. e478s.

146. Sears, C.R. and J.J. Turchi, *Complex cisplatin-double strand break (DSB) lesions directly impair cellular non-homologous end-joining (NHEJ) independent of*

downstream damage response (DDR) pathways. J Biol Chem, 2012. **287**(29): p. 24263-72.

147. Frankenberg-Schwager, M., et al., *Cisplatin-mediated DNA double-strand breaks in replicating but not in quiescent cells of the yeast Saccharomyces cerevisiae.* Toxicology, 2005. **212**(2-3): p. 175-84.

148. Binaschi, M., F. Zunino, and G. Capranico, *Mechanism of action of DNA topoisomerase inhibitors.* Stem Cells, 1995. **13**(4): p. 369-379.

149. Ming, X., et al., *Mass Spectrometry Based Proteomics Study of Cisplatin-Induced DNA–Protein Cross-Linking in Human Fibrosarcoma (HT1080) Cells.* Chemical Research in Toxicology, 2017. **30**(4): p. 980-995.

150. Degner, A., et al., *Discovery of Novel N-(4-Hydroxybenzyl)valine Hemoglobin Adducts in Human Blood.* Chem Res Toxicol, 2018. **31**(12): p. 1305-1314.

151. Michaelson-Richie, E.D., et al., *DNA-protein cross-linking by 1,2,3,4-diepoxybutane.* J Proteome Res, 2010. **9**(9): p. 4356-67.

152. Ham, Y.-H., et al., *Proteomics Study of DNA–Protein Crosslinks in Methylmethanesulfonate and Fe2+-EDTA-Exposed Human Cells.* Chemical Research in Toxicology, 2020. **33**(11): p. 2739-2744.

153. Nakano, T., et al., *T7 RNA polymerases backed up by covalently trapped proteins catalyze highly error prone transcription.* J Biol Chem, 2012. **287**(9): p. 6562-72.

154. Nakano, T., et al., *Translocation and stability of replicative DNA helicases upon encountering DNA-protein cross-links.* J Biol Chem, 2013. **288**(7): p. 4649-58.

155. Kuo, H.K., J.D. Griffith, and K.N. Kreuzer, *5-Azacytidine induced methyltransferase-DNA adducts block DNA replication in vivo.* Cancer Res, 2007. **67**(17): p. 8248-54.

156. Wong, V.C.-L., et al., *S-phase sensing of DNA-protein crosslinks triggers TopBP1-independent ATR activation and p53-mediated cell death by formaldehyde.* Cell Cycle, 2012. **11**(13): p. 2526-2537.

157. Chválová, K., V. Brabec, and J. Kašpárková, *Mechanism of the formation of DNA–protein cross-links by antitumor cisplatin.* Nucleic Acids Research, 2007. **35**(6): p. 1812-1821.

158. Chu, G., *Cellular responses to cisplatin. The roles of DNA-binding proteins and DNA repair.* J Biol Chem, 1994. **269**(2): p. 787-90.

159. Galluzzi, L., et al., *Molecular mechanisms of cisplatin resistance.* Oncogene, 2012. **31**(15): p. 1869-1883.

160. Skok, Ž., et al., *Dual Inhibitors of Human DNA Topoisomerase II and Other Cancer-Related Targets.* Journal of Medicinal Chemistry, 2020. **63**(3): p. 884-904.

161. Rasheed, Z.A. and E.H. Rubin, *Mechanisms of resistance to topoisomerase I-targeting drugs.* Oncogene, 2003. **22**(47): p. 7296-7304.

162. Ledesma, F.C., et al., *A human 5'-tyrosyl DNA phosphodiesterase that repairs topoisomerase-mediated DNA damage.* Nature, 2009. **461**(7264): p. 674-678.

163. Yang, S.W., et al., *A eukaryotic enzyme that can disjoin dead-end covalent complexes between DNA and type I topoisomerases.* Proceedings of the National Academy of Sciences, 1996. **93**(21): p. 11534-11539.

164. Ali Azam, T., et al., *Growth Phase-Dependent Variation in Protein Composition of the Escherichia coli Nucleoid.* Journal of Bacteriology, 1999. **181**(20): p. 6361-6370.

165. Sung, P. and H. Klein, *Mechanism of homologous recombination: mediators and helicases take on regulatory functions.* Nature Reviews Molecular Cell Biology, 2006. **7**(10): p. 739-750.

166. Đermić, E., et al., *3'-Terminated Overhangs Regulate DNA Double-Strand Break Processing in Escherichia coli.* G3 Genes|Genomes|Genetics, 2017. **7**(9): p. 3091-3102.

167. Choi, J.-H., et al., *Reconstitution of RPA-covered single-stranded DNA-activated ATR-Chk1 signaling.* Proceedings of the National Academy of Sciences, 2010. **107**(31): p. 13660-13665.

168. Baumann, P. and S.C. West, *Role of the human RAD51 protein in homologous recombination and double-stranded-break repair.* Trends Biochem Sci, 1998. **23**(7): p. 247-51.

169. Bhat, K.P. and D. Cortez, *RPA and RAD51: fork reversal, fork protection, and genome stability.* Nat Struct Mol Biol, 2018. **25**(6): p. 446-453.

170. Whelan, D.R., et al., *Spatiotemporal dynamics of homologous recombination repair at single collapsed replication forks.* Nature Communications, 2018. **9**(1): p. 3882.

171. Zhitkovich, A. and M. Costa, *A simple, sensitive assay to detect DNA-protein crosslinks in intact cells and in vivo.* Carcinogenesis, 1992. **13**(8): p. 1485-9.

172. Hughes, J.R. and J.L. Parsons, *The E3 Ubiquitin Ligase NEDD4L Targets OGG1 for Ubiquitylation and Modulates the Cellular DNA Damage Response.* Frontiers in Cell and Developmental Biology, 2020. **8**.

173. Robzyk, K., J. Recht, and M.A. Osley, *Rad6-dependent ubiquitination of histone H2B in yeast.* Science, 2000. **287**(5452): p. 501-4.

174. Pham, A.D. and F. Sauer, *Ubiquitin-activating/conjugating activity of TAFII250, a mediator of activation of gene expression in Drosophila.* Science, 2000. **289**(5488): p. 2357-60.

175. Yan, J., et al., *The ubiquitin-interacting motif containing protein RAP80 interacts with BRCA1 and functions in DNA damage repair response.* Cancer Res, 2007. **67**(14): p. 6647-56.

176. Lafranchi, L., et al., *APC/C(Cdh1) controls CtIP stability during the cell cycle and in response to DNA damage.* Embo j, 2014. **33**(23): p. 2860-79.

177. Kim, H., J. Chen, and X. Yu, *Ubiquitin-binding protein RAP80 mediates BRCA1-dependent DNA damage response.* Science, 2007. **316**(5828): p. 1202-5.

178. van Cuijk, L., et al., *SUMO and ubiquitin-dependent XPC exchange drives nucleotide excision repair.* Nature Communications, 2015. **6**(1): p. 7499.

179. Chauhan, A.K., et al., *Timely upstream events regulating nucleotide excision repair by ubiquitin-proteasome system: ubiquitin guides the way.* DNA Repair (Amst), 2021. **103**: p. 103128.

180. Takagi, Y., et al., *Ubiquitin Ligase Activity of TFIIH and the Transcriptional Response to DNA Damage.* Molecular Cell, 2005. **18**(2): p. 237-243.

181. Deshpande, Rajashree A., et al., *Nbs1 Converts the Human Mre11/Rad50 Nuclease Complex into an Endo/Exonuclease Machine Specific for Protein-DNA Adducts.* Molecular Cell, 2016. **64**(3): p. 593-606.

182. Hoege, C., et al., *RAD6-dependent DNA repair is linked to modification of PCNA by ubiquitin and SUMO.* Nature, 2002. **419**(6903): p. 135-141.

183. Chiu, R.K., et al., *Lysine 63-Polyubiquitination Guards against Translesion Synthesis–Induced Mutations.* PLOS Genetics, 2006. **2**(7): p. e116.

184. Qin, H. and Y. Wang, *Exploring DNA-binding proteins with in vivo chemical cross-linking and mass spectrometry.* J Proteome Res, 2009. **8**(4): p. 1983-91.

185. Kohn, K.W. and R.A. Ewig, *DNA-protein crosslinking by trans-platinum(II)diamminedichloride in mammalian cells, a new method of analysis.* Biochim Biophys Acta, 1979. **562**(1): p. 32-40.

186. Barker, S., et al., *A method for the isolation of covalent DNA-protein crosslinks suitable for proteomics analysis.* Anal Biochem, 2005. **344**(2): p. 204-15.

187. Spencer, V.A. and J.R. Davie, *Isolation of Proteins Cross-linked to DNA by Cisplatin*, in *The Protein Protocols Handbook*, J.M. Walker, Editor. 2002, Humana Press: Totowa, NJ. p. 747-751.

188. Ming, X., et al., *Mass Spectrometry Based Proteomics Study of Cisplatin-Induced DNA-Protein Cross-Linking in Human Fibrosarcoma (HT1080) Cells.* Chemical research in toxicology, 2017. **30**(4): p. 980-995.

189. Chichiarelli, S., et al., *Immunoprecipitation of DNA-protein complexes cross-linked by cis-diamminedichloroplatinum.* Anal Biochem, 2002. **302**(2): p. 224-9.

190. Meng, L.-H., et al., *DNA-protein crosslinks and replication-dependent histone H2AX phosphorylation induced by Aminoflavone (NSC 686288), a novel*

anticancer agent active against human breast cancer cells. Cancer Research, 2005. **65**(9_Supplement): p. 141-141.

191. Quievryn, G. and A. Zhitkovich, *Loss of DNA-protein crosslinks from formaldehyde-exposed cells occurs through spontaneous hydrolysis and an active repair process linked to proteosome function.* Carcinogenesis, 2000. **21**(8): p. 1573-80.
192. Yimit, A., et al., *Differential damage and repair of DNA-adducts induced by anti-cancer drug cisplatin across mouse organs.* Nature Communications, 2019. **10**(1): p. 309.
193. Nitiss, J.L., *Targeting DNA topoisomerase II in cancer chemotherapy.* Nature reviews. Cancer, 2009. **9**(5): p. 338-350.
194. Sannino, V., et al., *Xenopus laevis as Model System to Study DNA Damage Response and Replication Fork Stability.* Methods Enzymol, 2017. **591**: p. 211-232.
195. Maskey, R.S., et al., *Spartan deficiency causes genomic instability and progeroid phenotypes.* Nature communications, 2014. **5**: p. 5744-5744.
196. Saitoh, H. and J. Hinchey, *Functional heterogeneity of small ubiquitin-related protein modifiers SUMO-1 versus SUMO-2/3.* J Biol Chem, 2000. **275**(9): p. 6252-8.
197. Bruner, S.D., D.P. Norman, and G.L. Verdine, *Structural basis for recognition and repair of the endogenous mutagen 8-oxoguanine in DNA.* Nature, 2000. **403**(6772): p. 859-66.
198. Felgner, P.L., et al., *Lipofection: a highly efficient, lipid-mediated DNA-transfection procedure.* Proc Natl Acad Sci U S A, 1987. **84**(21): p. 7413-7.

199. Cardarelli, F., et al., *The intracellular trafficking mechanism of Lipofectamine-based transfection reagents and its implication for gene delivery.* Scientific Reports, 2016. **6**(1): p. 25879.

200. Hirt, B., *Selective extraction of polyoma DNA from infected mouse cell cultures.* J Mol Biol, 1967. **26**(2): p. 365-9.

201. Yoon, Y.G. and M.D. Koob, *Efficient cloning and engineering of entire mitochondrial genomes in Escherichia coli and transfer into transcriptionally active mitochondria.* Nucleic Acids Res, 2003. **31**(5): p. 1407-15.

202. Konac, E., et al., *Synergistic effects of cisplatin and proteasome inhibitor bortezomib on human bladder cancer cells.* Oncol Lett, 2015. **10**(1): p. 560-564.

203. Xu, Y., et al., *Proteasome inhibitor lactacystin enhances cisplatin cytotoxicity by increasing endoplasmic reticulum stress-associated apoptosis in HeLa cells.* Mol Med Rep, 2015. **11**(1): p. 189-195.